TROLL 4.0: representing water and carbon fluxes, leaf phenology and intraspecific trait variation in a mixed-species individual-based forest dynamics model – Part 1: Model description

Isabelle Maréchaux[1], Fabian Jörg Fischer[2,3], Sylvain Schmitt[1,4,5], Jérôme Chave[2]

1. AMAP, Univ Montpellier, CIRAD, CNRS, INRAE, IRD, 34000 Montpellier, France
2. CRBE, Université de Toulouse, CNRS, IRD, Toulouse INP, 118 route de Narbonne 31062 Toulouse, France
3. School of Biological Sciences, University of Bristol, Bristol, BS8 1TQ United Kingdom
4. CIRAD, UPR Forêts et Sociétés, F-34398, Montpellier, France
5. Forêts et Sociétés, Univ Montpellier, CIRAD, Montpellier, France

Correspondence to: Isabelle Maréchaux (isabelle.marechaux@inrae.fr)

Short summary: We describe TROLL 4.0, a simulator of forest dynamics that represents trees in a virtual space at one-meter resolution. Tree birth, growth, death and the underlying physiological processes such as carbon assimilation, water transpiration and leaf phenology depend on plant traits that are measured in the field for many individuals and species. The model is thus capable of jointly simulating forest structure, diversity and ecosystem functioning, a major challenge in modelling vegetation dynamics.

Abstract. TROLL 4.0 is an individual-based forest dynamics model that is capable of jointly simulating forest structure, diversity and ecosystem functioning, including the ecosystem water balance and productivity, leaf area dynamics and the tree community functional and taxonomic composition. It represents ecosystem flux processes in a manner similar to dynamic global vegetation models, while adopting a representation of plant community structure and diversity at a resolution consistent with that used by field ecologists. Specifically, trees are modeled as three-dimensional individuals with a metric-scale spatial representation, providing a detailed description of ecological processes such as competition for resources and tree demography. Carbon assimilation and plant water loss are explicitly represented at tree level using coupled photosynthesis and stomatal conductance models, depending on the micro-environmental conditions experienced by trees. Soil water uptake by trees is also modelled. Physiological and demographic processes are parameterized using plant functional traits measured in the field. Here we provide a detailed description and discussion of the implementation of TROLL 4.0. An evaluation of the model at two tropical forest sites is provided in a companion paper (Schmitt et al., submitted companion paper). TROLL 4.0's representation of processes reflects the state of the art, and we discuss possible developments to improve its predictive capability and its capacity to address challenges in forest monitoring, forest dynamics and carbon cycle research.

1 Introduction

Modelling vegetation dynamics remains a major challenge (Prentice et al., 2015; Song et al., 2021; Mahnken et al., 2022), and the wide variety of modelling concepts that coexist depend on models' initial objectives. Early versions of global vegetation models were developed to provide boundary conditions for energy, carbon and water budgets in global atmospheric models (Sellers et al., 1986, 1997). With the refinement of modeling concepts and computer power, feedback loops between the atmosphere and vegetation have gradually been taken into account (Charney, 1975; Cox et al., 2000; Meir et al., 2006), leading to an improved representation of fluxes of energy, carbon and water across the vegetation layer (Fisher et al., 2015; Moorcroft, 2003; Pitman, 2003). However, dynamic global vegetation models (DGVMs) typically adopt a simplified representation of floristic composition and vegetation structure (Fisher et al., 2014; Prentice et al., 2007). In many of these models, fluxes between vegetation and the atmosphere are still calculated in an average environment per grid cell (e.g. 1°*1°), for an average leaf of an individual drawn from a dozen of plant functional types (PFTs). The diversity of plant strategies is therefore typically represented by a small number of PFTs even in highly diverse tropical forests (Fisher et al., 2014; Poulter et al., 2011).

In parallel, stand-scale process-based models have been developed to better understand the exchanges between vegetation and the atmosphere through an up-scaling of fine-scale ecophysiological processes, and to account for within-stand micro-environmental heterogeneity (Wang and Jarvis, 1990; Gu et al., 1999; Williams et al., 1996; Ogée et al., 2003; Duursma and Medlyn, 2012; Fyllas et al., 2014). These process-based models are conceptually close to DGVMs, but they implement a more detailed representation of plant structure at the stand scale, and they have nurtured some important advances in DGVM-development over the past decades (e.g., Chen et al., 2016). Typically used to assimilate eddy-flux data, they do not include demographic processes however.

Forest growth models have a different history as they were initially developed to predict successional dynamics and inform forest management (Watt, 1947; Botkin et al., 1972; Vanclay, 1994; Porté and Bartelink, 2002; Liang and Picard, 2013). A key innovation have been gap models that represent recruitment, growth, mortality and competition between individual trees within forest patches. Forest patches are typically the size of a canopy opening created by the fall of a dominant tree (gap, or chablis, Bugmann 2001) and modelled as horizontally homogeneous, with a spatially implicit representation of tree positions. Through the simulation of a large number of patches, gap models can represent spatial heterogeneity due to gap dynamics within stands. Overall, these models adopt a finer representation of vegetation structure than classic DGVMs, but biogeochemical processes are generally modeled more coarsely, using ideal yield curves for tree growth rates combined with limiting factors imposed by the patch environment. Since these empirical relationships can only be parameterized on the basis of a large amount of data – readily available in plantations, but difficult to obtain elsewhere –, gap models typically also use plant functional types to simulate diverse forest stands. The number and definition of these groups has been much discussed in the literature, with no clear consensus (Botkin, 1975; Swaine and Whitmore, 1988; Vanclay, 1991; Köhler and Huth, 1998;

64 Köhler et al., 2000; Gourlet-Fleury et al., 2005; Kazmierczak et al., 2014), and these plant functional types are difficult to

65 transfer from one site to another (Picard and Franc, 2003; Picard et al., 2012).

66 Modelling vegetation from a completely different perspective and building upon flora distribution maps and

67 biogeographic concepts (Humboldt, 1849; Grisebach, 1872), plant species distribution models have been developed for long

68 (SDMs; Guisan et al., 2017). Generally, SDMs first estimate the envelope of environmental conditions for a species based on

69 species occurrence data (Guisan and Thuiller, 2005; Hutchinson, 1957; Soberón, 2007), which is used to infer a probability

70 distribution in space (Elith and Leathwick, 2009). These models require little knowledge on the processes underlying species

71 distribution, which explains their widespread use. However, because these models are statistical in nature, their ability to

72 project future states is unclear, and a great deal of research has been devoted to implementing process-based versions of these

73 SDMs (Chuine and Beaubien, 2001; Ferrier and Guisan, 2006; Morin and Lechowicz, 2008; Morin and Thuiller, 2009;

74 Kearney and Porter, 2009; Dormann et al., 2012; Journé et al., 2020).

75 From this brief and non exhaustive overview it emerges that each research community in vegetation modeling

76 emphasizes one representation of vegetation dimension – functioning, structure or diversity -- to the detriment of the others

77 (Maréchaux et al., 2021). Data availability and computing power partly explain such tradeoffs, and increasing model

78 complexity does not necessarily translate into an increase in reliability and robustness (Mahnken et al., 2022; Prentice et al.,

79 2015). However, a consensus has emerged in the literature that a better integration of plant species diversity, structure and

80 functioning should improve the predictive power of vegetation models (Purves and Pacala, 2008; Thuiller et al., 2008;

81 McMahon et al., 2011; Evans, 2012; Dormann et al., 2012; Mokany et al., 2016; Fisher et al., 2018). For example, tree species

82 diversity influences the productivity and resilience of forest ecosystems (Schnabel et al., 2019), and these biodiversity-

83 ecosystem functioning relationships result from local interactions where competition for resources is a key process (Fichtner

84 et al., 2018; Guillemot et al., 2020; Jourdan et al., 2020; Yu et al., 2024; Nemetscheck *et al.* 2024). Similarly, the fine details

85 of stand structure control the uptake of resources by vegetation (Braghiere et al., 2019, 2021; Brum et al., 2019; Ivanov et al.,

86 2012; De Deurwaerder et al., 2018), and they also determine the response to environmental stresses and disturbances

87 (Blanchard et al., 2023; Jucker et al., 2018; Seidl et al., 2014; De Frenne et al., 2019). More generally, the contribution of

88 vegetation in biogeochemical cycles, albeit typically quantified from stand to global scales (e.g. biomass, productivity),

89 ultimately depends on individual processes (e.g. mortality, Johnson et al., 2016) controlled by fine-scale heterogeneity and the

90 various ecological strategies of species (Poorter et al., 2015).

91 Therefore, recent developments in DGVMs have sought to better represent plant community structure and diversity.

92 Several cohort-based DGVMs have been developed to refine the representation of vegetation heterogeneity (Moorcroft et al.,

93 2001; Fisher et al., 2015; Longo et al., 2019; Smith et al., 2001). Continuous representations of functional diversity have also

94 been proposed using the distribution and co-variation of traits at the individual level or trait-climate relationships (Sakschewski

95 et al., 2015; Verheijen et al., 2015; Scheiter et al., 2013; Pavlick et al., 2013; Berzaghi et al., 2020; Van Bodegom et al., 2014).

96 These developments represent major advances in vegetation modelling, but scale mismatches between field data and model

97 representations limit the ability to assimilate data of various nature and resolution. While inverse modelling approaches can

98   partially alleviate these constraints (Hartig et al., 2012; Dietze et al., 2013; LeBauer et al., 2013; Fer et al., 2018; Lagarrigues

99   et al., 2015), they rely heavily on confidence in the model structure, can therefore raise equifinality issues (Medlyn et al.,

100   2005), and increase rapidly in computational complexity in high-dimensional parameter sets.

101   Finally, most of these challenges are exacerbated for tropical forests, as they are structurally complex (Doughty et al.,

102   2023), support a large number of tree species per hectare (up to several hundred, Wilson et al., 2012), and are more difficult

103   to access for evaluation in the field (Schimel et al., 2015). Given that they provide a range of ecosystem services and play a

104   major role in regional and global biogeochemical cycles (Beer et al., 2010; Bonan, 2008; Pan et al., 2011; Harper et al., 2013),

105   tropical forests and their responses to changing environmental factors have been identified as one of the greatest sources of

106   uncertainty in Earth system models (Koch et al., 2021; Powell et al., 2013; Restrepo-Coupe et al., 2017; Huntingford et al.,

107   2013). Thus, many advances in vegetation modelling have been, and still are, motivated by the challenge of tropical forests.

108   Here we describe a major upgrade of the TROLL forest dynamics model (Chave, 1999; Maréchaux and Chave, 2017;

109   Fischer, 2019), referred to here as TROLL 4.0. TROLL 4.0 brings together various modelling traditions, including elements

110   of DGVMs, stand-scale process-based models and forest gap models while adopting a species-level representation of plant

111   diversity, to jointly simulate the functioning, structure and diversity of forest ecosystems, and in particular tropical forests.

112   TROLL is a spatially explicit forest dynamics model, with an individual- and trait-based representation (Fig. 1). Individual

113   trees from 1cm diameter at breast height (*dbh*) are explicitly represented in a three-dimensional space discretized at a resolution

114   of one meter, allowing a fine representation of stand structure and local interactions via explicit competition for resources.

115   Each tree belongs to a species, with a list of mean traits per species provided as input. These traits control the physiological

116   and demographic processes of the tree's functioning and life cycle, from recruitment to growth, to seed dispersal and death.

117   This type of trait-based parameterization is based on recent advances in plant physiology and functional ecology, has been

118   facilitated by the expansion of large databases of functional traits (Díaz et al., 2016, 2022; Kattge et al., 2011, 2020), in

119   particular for tropical trees (Baraloto et al., 2010a; Vleminckx et al., 2021).

120   In TROLL 4.0, carbon assimilation and water loss by transpiration are represented explicitly using a photosynthesis

121   model coupled with a stomatal conductance model. Both take into account variation in micro-environmental conditions

122   between and within tree crowns, as well as the tree's access to soil water. A water cycle is now simulated, with the state and

123   dynamics of soil water explicitly represented and coupled with the vegetation dynamics. The influence of water availability

124   on leaf-level gas exchanges, leaf phenology, tree recruitment and death is parameterized through the leaf water potential at

125   turgor loss point (Bartlett et al., 2012) and mechanistic-based coordination with other hydraulic traits (Bartlett et al., 2016).

126   Carbon that is not consumed by the respiration of living tissues is then allocated to leaf production, carbon storage and tree

127   growth through allometric relationships. Compared to TROLL version 2.3.2 (Maréchaux and Chave, 2017), TROLL 4.0

128   includes other improvements: plant functional traits can vary among trees of the same species; tree crown shapes can be more

129   realistic than cylinders; and leaf density can vary within the tree crowns.

130   In this contribution, we provide a detailed description of the structure and objectives of the TROLL 4.0 model,

131   discussing how new modeling representations are an outcome of the state of knowledge and the availability of data. Finally,

132 we discuss the limitations of the model and future developments. An evaluation of the model's ability to simulate forest
133 structure, diversity and functioning for two Amazonian forest sites is reported in a companion paper (Schmitt et al., submitted
134 companion paper). The model is written in C++ and wrapped in the R environment through a dedicated package named
135 *rcontroll* (Schmitt et al. 2023).

136
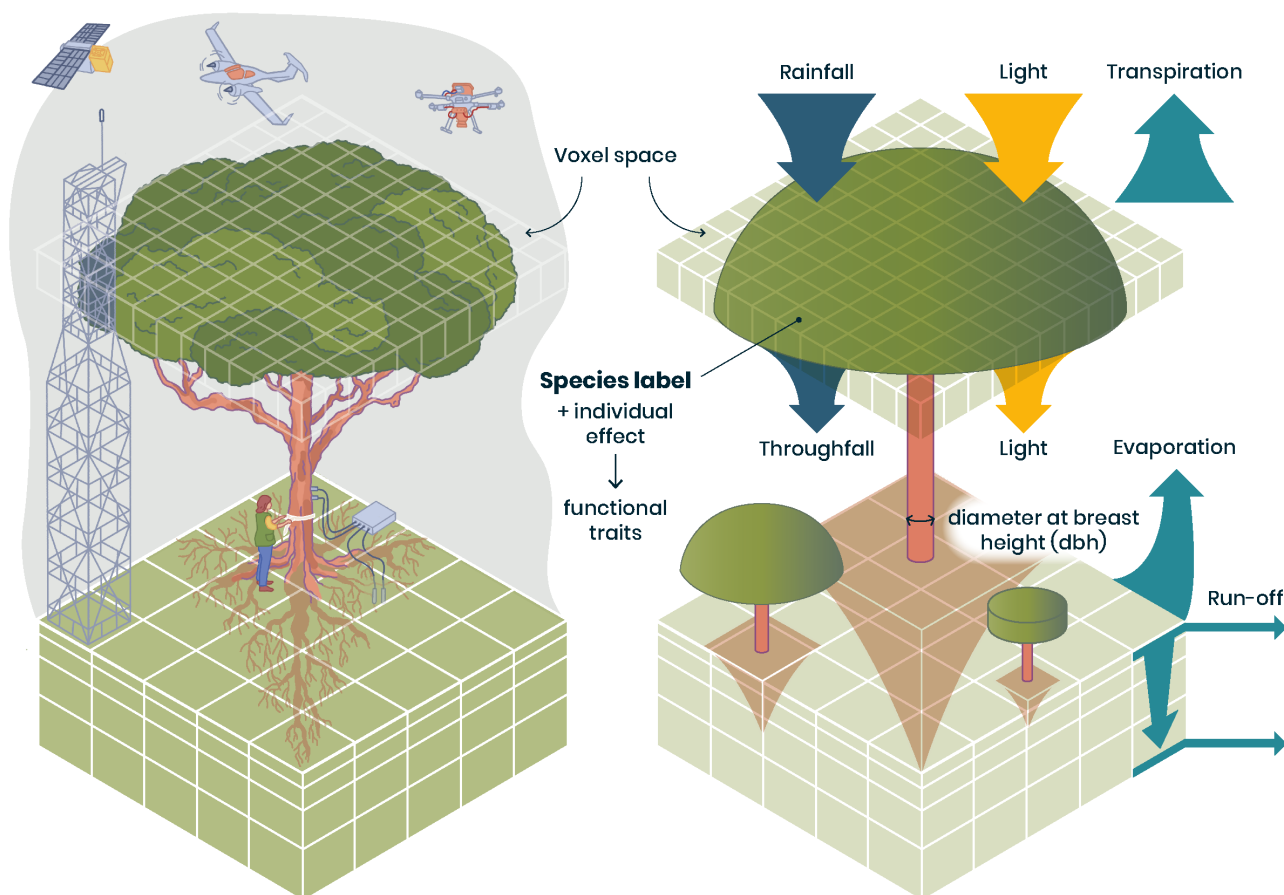
137

138 **Figure 1: Representation of individual trees in a spatially explicit environment in TROLL 4.0 (right) allowing direct comparison**
139 **with data of various nature (left). In TROLL 4.0, each tree is composed of a trunk, a crown, whose shape evolves from a cylinder to**
140 **an umbrella as the tree grows, and root biomass that decreases exponentially with soil depth. Tree dimensions are updated at each**
141 **timestep, depending on the net assimilated carbon that is allocated to growth, and following allometric relationships depending on**
142 **tree diameter at breast height (*dbh*). Each tree has a species label associated with plant functional traits, which, together with an**
143 **individual effect randomly attributed at tree birth, determines the tree's functional traits. These traits are used to parameterize**
144 **physiological and demographic processes that govern tree functioning throughout its life cycle. Light diffusion is computed explicitly**
145 **at each time step and within each voxel from the canopy top to the ground. Water balance is also computed at each timestep, and**
146 **the resulting water availability across soil voxels influence tree functioning. With this representation of forest structure, composition**
147 **and functioning, model outputs can be directly compared with a wide range of data, including carbon and water fluxes provided by**
148 **eddy-flux towers, field inventories, and 3D structure estimates from remote sensing (left). In TROLL 4.0, aboveground voxels**
149 **typically have a finer horizontal resolution than belowground voxels, but the latter are vertically finer and increasing in thickness**
150 **with depth (right). This resolution matches the one of fine-scale remote-sensing products or soil water content monitoring (left).**

151

2 Model description

2.1 Environmental conditions

TROLL 4.0 simulates an idealized forest stand with a typical size of 1 to 100 ha. Parallel computing may be used to simulate several times the same stand, or to simulate several forest stands with different environmental conditions. Climatic drivers are similar to those represented in many DGVMs (air temperature, vapor pressure deficit, wind speed, and light intensity above the canopy, as well as precipitation). The forest ecosystem is divided into an above-ground and below-ground part. Soil is explicitly represented as a water reservoir, but soil nutrients are not modeled. The topography within a stand is assumed to be flat.

2.2 Light availability and aboveground variation in micro-climate

Above ground, the simulated forest stand is represented as a discrete grid of 1m^3 cubic voxels. Light diffuses through the forest's leaf layers from the top of the canopy to the ground, with one recalculation each day. In a given voxel, light availability is the photosynthetic photon flux density in μmol photons m^{-2} s^{-1} and is computed as a function of the incident light intensity at top canopy (PPFD$_{top}$, see Table A1 for a list of symbols), the cumulated leaf density of voxels above and the (constant) leaf density within the voxel itself. The Beer-Lambert extinction of light within the canopy allows to calculate the incident PPFD (per unit ground area) above any layer at vertical extent v as:

$$PPFD(v) = PPFD_{top} \times \exp[-k \times LAI(v)] \qquad (1)$$

where $LAI(v)$ is the cumulated leaf area above height v, and k is the extinction coefficient. We here define $k = k_{geom} \times$ absorptance$_{leaves}$, where k_{geom} reflects the geometric arrangement of leaves in the voxel (a value of 0.5 reflecting spherical leaf distribution; Ross, 1981) and absorptance$_{leaves}$, the fraction of absorbed light within a single leaf (Long et al., 1993; Poorter et al., 1995). The absorbed light in a layer a of thickness Δa is then

$$PPFD_{abs}(a) = PPFD_{top} \times \exp[-k \times LAI(a)] - PPFD_{top} \times \exp[-k \times LAI(a + \Delta a)] \qquad (2)$$

Assuming that leaf area per unit ground area (m^2 m^{-2}), or $dens(a)$, is constant within the layer, this simplifies to:

$$PPFD_{abs}(a) = PPFD_{top} \times \exp[-k \times LAI(a)] \times (1 - \exp[-k \times dens(a)]) \qquad (3)$$

For photosynthesis calculations, absorbed PPFD per unit ground area is converted into absorbed PPFD per unit leaf area by dividing $PPFD_{abs}(a)$ by $dens(a)$.

Air microenvironmental variation within the canopy is represented as follows. Nighttime temperature (T$_{night}$) is assumed constant throughout the night and within the canopy, while temperature (T) and vapor pressure deficit (VPD) vary across voxels depending on the variable $\lambda(v) = \frac{LAI(v)}{LAI_{sat}}$ with LAI_{sat} a threshold LAI and LAI(v) the LAI above voxel v. At height v above ground, we calculate temperature and VPD as follows:

181 $T(v) = T_{top} - \Delta T \times \lambda(v)$ (4)

182 $VPD(v) = VPD_{top} \times \left[C_{VPD0} + (1 - C_{VPD0}) \sqrt{(1 - \lambda(v))} \right]$ (5)

183 where ΔT and C_{VPD0} are set parameters and T_{top} and VPD_{top} are values at the top of canopy. For any given layer a of depth

184 Δa, temperatures and VPDs are then calculated by averaging both functions from a to $a + \Delta a$:

185 $T_{mean}(a) = \frac{1}{\Delta a} \int_a^{a+\Delta a} (T_{top} - \frac{\Delta T}{LAI_{sat}} \times LAI(v)) dv$ (6)

186 $VPD_{mean}(a) = \frac{1}{\Delta a} \int_a^{a+\Delta a} VPD_{top} \times \left[C_{VPD0} + \frac{(1-C_{VPD0})}{\sqrt{LAI_{sat}}} \sqrt{(LAI_{sat} - LAI(v))} \right] dv$ (7)

187 Equations 6 and 7 can then be simplified using the assumption of constant leaf density within a layer and redefining v with

188 respect to the current layer a, so that $LAI(v) = LAI(a) + dens(a) \times v$.

189 This representation of variation of T and VPD within the canopy is in qualitative agreement with empirical

190 observations of microclimate gradients within tropical forest canopies (Camargo and Kapos, 1995; Shuttleworth, 1985;

191 Shuttleworth et al., 1989, Tymen et al. 2017), with a consistent buffering effect of forest canopies on understory micro-

192 environment (De Frenne et al., 2019), and a strong control by forest structure (Gril et al., 2023b, a; Tymen et al., 2017;

193 Zellweger et al., 2019).

194 Wind speed attenuation inside the canopy is simulated as described in Rau et al. (2022), who explored the effect of

195 wind speed on forest structure in a forest exposed to cyclones using TROLL. Wind speed is usually measured above the canopy

196 and decreases as one approaches the canopy top layer, so wind speed at the top of the canopy is (Monteith & Unsworth 2008):

197 $u(z) = \frac{u_*}{\kappa} \ln \left(\frac{z-d}{z_0} \right), \; if \; z \geq H$ (8)

198 where $u(z)$ is the horizontal wind speed in m s⁻¹ at a height z (in m) above ground, H the height of the top of the canopy (in

199 m), u_* is the friction velocity, κ the von Karman constant ($\kappa=0.40$), d the zero-plane displacement height, here assumed to be

200 equal to 0.8H, and z_0 the aerodynamic roughness, here assumed to be equal to 0.06H (Rau et al., 2022). Within the canopy,

201 wind speed decreases as (Inoue 1963):

202 $u(z) = u(H) \exp \left(-\alpha \left(1 - \frac{z}{H} \right) \right), \; if \; z < H$ (9)

203 with $\alpha \approx 3$ (Raupach et al., 1996). Wind speed was not computed at the voxel scale, but using the coarser horizontal resolution

204 of the belowground field (see section 2.3 below, e.g. 25x25 m), and a mean top canopy height H was computed as input to Eqs

205 (8) and (9).

206 **2.3 Soil water availability**

207 In TROLL 4.0, the belowground part of the ecosystem is explicitly represented, and its discretization is specified by the user,

208 including the number and depth of layers, and horizontal dimensions of the cells. Belowground voxels are typically coarser

209 horizontally (e.g. 25m x 25m, as commonly implemented in gap models Bugmann, 2001), but finer vertically, than

210 aboveground 1-m³ voxels. Metric-scale lateral water fluxes are difficult to parameterize and evaluate, and neglecting them

211   here limits the computational burden. Soil layers typically increase in thickness with depth, as in most DGVMs or forest

212   physiological models (Prentice et al., 2015) and in standard soil assessments (e.g. Hengl et al., 2017). In this representation,

213   contrasting root depth and access to water can be represented across individual trees together with potential variation in soil

214   properties and hydraulic state. This approach contrasts with some forest dynamics models that use a single-layer belowground

215   representation (e.g. Gutiérrez et al., 2014; Christoffersen et al., 2016; Fyllas et al., 2014).

216   The water content in each belowground voxel is simulated using a bucket model, which relies on the vertical water

217   balance for each voxel. Neglecting horizontal lateral fluxes, the water balance for a given soil column amounts to:

218    $\Delta SWC = P - I - Q - E - T - L$ (10)

219   where SWC is the soil water content, P the incident rainfall, I the canopy interception, Q the run-off, E the evaporation from

220   the soil, T the transpiration, i.e. the plant water uptake, and L the leakage. This water balance is established for each soil layer,

221   with inputs from upwards and outputs downwards starting from the top layer (l=1): outputs of layer l are inputs for layer $l+1$,

222   with L corresponding to the output of the deepest layer, and P-I-Q to the input of the top layer. Note that this downward

223   iteration neglects: (i) potential hydraulic lift (upward water redistribution, see e.g. Dawson, 1993; Burgess et al., 1998; Oliveira

224   et al., 2005); and (ii) potential interaction with the water table (Costa et al., 2023; Sousa et al., 2022). Further developments

225   could account for these two mechanisms where they are expected to play a significant role. In particular, flooded areas could

226   be easily represented, with a shallower soil depth and a prescribed boundary condition, i.e. a shallower water table. We now

227   describe and discuss each term of the water balance and the corresponding modeling choices.

228   *Rainfall.* Rainfall (*P*, in mm) is a model input. It is assumed that the total daily rainfall corresponds to a single event

229   of rain per day (one storm, as in, e.g., Rodriguez-Iturbe et al., 1999; Laio et al., 2001; Fischer et al., 2014; Gutiérrez et al.,

230   2014).

231   *Interception.* Rainfall interception by the canopy is simulated using a model where interception depends on LAI, as

232   proposed by Liang et al. (1994):

233    $I = \min(P, K \times LAI)$ (11)

234   where K=0.2mm and LAI corresponds to the leaf area index at ground level, averaged across the ground-level aboveground

235   voxels that contribute to a single belowground voxel (typically $625=25^2$ aboveground voxels contribute to one belowground

236   voxel). Similar simple formulations of canopy interception have been used elsewhere (e.g. Liu et al., 2017), and this choice is

237   justified by the lack of relevant data to properly parameterize more complex formulations at most field sites. More complex

238   models of rainfall interception also exist however (Rutter and Morton, 1977; Gash, 1979; Gash et al., 1995).

239   *Run-off and infiltration.* As in most bucket models coupled with a forest dynamics model, the temporal propagation

240   of the wetting front into the soil is not explicitly simulated here, because of the daily timestep and the vertically lumped

241   representation of soil moisture dynamics (e.g., Laio et al., 2001, Guimberteau et al., 2014). When the soil top layer has enough

242   available storage to absorb the totality of the throughfall (*i.e.* when throughfall is smaller than the layer water content at field

243   capacity minus the current soil water content), it is assumed that the increment in soil water content of that top layer is equal

244   to the throughfall. Otherwise, the excess water percolates to the next layer below. In the absence of an explicit wetting front,

245   runoff occurs only when the superficial layer is already saturated, which is similar to Dunne run-off (Dunne and Black, 1970).

246   More complex formulations of run-off exist (d'Orgeval et al., 2008; Guimberteau et al., 2014; Horton, 1933), but because of

247   the high porosity of many tropical forest soils (Hodnett and Tomasella, 2002; Sander 2002) and the lack of explicit topography

248   in this version, our choice is parsimonious.

249   *Soil evaporation.* We assumed that water evaporates from the top soil layer only, a reasonable assumption if the top

250   soil layer is not too thin. We followed Sellers et al. (1992) under which evaporation from the soil is expressed as (see Merlin

251   et al., 2016 for a review of alternatives):

252    $E = \frac{M_w}{RT_s} \times \frac{e_s - e_a}{r_{soil} + r_{aero}}$ (12)

253   where E is in kg m^{-2} s^{-1}, M_w is the molar mass of water vapor (M_w=18 kg mol^{-1}), R is the ideal gas constant (R=8.31 J mol^{-1}

254   K^{-1}), T_s is the temperature at soil surface in K, e_s is the vapor pressure of the soil surface in Pa, e_a is the vapor pressure of air

255   above the soil surface in Pa, r_{soil} is the soil surface resistance in s m^{-1}, and r_{aero} is the aerodynamic resistance to heat transfer

256   in s m^{-1}. Soil water pressure e_s is a function of the water potential of the top soil belowground voxel ($\psi_{soil,top}$, in MPa; Jones,

257   2013, Eq. (5.14) therein):

258    $e_s = e_{sat}(T_s) \times \exp\left(\frac{V_w}{RT_s} \times \psi_{soil,top}\right) = e_{sat}(T_s) \times \exp\left(2.17 \times \frac{\psi_{soil,top}}{T_s}\right)$ (13)

259   Where V_w is the partial molal volume of water ($V_w = 18 \times 10^{-6}$ m^3 mol^{-1}), and $e_{sat}(T_s)$ is the saturated vapor pressure at T_s

260   computed following the Buck equation (Jones, 2013, Appendix 4 therein). e_a is by definition equal to $e_{sat}(T_s) - VPD_{ground}$,

261   where the latter is the VPD at ground level in Pa. r_{soil} is computed following Sellers et al. (1992, Eq. (19) therein, see also

262   Merlin et al., 2016, Eq. (12)):

263    $r_{soil} = \exp\left(8.206 - 4.255 \times \frac{\theta_{top}}{\theta_{fc,top}}\right)$ (14)

264   where θ_{top} is the water content of the top soil belowground voxel and $\theta_{fc,top}$ is its water content at field capacity (in m^3).

265   Aerodynamic resistance r_{aero} is computed as follows (Merlin et al., 2016, Eq. (B10) therein):

266    $r_{aero} = \frac{1}{\kappa^2 \times u(Z)} \ln\left(\frac{Z}{Z_m}\right)^2$ (15)

267   with κ again the von Karman constant (κ=0.40), $u(Z)$ is the wind seed (in m s^{-1}) at reference height Z, here taken at 1m above

268   ground, and Z_m is the momentum soil roughness in m, set to 0.001m.

269   *Transpiration.* Trees transpire soil water from the belowground voxel they are rooted in (see section 2.4.3). For a

270   given tree, the total daily soil water uptake is the sum of the water transpired by leaves across its crown and across day-time

271   half hours (see section 2.5.2). Soil layers contribute to water uptake as a function of tree-dependent weights, w_l (see Eq. (21),

272   section 2.4.3), which depend on root biomass and on the soil hydraulic state in each layer.

273   For each belowground voxel in layer l, the soil water potential (ψ_l) and the soil hydraulic conductivity (K_l) are

274   computed at each time step from the soil water content in the focal voxel using the van Genuchten-Mualem soil characteristic

275   and hydraulic conductivity curves (Mualem, 1976; van Genuchten, 1980; see Table 1 in Marthews et al., 2014). Parameters of

276 these curves are estimated using regression models (pedotransfer functions) for tropical soils (Hodnett and Tomasella, 2002),
277 except the saturated hydraulic conductivity, which is computed following Cosby et al. (1984; see Table 2 in Marthews et al.,
278 2014). In practice, when only soil texture data is available, TROLL 4.0 contains a default option to apply the texture-based
279 only pedotransfer function provided by Tomasella and Hodnett (1998), coupled to the soil characteristic and hydraulic
280 conductivity curves of Brooks and Corey (1964) (see Tables 1 and 2 in Marthews et al., 2014).

281 **2.4 Representation of trees in the model**

282 **2.4.1 Species affiliation and intra-specific trait variability**

283 In TROLL 4.0, each tree (and seed) is attributed a botanical species defined by a taxonomic binomial. It is assumed that the
284 user has sufficiently good knowledge of the tree species growing in the study area so that a list of species-specific mean plant
285 functional trait values can be provided as input. These are the leaf mass per area (LMA, in g m^{-2}), the leaf area (LA, cm^2), the
286 leaf nitrogen content per dry mass (N, in mg g^{-1}), the leaf phosphorous content per dry mass (P, in mg g^{-1}), the wood specific
287 gravity (wsg, in g cm^{-3}), the leaf water potential at turgor loss point (π_{tlp}, in MPa), and three allometric parameters (dbh$_{thres}$,
288 h$_{lim}$, a$_h$, all in m; see section 2.4.2). The number of species provided in input is not limited. In addition to mean plant functional
289 trait values, it is possible to input individual trait values from which a trait variance-covariance matrix is computed
290 (alternatively the trait variance-covariance matrix can be prescribed). With this option, for each recruited tree, the trait values
291 are drawn from a distribution rather than attributed the species-specific mean value. For each trait i and tree j, the species-
292 specific mean value is multiplied by a factor $e^{\varepsilon_{i,j}}$ where $\varepsilon_{i,j} \sim N(0, \sigma_i)$ where σ_i the trait-specific standard deviation on a
293 logarithmic scale (lognormal variation). The sole exception is wood specific gravity, which we assume to be normally
294 distributed around the mean with $\varepsilon_{wsg,j} \sim N(0, \sigma_{wsg})$. Trait covariance is only considered for leaf N, leaf P and LMA, and
295 other traits are assumed to be decoupled (Baraloto et al., 2010b). Note that with this implementation, intraspecific variation is
296 not structured in space or time nor heritable, and is thus a surrogate for variability emerging from genetic variation or plasticity
297 (Girard-Tercieux et al., 2023; 2024). A more realistic representation of the latter is left for future version.

298 **2.4.2 Aboveground structure**

299 Above ground, the tree geometry is represented as a three-dimensional object within the voxelized space and consists of a
300 trunk and a crown filled with leaves. The trunk is assumed to be a cylinder characterized by its total height and its diameter
301 (*dbh*, for diameter at breast height, by analogy with forest inventories). The aboveground dimensions of trees are predicted
302 from their *dbh* via scaling rules. For tree j with *dbh$_j$*, we calculate its height h$_j$, its crown radius cr$_j$, and its crown depth cd$_j$ as
303 follows:

304 $$h_j = \frac{h_{lim} \times dbh_j}{(a_h + dbh_j)} \times e^{\varepsilon_{h,j}} \tag{16}$$

305 $$cr_j = e^{a_{cr}} \times dbh^{b_{cr}} \times e^{\varepsilon_{cr,j}} \tag{17}$$

306     $cd_j = \min\left(\frac{h_j}{2}, (a_{cd} + b_{cd} \times h_j) \times e^{\varepsilon_{cd,j}}\right)$ (18)

307   where h_{lim} and a_h are species-specific coefficients of the Michaelis-Menten function, and a_{cr}, b_{cr}, a_{cd}, and b_{cd} allometric

308   coefficients that are species independent. $\varepsilon_{h,j}$, $\varepsilon_{cr,j}$ and $\varepsilon_{cd,j}$ are variance terms to simulate intraspecific variation with

309     $\varepsilon_{h,j} \sim N(0, \sigma_h)$, $\varepsilon_{cr,j} \sim N(0, \sigma_{cr})$, and $\varepsilon_{cd,j} \sim N(0, \sigma_{cd})$. Tree crown architecture is known to depend on species ecological

310   strategies (Bohlman and O'Brien, 2006; Iida et al., 2012; Poorter et al., 2006; Laurans et al., 2024), but given that crown

311   extents are difficult to measure reliably in the dense canopies of tropical forests, we used a single set of parameters for all the

312   species.

313   In the previous published version (Maréchaux and Chave, 2017), tree crowns were represented as cylinders with

314   homogeneous leaf densities. Since v.3.0, TROLL can also model tree crowns as flexible, umbrella-like shapes with

315   heterogeneous leaf density distributions. Small tree crowns are simulated as cylinders, but consist of up to three separate 1-m

316   layers of leaves (top, intermediate and bottom layer). Each layer can be assigned a percentage of the total leaf area (e.g., 50%,

317   30%, 20%) to reflect gradients in leaf densities from the upmost to lower crown layers (Kitajima et al., 2005), but the default

318   is an equal distribution (33%, 33%, 33%) across all layers. Once a tree surpasses 3 m in crown depth, no new layers are added.

319   Instead, the treetop grows quicker in height than the outer crown parts. As a result, the three 1-m layers are folded around the

320   tree trunk like an umbrella at various stages of opening (see Fig. 1b in Schmitt et al., 2023, and similar tree representations in

321   Strigul et al., 2008). Different functional forms are available to describe height variation from treetop to crown edge, but here

322   we chose a simple linear decrease between the radius at the top of the crown to the radius at the bottom of the crown. The ratio

323   between both radii is controlled through the global parameter *shape_crown*, which varies between 0 (conical shape) and 1

324   (cylinder), and thus allows for various "conifer-like" and "broadleaf-like" shapes in between.

325   We also relax the assumption that tree crowns are homogeneously filled across their horizontal extent. In TROLL

326   4.0, crowns have small 1-m^2 openings (or gaps) in their crowns, parameterized as percentage of total crown area that is not

327   filled with leaves, f_{gap}. This allows for the modelling of a spatially heterogeneous light environment in the understory (Tymen

328   et al., 2017), with a theoretical range from $f_{gap} = 0\%$ (full crown cover, no openings) to $f_{gap} = 100\%$ (a hypothetical crown with

329   no leaf area). When calibrating TROLL for tropical forests with airborne laser scanning (Fischer et al., 2019), we found a value

330   of $f_{gap} = 15\%$ to be a good approximation for this within-crown gap fraction. If intraspecific variation in crown extent is

331   explicitly modelled, the fraction of crown gaps is rescaled so that the absolute crown cover stays constant (i.e., the fraction of

332   crown gaps is divided by $e^{2\varepsilon_{cr,j}}$). Within species, variation in crown extent is thus assumed as decoupled from variation in leaf

333   area, i.e., reflecting variation in branch angles and directions, but not branch number or biomass.

334   **2.4.3 Belowground structure**

335   TROLL 4.0 makes the common assumption that total fine root biomass is equal to leaf biomass. Future developments should

336   endeavor to represent a more explicit belowground allocation scheme (Merganičová et al., 2019; Huaraca Huasco et al., 2021).

337   Direct estimates of individual tree root depth and root distribution are rare in moist tropical forests (Canadell et al., 1996;

338   Jackson et al., 1996, 1999; Nepstad et al., 1994; Cusack et al., 2024; Guerrero-Ramírez et al., 2021). Some studies have

339   quantified the depth of tree water uptake using indirect methods, such as predawn leaf water potential, or isotope labeling

340   (Brum et al., 2019; Stahl et al., 2013), but this does not give access to the actual rooting depth. Tree root depth was here

341   assumed to increase with tree size, and was computed as a function of tree *dbh* as follows (Kenzo et al., 2009, Fig. 4 therein):

342   $RD = 0.35 \times dbh^{0.54}$ (19)

343   with root depth, RD, in m, and diameter at breast height, dbh, in cm. As in Xu et al. (2016), the exponent was based on Kenzo

344   et al. (2009), who reported on data from excavated trees in secondary forests in Malaysia. The first parameter (0.35, root depth

345   at dbh=1cm) was adjusted to avoid unrealistic water depletion of the top soil layer. In the absence of relevant species-specific

346   data, this allometric equation was assumed to hold for all species, even if root depth is known to be highly plastic (e.g. Rowland

347   et al., 2023). Correlations between rooting depth and leaf phenological habit have been reported, but in drier or more seasonal

348   sites than Amazonian rainforests (Brum et al., 2019; Hasselquist et al., 2010; Smith-Martin et al., 2020), and trait coordination

349   are known to be typically stronger under harsher environmental conditions (Dwyer and Laughlin, 2017; Delhaye et al., 2020).

350   We assumed that vertical tree root distribution follows an exponential profile, as observed empirically at the stand

351   scale (Fisher et al., 2007; Humbel, 1978; Jackson et al., 1996). The fine root biomass in layer l, at depths ranging from z_l to

352   $z_{l+1} (> z_l)$ is computed as:

353   $RB_l = RB_t \times \left(\exp\left(-3\frac{z_l}{RD}\right) - \exp\left(-3\frac{z_{l+1}}{RD}\right) \right)$ (20)

354   where RB$_t$ is the total tree fine root biomass (in g), RB$_l$ the fine root biomass in layer l (in g), RD the tree rooting depth (in m).

355   The factor 3 was determined so that about 95% of the tree biomass is contained between soil surface and RD (note that -

356   log(0.05)≈3) (Arora and Boer, 2003). Tree roots are distributed across vertical layers, but do not spread across belowground

357   voxels horizontally. As a result, trees only deplete the water content of the belowground voxels located below their trunk

358   position (see section 2.3).

359   The soil water potential in the root zone, ψ_{root} (in MPa), captures how the plant equilibrates with the soil water state

360   across its root profile. It is computed as the weighted mean of the belowground voxel water potentials across layers. We used

361   the weighting scheme proposed by Williams et al. (2001; see also Bonan et al., 2014; Duursma and Medlyn, 2012), which

362   accounts for the variation of soil water availability and conductance across layers as follows:

363   $\psi_{root} = \sum_l w_l \times \psi_l$ with $w_l = \frac{(\psi_l - \psi_{R,min}) \times G_l}{\sum_{ll}(\psi_{ll} - \psi_{R,min}) \times G_{ll}}$ (21)

364   where ψ_l is the soil water potential in layer l, and $\psi_{R,min}$ is the root water potential below which there is no water uptake

365   within the layer (minimal root water potential, assumed to be -3 MPa as in Duursma and Medlyn, 2012). G$_l$, the soil-to-root

366   water conductance in layer l, in mmol H$_2$0 m^{-2} s^{-1} MPa^{-1}, computed as follows (Gardner, 1964):

367   $G_l = \frac{2\pi L_{a,l} K_l}{\log\left(\frac{r_s}{r_r}\right)}$ (22)

368   In Eq (22), L$_{a,l}$ is the total root length per unit area in the layer (in m m^{-2}), with the total root length in the layer computed as

369   $RB_l \times SRL$ where SRL is the specific root length, here assumed to be constant (10 m g^{-1}, Bonan et al., 2014; Metcalfe et al.,

370   2008; Weemstra et al., 2016). K_l is the soil hydraulic conductivity of layer l (in mmol H_2O m^{-1} s^{-1} MPa^{-1}, see section 2.3), r_r is

371   the mean fine root radius, here set at 1mm, and r_s is half the mean distance between roots, calculated with the assumption of

372   uniform root spacing in a given layer (Newman, 1969):

373   $$r_s = \frac{1}{\sqrt{\pi L_{v,l}}}$$ (23)

374   where $L_{v,l}$ is the total root length per unit soil volume in the layer (in m m^{-3}), computed in the same way as $L_{a,l}$, but also divided

375   by layer depth.

376   A range of other models have been used to infer ψ_{root} using the relative tree root biomass in each layer directly as

377   weights (De Kauwe et al., 2015; Naudts et al., 2015; Powell et al., 2013; Schaphoff et al., 2018; Sakschewski et al., 2021;

378   Verbeeck et al., 2011). However, trees do not uptake water simply as a proportion of root density, but can equilibrate with the

379   wettest soil layers (Schmidhalter, 1997; Duursma and Medlyn, 2012): the contrasting temporal variations in water availability

380   across layers result in seasonal changes in the depth of active water withdrawal (Bruno et al., 2006; Joetzjer et al., 2022). For

381   instance, cavitation in the driest part of the soil disconnects roots from the soil (Sperry et al., 2002; see also Fisher et al., 2006).

382   This is likely why deeper roots, although often very rare, disproportionately contribute to sustain forest productivity during

383   dry seasons.

2.5 Leaf physiology

385   The carbon assimilated and the water transpired by a tree within a day are the sum of the leaf-level carbon and water fluxes

386   across day-time half hours. Leaf-level carbon assimilation is computed per crown layer of each tree, using the Farquhar-von

387   Caemmerer-Berry model of C$_3$ photosynthesis (Farquhar et al., 1980, see section 2.5.1), coupled to the model of stomatal

388   conductance of Medlyn et al. (2011; see section 2.5.2) as in Maréchaux and Chave (2017). In TROLL 4.0 the dependences on

389   leaf temperature (T_l), vapor pressure deficit at the leaf surface (VPD$_s$), and CO$_2$ concentration at the leaf surface (c_s) are now

390   determined iteratively at the leaf surface, starting from air temperature (T), air vapor pressure deficit (VPD$_a$) and air CO$_2$

391   concentration (c_a) averaged across the tree crown layer (see sections 2.2 and 2.4.2) and with transpiration computed using the

392   Penman-Monteith equation (see section 2.5.4).

2.5.1 Photosynthesis

394   In Farquhar et al. (1980), leaf-level net carbon assimilation rate (A_n, µmol CO_2 m^{-2} s^{-1}) is limited by either Rubisco activity

395   (A_v, µmol CO_2 m^{-2} s^{-1}), or RuBP regeneration (A_j, µmol CO_2 m^{-2} s^{-1}):

396   $$A_n = min\{A_v, A_j\} - R_p(T_l) \quad ; \quad A_v = V_{cmax}(T_l, \psi_{pd}) \times \frac{c_i - \Gamma^*}{c_i + K_m(T_l)} \quad ; \quad A_j = \frac{J}{4} \frac{c_i - \Gamma^*(T_l)}{c_i + 2\Gamma^*(T_l)}$$ (24)

397   where R_p is the photorespiration rate (µmol C m^{-2} s^{-1}), V_{cmax} is the maximum rate of carboxylation (µmol CO_2 m^{-2}s^{-1}), c_i the

398   CO$_2$ partial pressure at carboxylation sites, Γ^* the CO$_2$ compensation point in the absence of dark respiration, K_m the apparent

399 kinetic constant of the Rubisco (von Caemmerer, 2000), and J the electron transport rate (µmol e^- m^{-2} s^{-1}), which depends on

400 PPFD through:

401
$$J = \frac{1}{2\theta}\left[\alpha \times PPFD + J_{max}(T_l, \psi_{pd}) - \sqrt{\left(\alpha \times PPFD + J_{max}(T_l, \psi_{pd})\right)^2 - 4\theta \times \alpha \times PPFD \times J_{max}(T_l, \psi_{pd})}\right] \quad (25)$$

402 J$_{max}$ is the maximal electron transport capacity (µmol e^- m^{-2} s^{-1}), θ the curvature factor (unitless), and α the apparent quantum

403 yield to electron transport (mol e^- mol *photons*$^{-1}$), computed following von Caemmerer (2000) as $\alpha = (1 - LSQ) \times 0.5$, with

404 LSQ the effective spectral quality of light, fixed at 0.15, and the factor 0.5 accounts for the fact that each photosystem absorbs

405 half of the photons.

406   The V_{cmax} and J_{max} parameters depend on leaf properties, leaf temperature (T_l) and water state (through the leaf

407 predawn water potential, ψ_{pd}, see Eq. (37)) and represent a large source of uncertainty in vegetation models (Zaehle et al.,

408 2005; Mercado et al., 2009; Rogers et al., 2017). In tropical forest environments, Domingues et al. (2010) suggested that V_{cmax}

409 and J_{max} are co-limited by the leaf concentration of nitrogen and phosphorus as follows (see also Walker et al., 2014):

410 $V_{cmax-M}(25°C) = min\{-1.56 + 0.43 \times N - 0.37 \times LMA \; ; \; -0.80 + 0.45 \times P - 0.25 \times LMA \;\}$ (26)

411 $J_{max-M}(25°C) = min\{-1.50 + 0.41 \times N - 0.45 \times LMA \; ; \; -0.74 + 0.44 \times P - 0.32 \times LMA \;\}$ (27)

412 with V_{cmax-M} and J_{max-M} the photosynthetic capacities at 25°C of unstressed mature leaves on a leaf dry mass basis, in µmol

413 CO_2 g^{-1} s^{-1} and µmol e^- g^{-1} s^{-1}, respectively. N and P are leaf nitrogen and phosphorus concentrations in mg g^{-1}, and LMA is the

414 leaf mass per area in g cm^{-2}. V_{cmax-M} and J_{max-M} can be converted into area-based V_{cmax} and J_{max} by multiplying by LMA.

415 We used this leaf trait-based parameterization of $V_{cmax}(25°C)$ and $J_{max}(25°C)$ in the absence of water stress (as in Fyllas et

416 al., 2014; Mercado et al., 2011). The dependence of V_{cmax} and J_{max} with temperature was given by equations in Bernacchi et

417 al. (2003), and the dependence with water availability was modelled by a function of ψ_{pd} (WSF_{ns}, see section 2.5.3, Eq. (40)):

418 $V_{cmax}(T_l, \psi_{pd}) = V_{cmax}(25°C) \times e^{\left(26.35 - \frac{65.33}{R \times (T_l + 273.15)}\right)} \times WSF_{ns}(\psi_{pd})$ (28)

419 $J_{max}(T_l, \psi_{pd}) = J_{max}(25°C) \times e^{\left(17.57 - \frac{43.54}{R \times (T_l + 273.15)}\right)} \times WSF_{ns}(\psi_{pd})$ (29)

420 where R is the molar gas constant (0.008314 kJ K^{-1} mol^{-1}), and T_l is the internal leaf temperature in Celsius degrees. The

421 temperature dependence of Γ^* and K_m followed von Caemmerer (2000):

422 $\Gamma^*(T_l) = 37 \times e^{23.4 \times \frac{(T_l - 25)}{298 \times R \times (273 + T_l)}}$ (30)

423 $K_m(T_l) = 404 \times e^{59.36 \times \frac{(T_l - 25)}{298 \times R \times (273 + T_l)}} \times \left(1 + \frac{210}{248 \times e^{35.94 \times \frac{T_l - 25}{298 \times R \times (273 + T_l)}}}\right)$ (31)

424 Temperature dependencies in Eqs (28)-(31) are consistent with Domingues et al. (2010), following recommendations from

425 Rogers et al. (2017).

426   Leaf photorespiration rate R_p was assumed to be a fixed fraction (40%) of leaf dark respiration rate (Atkin et al.,

427 2000). We used Atkin et al. (2015) 'broadleaved trees' empirical model to estimate mature leaf dark respiration rates as a

428 function of plant functional traits:

429     $R_{d-M}(25°C) = 8.5341 - 0.1306 \times N - 0.5670 \times P - 0.0137 \times LMA + 11.1 \times V_{cmax-M} + 0.1876 \times N \times P$ (32)

430   with R_{d-M} the leaf dark respiration rate on a dry mass basis and at reference temperature of 25°C (in nmol CO_2 g^{-1}s^{-1}).

431   Multiplying R_{d-M} by LMA gives the area-based leaf dark respiration R_d (in μmol C m^{-2} s^{-1}). The temperature dependence of

432   mature leaf dark respiration rates was calculated as (Atkin et al., 2015, Eq. (1) therein; see also Heskel et al. 2016):

433     $R_d(T_l) = R_d(25°C) \times \left[3.09 - 0.043 \times \frac{(T_l+25)}{2} \right]^{\frac{(T_l-25)}{10}}$ (33)

434   Long-term acclimation to temperature is not considered in TROLL 4.0 (Kattge and Knorr, 2007; Smith and Dukes, 2013).

435   **2.5.2 Stomatal conductance**

436   Carbon assimilation by photosynthesis is limited by the CO_2 partial pressure at carboxylation sites, which is controlled by

437   stomatal transport as modeled by the diffusion equation:

438     $A_n = g_s(c_s - c_i)$ (34)

439   with g_s the stomatal conductance to CO_2 (mol CO_2 m^{-2} s^{-1}). The representation of stomatal conductance varies greatly across

440   vegetation models (Damour et al., 2010; Bonan et al., 2014; Rogers et al., 2017; see Appendix B, Table B1) and remains an

441   active research topic (Anderegg et al., 2018; Dewar et al., 2018; Lamour et al., 2022; Sperry et al., 2017; Wolf et al., 2016;

442   Sabot et al., 2022). In TROLL 4.0, stomatal conductance to water vapor is simulated as (Medlyn et al., 2011):

443     $g_{sw} = g_0 + 1.6 \times \left(1 + \frac{g_1}{\sqrt{VPD_s}} \right) \times \frac{A_n}{c_s}$ (35)

444   where g_{sw} is the stomatal conductance to water vapor in mol H_2O m^{-2} s^{-1}, 1.6 is the factor needed to convert one mole of CO_2

445   into one mole of H_2O, VPD_s is the vapor pressure deficit at the leaf surface in kPa, A_n is the assimilation rate in μmol CO_2 m^{-}

446   ^{2} s^{-1} (Eq. (24) above), c_s is the CO_2 concentration at the leaf surface in ppm, g_0 is the minimum conductance for water vapor

447   in mol H_2O m^{-2} s^{-1} (Duursma et al., 2019), and g_1 is a model parameter in kPa$^{1/2}$. Equations 24, 34 and 35 taken together lead

448   to two quadratic equations for c_i, one when Rubisco activity is limiting and one when RuBP regeneration is limiting, and the

449   solution is the highest root.

450   The parameter g_1 varies with species ecological strategies and carbon cost of water use (Domingues et al., 2014;

451   Franks et al., 2018; Héroult et al., 2013; Lin et al., 2015; Wolz et al., 2017). Consequently, it is expected that g_1 should differ

452   across plant functional types (e.g. Xu et al., 2016). Here we assumed a dependence of g_1 with wood density (wsg, in g cm^{-3})

453   as in Lin et al. (2015). We also assumed a dependence with water availability, modelled by a function of ψ_{pd} (WSF_s; see

454   section 2.5.3):

455     $g_1 = (-3.97 \times wsg + 6.53) \times WSF_s(\psi_{pd})$ (36)

456   This parameterization of g_1 based on wood density is a matter of debate however, and alternatives have been proposed (Wu

457   et al., 2020; Lamour et al., 2023).

458   The parameter g_0 quantifies water fluxes through the leaf cuticle (cuticular conductance) and from stomatal leaks.

459   Although it is increasingly recognized as a key parameter explaining tree water loss in drought conditions (Cochard, 2021;

460   Martin-StPaul et al., 2017), its values and variation with other functional traits is poorly documented (Duursma et al., 2019;

461   Slot et al., 2021; Nemetschek et al., 2024), and we here assumed a fixed value. Note that some previous studies have defined

462   g_0 as cuticular conductance only, ignoring stomatal leak effects, and thus underestimating g_0.

463   Both g_0 and g_1 were assumed not to depend on temperature in the absence of clear empirical evidence for tropical

464   forest trees (Duursma et al., 2019; Slot et al., 2021; Rogers et al., 2017), but this may be further explored in the future through

465   measurement and experiment (Cochard, 2021).

2.5.3 Effect of water availability on leaf-level gas exchange

467   Under water stress, leaf-level gas exchanges and photosynthesis are impaired, but how this is represented varies greatly across

468   models (Appendix B, Table B1; Powell et al., 2013; Trugman et al., 2018; Verhoef and Egea, 2014). A common approach is

469   to define a single integrative water stress factor cumulating all effects along the soil-plant-atmosphere pathway, some of which

470   being difficult to evaluate empirically (e.g. Fischer et al., 2014; Gutiérrez et al., 2014; Krinner et al., 2005; Clark et al., 2011).

471   This factor is then used to modify the parameters of the stomatal conductance and/or photosynthesis models (Egea et al., 2011;

472   Verhoef and Egea, 2014). Depending on models, water stress factors have been assumed to depend on soil water content or on

473   soil water potential in the root zone (De Kauwe et al., 2015; Drake et al., 2017; Joetzjer et al., 2014; Powell et al., 2013;

474   Trugman et al., 2018). Alternatively, some models have implemented a water stress factor as a function of leaf water potential

475   (ψ_{leaf}; Christoffersen et al., 2016; Duursma and Medlyn, 2012; Kennedy et al., 2019; Xu et al., 2016; see also the pioneer

476   work of Tuzet et al., 2003) or used optimization approaches (Williams et al., 1996; Anderegg et al., 2018; Sabot et al., 2020;

477   Sperry et al., 2017; Wolf et al., 2016), to account for the cost of water uptake and transportation in the plant water column.

478   The shape of such functions remains contentious however (Table B1), resulting in substantial differences in model predictions.

479   Also, there is no consensus on the relative role of stomatal and non-stomatal limitations on leaf CO_2 assimilation

480   under drying conditions, reflecting contrasted experimental results (Drake et al., 2017; Zhou et al., 2014; Keenan et al., 2010;

481   Appendix B, Table B2). Under stomatal limitation, stomatal closure reduces leaf gas exchanges, and the water stress factor is

482   applied on stomatal conductance, or stomatal conductance model parameters (e.g. g_1). Under non-stomatal limitations, drought

483   (leading to increased leaf temperature and/or decreased leaf water potential) impairs the biochemical photosynthesis apparatus,

484   which results in a reduction of photosynthetic capacities, and/or mesophyll conductance (Flexas et al., 2004, 2012). In this

485   latter case, the water stress factor is applied on V_{cmax} and J_{max} (Drake et al., 2017; Keenan et al., 2010). Some models consider

486   only one limitation, and others both (Appendix B, Table B1).

487   In TROLL 4.0, two water stress factors are used, one for stomatal limitation, modifying the g_1 parameter (WSF_s; Eq.

488   (36)), and one for non-stomatal limitations, modifying the V_{cmax} and J_{max} parameters of the photosynthesis model (WSF_{ns}; Eq.

489   (28) and (29)). Both water stress factors are assumed to depend on the leaf predawn water potential (ψ_{pd}; De Kauwe et al.,

490   2015; Verhoef and Egea, 2014), which is a function of the soil water potential in the root zone (ψ_{root}, Eq. (21)) (Stahl et al.,

491   2013, but see Bucci et al., 2004; Donovan et al., 2003) as follows (Jones, 2013; Eq. (4.9) therein):

492 $\quad \psi_{pd} = \psi_{root} - \rho g h \simeq \psi_{root} - 0.01 \times h$ (37)

493 where ρ is the density of water, g the gravitational force (g=9.81 m s^{-2}), and h total tree height in m. Here, WSF_s was computed

494 as (Zhou et al., 2013; De Kauwe et al., 2015):

495 $\quad WSF_s = \exp(b \times \psi_{pd})$ (38)

496 where b is a parameter. To parameterize b, we used the relationship between the leaf water potential at turgor loss point (π_{tlp}

497 in MPa) and the water potential causing 90% of stomatal closure (ψ_{gs90}, in MPa): $\pi_{tlp} = 0.97 \times \psi_{gs90}$ (P<0.01, R^2=0.4; Fig.

498 1 in Martin-StPaul et al. 2017), and assumed that $WSF_s \approx 0.1$ at ψ_{gs90} (an approximation given the shape of Eq. (35)), leading

499 to:

500 $\quad WSF_s = \exp\left(-2.23 \times \frac{\psi_{pd}}{\pi_{tlp}}\right)$ (39)

501 The link between the leaf water potential at stomatal closure and the leaf water potential at turgor loss point is supported by

502 several studies (Bartlett et al., 2016b; Brodribb et al., 2003; Farrell et al., 2017; Martin-StPaul et al., 2017; Meinzer et al.,

503 2016; Rodriguez-Dominguez et al., 2016; Trueba et al., 2019). The formulation of WSF_s in Eq (39) was preferred over

504 alternatives, such as a linear relationship between WSF_s and ψ_{pd} (Oleson et al., 2008; Powell et al., 2013; Verhoef and Egea,

505 2014). The latter is less supported by data and leads to threshold responses as soil water content declines and similar responses

506 across species, in contrast with empirical evidence (Kursar et al., 2009; Zhou et al., 2013).

507 $\quad$ The water stress factor for non-stomatal limitation (WSF_{ns}) was computed following Xu et al. (2016):

508 $\quad WSF_{ns} = \left(1 + \left(\frac{\psi_{pd}}{\pi_{tlp}}\right)^a\right)^{-1}$ (40)

509 with a=6 estimated from data reported in Brodribb et al. (2003). In this formula, $WSF_{ns} = \frac{1}{2}$ when $\psi_{pd} = \pi_{tlp}$, in agreement

510 with empirical findings (Brodribb et al., 2002; Manzoni, 2014).

511 $\quad$ The parameterization of WSF_s and WSF_{ns} based on π_{tlp} is supported by the fact that leaf cells need to maintain turgor

512 to sustain functioning (Hsiao, 1973). These functions do not depend on π_{tlp} when $\psi_{pd} = \pi_{tlp}$, so there is a simple link between

513 the leaf drought tolerance, as informed by π_{tlp}, and the response of leaf-level gas exchange to water availability. Also, these

514 equations predict that the decline of stomatal conductance as water availability decreases precedes that of photochemistry,

515 consistent with observations (Fig. 2; Fatichi et al., 2016; Trueba et al., 2019).

516 $\quad$ Note that, since mesophyll conductance is not explicitly represented here, the effect of water stress on photosynthetic

517 capacities (WSF_{ns}) includes both direct effects on the photosynthetic machinery and indirect effects from the reduction of

518 mesophyll conductance (Drake et al., 2017; Keenan et al., 2010). Alternative shapes of water stress factors could be explored

519 in the future, and a more explicit representation of the water flow through the plant water column could be implemented

520 (Paschalis et al., 2024). In the absence of a clear consensus on the effect of water stress on respiration, TROLL 4.0 does not

521 assume that respiration depends on water availability (Flexas et al., 2006, 2005; Rowland et al., 2018, 2015; Santos et al.,

522 2018; Stahl et al., 2013b).

523

524
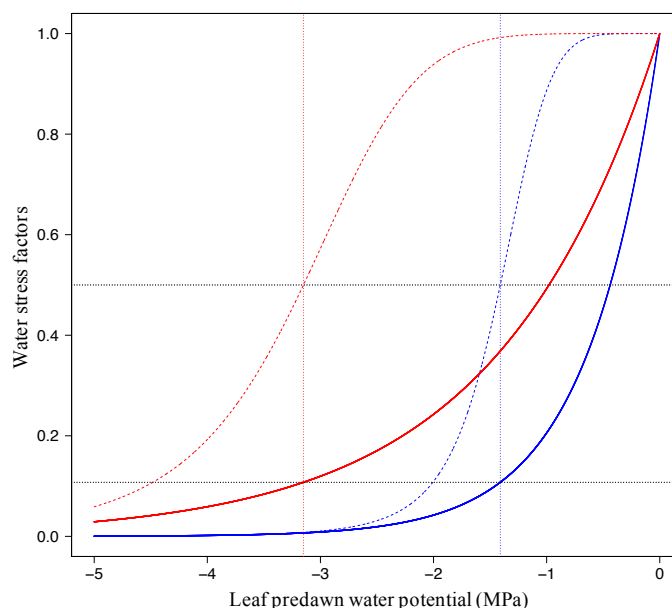
Figure 2: Responses of leaf-level gas exchange to water stress, depending on the leaf drought tolerance. Water stress factors for the stomatal conductance parameter g_1 (stomatal limitation, WSF$_s$, Eq. (39); solid lines) and for the photosynthetic capacities J$_{max}$ and V$_{cmax}$ (non-stomatal limitation, WSF$_{ns}$, Eq. (40); dashed lines) as a function of leaf predawn water potential (ψ_{pd}, in MPa). WSFs are shown for a a drought vulnerable species (π_{tlp}=-1.41 MPa, the least negative value reported in Maréchaux et al., 2015; blue lines), and for a drought tolerant species (π_{tlp}=-3.15 MPa, the most negative value reported in Maréchaux et al., 2015). Vertical dotted lines: π_{tlp}, horizontal dotted black lines: WSF$_s$ and WSF$_{ns}$ at π_{tlp}.

2.5.4 Leaf energy balance

In TROLL 4.0, leaf temperature (T_l), vapor pressure deficit (VPD$_s$) and CO$_2$ concentration (c_s) at the leaf surface are computed through an iterative scheme that solves the leaf energy balance (Medlyn et al., 2007; Wang and Leuning, 1998; Duursma, 2015; Vezy et al., 2018). This is an important step because the leaf boundary layer plays a key role on gas exchanges, and especially so in dense tropical moist forests, given the large size of tropical tree leaves and the low wind speeds within canopies (De Kauwe et al., 2017; Jarvis and McNaughton, 1986; Meinzer et al., 1997). The iterative scheme is as follows. Initially, T_l, VPD$_s$ and c_s are set equal to surrounding air values (T, VPD and c_a). Leaf photosynthesis (A_n) and stomatal conductance (g_{sw}) are computed using Eqs (24), (34) and (35); next, the boundary layer conductance and radiation conductance are computed; and finally leaf-level transpiration rate is deduced from the Penman-Monteith equation (Eq. (41) below). After these steps, new values for T_l, VPD$_s$ and c_s are computed, and the above steps are repeated until leaf temperature converges, i.e., when the absolute difference between the T_l of two consecutive iteration is lower than 0.01°C.

Leaf-level transpiration rate E_l (in mol H$_2$0 m^{-2} s^{-1}) is calculated as:

543 $E_l = \frac{1}{\lambda} \times \frac{sR_{ni} + VPD_a g_H C_p M_a}{s + \gamma \frac{g_H}{g_w}}$ (41)

544 where λ is the latent heat of water vapor (in J mol^{-1}), s is the slope of the (locally linearized) relationship between saturated

545 vapor pressure and temperature (in Pa K^{-1}, see Jones, 2013, Eq. (5.15) therein), R_{ni} is the isothermal net radiation (in J m^{-2} s$^-$

546 ^{1}), g_H is the total leaf conductance to heat (in mol m^{-2} s^{-1}), C_p is the heat capacity of air (1010 J kg^{-1} K^{-1}), M_a is the molecular

547 mass of air (28.96×10^{-3} kg mol^{-1}), γ the psychrometric constant (in Pa K^{-1}), and g_w the total conductance to water vapor

548 (mol H$_2$0 m^{-2} s^{-1}). The latent heat of water vapor λ depends on air temperature as follows:

549 $\lambda = (2.501 \times 10^3 - 2.365 \times T) \times 18$ (42)

550 The isothermal net radiation R_{ni} has two components, the absorbed solar radiation (S_{abs}), including both PAR and NIR

551 wavebands, and the net longwave radiation (Leuning et al., 1995; Appendix D therein):

552 $R_{ni} = S_{abs} - B_{n,0} \times k_d \exp(-k_d LAI)$ (43)

553 where $B_{n,0}$ is the net longwave radiation at the top of the canopy, and $k_d \exp(-k_d LAI)$ accounts for its extinction within the

554 canopy, with k_d set equal to 0.8. To account for the absorbed NIR radiation at a given height within the canopy in S_{abs}, we

555 used the relationship reported by Kume et al. (2011; Fig. 4 therein) that links the transmitted NIR to the transmitted and incident

556 PAR, and assumed a leaf absorptance in the NIR equal to 0.1. $B_{n,0}$ is then computed as the absorbed minus the emitted

557 longwave radiation:

558 $B_{n,0} = \varepsilon_l (1 - \varepsilon_a) \sigma T_{top}^4$ (44)

559 where T_{top} is the top canopy air temperature in K, σ is the Stefan-Boltzmann constant ($\sigma = 5.67 \times 10^{-8}$ W m^{-2} K^{-4}), ε_l is the

560 emissivity of the canopy leaves, here assumed to be 1, and ε_a the emissivity of the atmosphere. Several models exist for ε_a,

561 with varying performance depending on the sky conditions (Marthews et al., 2012). We here used Dilley and O'Brien (1998),

562 which compromises between parsimony and performance across sky conditions (Marthews et al., 2012; Tables 2 and 5 therein).

563   g_H, the total leaf conductance to heat, has three components, the boundary layer conductance for free convection g_{bHf},

564 the boundary layer for forced convection g_{bHu}, and the radiation conductance g_r (Leuning et al., 1995; Jones, 2013):

565 $g_H = 2 \times (g_{bHf} + g_{bHu} + g_r)$ (45)

566 where the factor 2 accounts for the two sides of the leaves. g_{bHf}, the boundary layer conductance for free convection, is given

567 by:

568 $g_{bHf} = 0.5 \times D_H \times \left(\frac{1.6 \times 10^8 \times |T_l - T|}{w_l} \right)^{0.25} \times \frac{P_{ress}}{RT}$ (46)

569 where D_H is the molecular diffusivity to heat ($D_H = 21.5 \times 10^{-6}$ m^2 s^{-1}), P$_{ress}$ the atmospheric pressure (in Pa), R the universal

570 gas constant (R=8.314 J mol^{-1} K^{-1}) and T the temperature of surrounding air in K. Leaf width w_l (in m) is estimated as the

571 square root of leaf area ($w_l = \sqrt{LA}$). g_{bHu}, the boundary layer for forced convection (in mol m^{-2} s^{-1}), is given by:

572 $g_{bHu} = 0.003 \times \sqrt{\frac{u}{w_l}} \times \frac{P_{ress}}{RT}$ (47)

573 where u is the wind speed in m s^{-1} (see Eq. (9)). g_r, the radiation conductance in mol m^{-2} s^{-1} varies with T_a as follows (Jones,

574 2013, p.101 therein):

575 $g_r = \frac{4 \times \varepsilon_l \sigma T^3}{C_p M_a}$ (48)

576 g_w the total conductance to water vapor has two components that represent hydraulic resistances in series: the stomatal

577 conductance (g_{sw}, in mol H$_2$0 m^{-2} s^{-1}, Eq. (35)) and the boundary layer conductance (g_{bw} in mol H$_2$0 m^{-2} s^{-1}) to water vapor:

578 $g_w = \frac{g_{bw} \times g_{sw}}{g_{bw} + g_{sw}}$ (49)

579 with $g_{bw} = 1.075 \times \left(g_{bHf} + g_{bHu} \right)$ (50)

580 where 1.075 accounts for the relative diffusivities of heat and water vapor in air. Equations (49) and (50) assume that all leaves

581 are hypostomatous (stomates on the ground-facing side of the leaves only), a reasonable assumption in tropical forests (Drake

582 et al., 2019; Muir, 2015).

583 **2.6 Carbon allocation**

584 **2.6.1. Net carbon uptake: whole-tree integration and respiration**

585 At each daily timestep, the individual tree net primary productivity of carbon, NPP_{ind} (in gC), is obtained by the following

586 balance equation (Fig. 3):

587 $NPP_{ind} = GPP_{ind} - R_{maintenance} - R_{growth}$ (51)

588 GPP_{ind} (in gC) is computed each half hour as the carbon assimilation rate A_n (Eq. (19)), multiplied by the leaf area in each

589 tree crown layer (LA_l, in m^2), then summed over tree crown layers and cumulated across the day.

590   Young leaves and old leaves have been reported to have lower photosynthetic capacities and activities than mature

591 leaves (Doughty and Goulden, 2008; Kitajima et al., 2002, 1997b; Wu et al., 2016; Albert et al., 2018; Menezes et al., 2021).

592 For each tree, total leaf area (LA$_t$) is partitioned into three leaf age pools: young, mature and old leaves, so that LA$_t$= LA$_{young}$

593 + LA$_{mature}$ + LA$_{old}$ (all in m^2). These three leaf age pools are assumed to be uniformly distributed within the tree crown. In

594 young and old leaves, net assimilation rate is a fraction $\varrho < 1$ of that of mature leaves, so that:

595 $GPP_{ind} = C_{GPP} \times \frac{(\varrho \times LA_{young} + LA_{mature} + \varrho \times LA_{old})}{LA_t} \sum_l \sum_t A_n(t, l) \times LA_l$ (52)

596 where the factor C_{GPP} is a conversion factor, t depicts the daytime half-hours and l the tree crown layers. Here we assume that

597 the carbon uptake efficiency ϱ relative to mature leaves is the same in young and old leaves and $\varrho = 0.5$, a value consistent

598 with observations.

599   TROLL 4.0 partitions autotrophic respiration into maintenance respiration and growth respiration, even if both come

600 from the same biochemical pathways (Amthor, 1984; Thornley and Cannell, 2000). Maintenance respiration (R$_{maintenance}$) has

601 seldom been documented for stem and roots and is inferred empirically (Cavaleri et al., 2008; Meir et al., 2001; Slot et al.,

602 2013; Weerasinghe et al., 2014). Nighttime leaf maintenance respiration is computed using Eqs (32) and (33), using the mean

603   nighttime temperature. As stomatal conductance and dark respiration vary less with leaf age than carbon assimilation rate
604   (Albert et al., 2018; Kitajima et al., 2002; Villar et al., 1995), we assumed that young and old leaves have respiration and
605   transpiration rate equal to $\varrho' = 0.75$ that of mature leaves, leading to lower water use efficiency than mature leaves. Tree-level
606   nighttime leaf respiration and daytime transpiration are computed as follows at each timestep:

607   $$X_{ind} = C_X \times \frac{(\varrho' \times LA_{young} + LA_{mature} + \varrho' \times LA_{old})}{LA_t} \sum_l (\sum_i X(i,l)) \times LA_l \qquad (53)$$

608   where X_{ind} is either the carbon respired by leaves during the night or the total water transpired by the tree, in gC or m^3
609   respectively, X being the leaf dark respiration (Eqs. (32) and (33)) or the leaf-level transpiration rate (Eq. (41)) respectively,
610   and C_X is a conversion factor.

611   Stem maintenance respiration (R_{stem}, in μmol C s^{-1}) was modeled assuming a constant respiration rate per volume of
612   sapwood (39.6 μmol m^{-3} s^{-1}, Ryan et al., 1994), so that:

613   $$R_{stem} = C_{sresp} \times 39.6 \times SA \times (h - cd) \qquad (54)$$

614   where SA is the tree sapwood area (in m^2) and C_{sresp} is a conversion factor. Stem respiration response to temperature was
615   modeled using a Q_{10} value of 2.0 (Meir and Grace, 2002; Ryan et al., 1994), and using mean daytime and nighttime
616   temperatures. Stahl et al. (2011) reported that R_{stem} varies among individual trees, even when controlling for sapwood volume.
617   However, in absence of a clear understanding of the drivers, Eq. (54) is a parsimonious choice. In TROLL 4.0, sapwood area
618   is computed dynamically. We used an inversion of the pipe model to derive sapwood area from the tree's leaf area (LA$_t$, in
619   m^2), height (h, in m) and wood density following Fyllas et al. (2014; Eqs (7) and (8) therein):

620   $$SA = C_{SA} \frac{2 \times LA_t}{\lambda_1 + \lambda_2 \times h + \delta_1 + \delta_2 \times wsg} \qquad (55)$$

621   with λ_1= 0.066 m^2 cm^{-2}, λ_2=0.017 m cm^{-2}, δ_1=-0.018 m^2 cm^{-2}, and δ_2 =1.6 cm^3 g^{-1}, and C$_{SA}$ a conversion factor. In addition
622   to Eq. (55), there are both lower and upper limits on sapwood extent. Sapwood has a minimum thickness of 0.5 cm and any
623   newly grown wood is always considered sapwood, irrespective of leaf area. TROLL 4.0 also imposes an upper limit on
624   sapwood growth based on stem diameter growth, so that increases in living tissue cannot exceed increases in total tissue.

625   Other contributions of maintenance respiration were prescribed as proportions of leaf and stem maintenance
626   respiration. Fine root maintenance respiration was assumed to be half of leaf maintenance respiration (Malhi, 2012), and coarse
627   root and branch maintenance respirations were assumed to account for half of stem respiration (Asao et al., 2015; Cavaleri et
628   al., 2006; Meir and Grace, 2002).

629   Growth respiration (R$_{growth}$) was assumed to account for 30% of the carbon uptake by photosynthesis (gross primary
630   productivity) minus the maintenance respiration (Cannell and Thornley, 2000). These assumptions are commonly made in the
631   literature, but remain a major source of uncertainty in the carbon flux modeling (Atkin et al., 2014; Huntingford et al., 2013).

632   Contrary to the last published version of TROLL, in which the allocation of NPP$_{ind}$ to plant organs was fully prescribed
633   by fixed factors (f$_{canopy}$= f$_{leaves}$ + f$_{fruit}$ + f$_{twigs}$ and f$_{wood}$, Maréchaux and Chave, 2017), the allocation scheme implemented in
634   TROLL 4.0 can now be additionally modulated depending on the current tree state and it includes an explicit carbon storage
635   compartment (sections 2.6.2 and 2.6.3; Fig. 3).

636

637
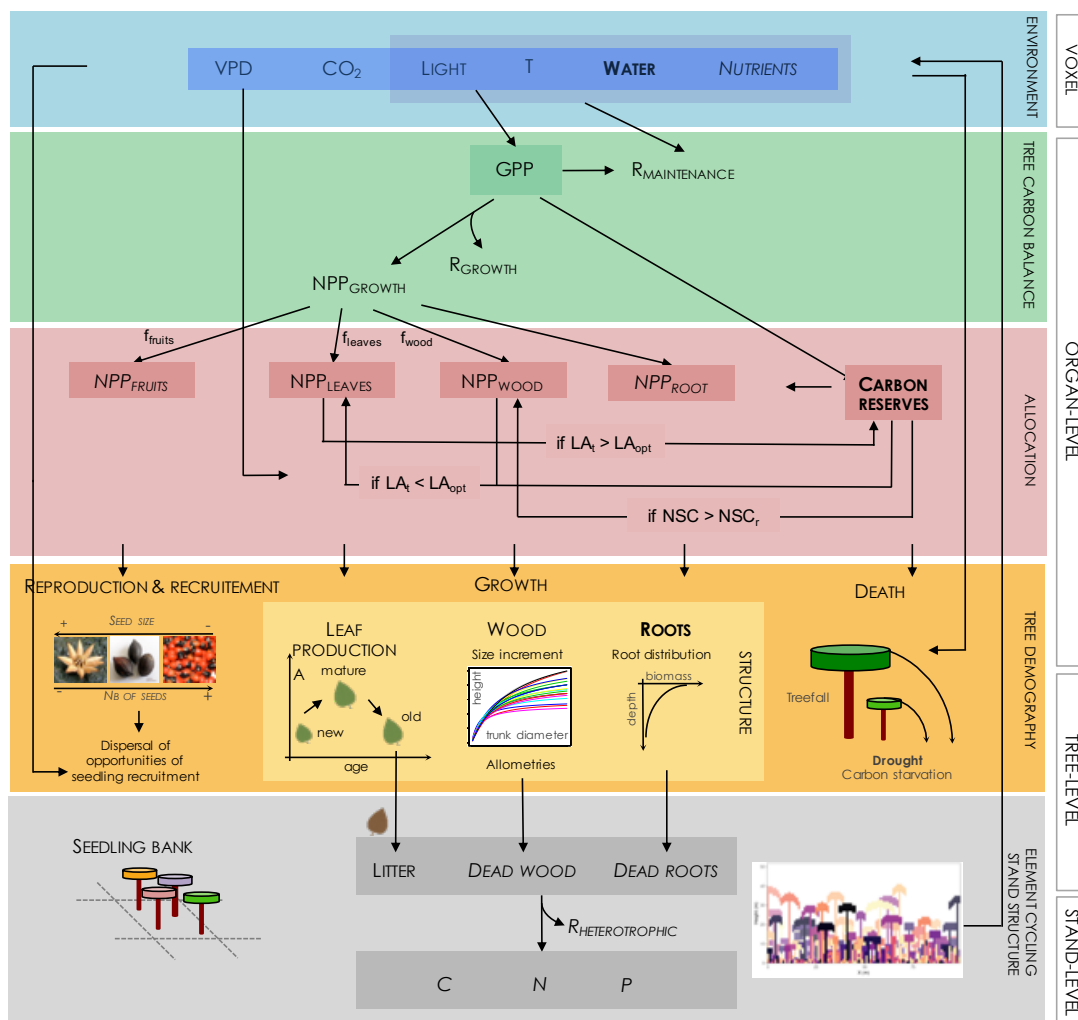
Figure 3: Diagram of structures and processes driving individual and community dynamics, as investigated under the modeling
approach adopted in TROLL 4.0. Elements in bold letters refer to novel implementation in comparison to the previous published
version, while italic letters refer to elements still not included in this present version. Abiotic environment is modeled at the voxel
scale and drive C assimilation in the leaves (gross primary productivity, GPP) and maintenance respiration rates of the different
plant organs (R$_{MAINTENANCE}$). The C amount resulting from the balance between GPP and R$_{MAINTENANCE}$ can be used for tissue
production (NPP$_{FRUITS}$, NPP$_{LEAVES}$, NPP$_{WOOD}$ and NPP$_{ROOTS}$) or stored (CARBON RESERVES) in the different tree organs. Both
allocations induce metabolic costs (R$_{GROWTH}$ and R$_{STORAGE}$; but the latter is not represented nor included). CARBON RESERVES
represents non-structural carbohydrates (NSC), mainly stored as sugar or starch, and its maximal storage capacity is given by NSC$_r$.
Allocation to these different compartments follows a hierarchical scheme initialized by default proportions (f$_{fruits}$, f$_{leaves}$, f$_{wood}$). If the
tree leaf area (LA$_t$) exceeds the optimal leaf area (LA$_{opt}$, a function of both tree properties and its micro-environment), then the
surplus of NPP$_{LEAVES}$ is allocated to carbon reserves. If the tree leaf area is lower than optimal, then NPP$_{WOOD}$, and if further needed,
carbon reserves, are mobilized for leaf production. If carbon reserves surpass storage capacity (NSC$_r$), then stored carbohydrates
are used for woody growth. C allocated to tissue production leads to an increment of trunk diameter and height following allometric
relationhips, and the production of new young leaves and roots. Simultaneously with tissue turnover, this leads to the update of leaf
density and root biomass distribution, influencing both abiotic environment (eg. light diffusion and water interception) and light
and element acquisition, and thus carbon assimilation and metabolism. C allocated to reproduction leads to the production of seeds,
which are dispersed randomly. This generates a spatially-explicit seedling bank, from which winners are locally recruited depending

660 **2.6.2 Leaf production and leaf shedding**

661 Leaf phenology is a key driver of the variation of tropical forest productivity (Manoli et al., 2018; Restrepo-Coupe et al., 2013;

662 Wu et al., 2017). However, its underlying drivers remain poorly understood, and its representation in vegetation models

663 remains challenging (Chen et al., 2020; Restrepo-Coupe et al., 2017). In ORCHIDEE, Chen et al. (2020, 2021) proposed a leaf

664 phenological scheme in which the production of young leaves is partly controlled by incident shortwave radiation, while the

665 shedding of old leaves is controlled by vapor pressure deficit. This scheme reproduces the simultaneous increase in leaf

666 production and litterfall observed in many Amazonian rainforest sites where productivity increases during the dry season

667 (Chave et al., 2010; Wagner et al., 2016; Yang et al., 2021), but not the observed seasonality in productivity at some sites (e.g.

668 GUYAFLUX eddy-flux site in French Guiana, Chen et al., 2020). Additionally, this scheme overlooks the contrasted leaf

669 phenological patterns observed across canopy individuals within and across species within communities (Nicolini et al., 2012;

670 Loubry, 1994). In ED2, Xu et al. (2016) implemented a leaf phenological scheme driven by water availability in the root zone

671 in a seasonally dry tropical forest. Since leaf shedding is often triggered by drought-induced loss of leaf turgor in these systems

672 (Sobrado, 1986), leaf shedding and production are assumed to depend on the difference between leaf predawn water potential

673 and leaf water potential at turgor loss point. However, such a scheme cannot simulate the simultaneous leaf production and

674 shedding observed in moist tropical forests.

675   In TROLL 4.0, we propose an alternative approach. At each timestep, the optimal tree total leaf area (LA$_{opt}$) is

676 estimated as the leaf area beyond which producing more leaves leads to a net carbon loss due to self-shading and respiration

677 costs. LA$_{opt}$ depends on tree crown size and leaf area density (section 2.4.2), leaf photosynthetic capacities and respiration rate

678 (section 2.5.1), and local light environment. At each timestep, the amount of carbon allocated to the production of new young

679 leaves, NPP_{leaves}, and to woody growth, NPP_{wood}, are determined by default as: $NPP_{leaves} = f_{leaves} \times NPP_{ind}$, with

680 $f_{leaves} = 0.68 \times f_{canopy}$ (Chave et al., 2008, 2010; Maréchaux and Chave, 2017), and $NPP_{wood} = 0.6 \times f_{wood} \times NPP_{ind}$,

681 where the factor 0.6 accounts for the fact that about 40% of woody NPP is actually used for branch fall repair (Malhi et al.,

682 2011). When leaf area LA$_t$ exceeds LA$_{opt}$, NPP_{leaves} is reduced so that LA$_t$= LA$_{opt}$. Second, if the carbon allocated to leaf

683 production is not sufficient to compensate leaf loss, then the carbon attributed by default to tree woody growth is mobilized

684 for leaf production until leaf loss is compensated. If not sufficient, the tree carbon storage (see section 2.6.3) is then also

685 mobilized. Hence this scheme prioritizes the maintenance of the assimilating tissues over woody growth (Schippers et al.,

686 2015). The variation of leaf area for each leaf age pool is then computed as follows:

687 $\Delta LA_{young} = \frac{2 \times NPP_{leaves}}{LMA} - \frac{LA_{young}}{\tau_{young}}$

688    $\Delta LA_{mature} = \frac{LA_{young}}{\tau_{young}} - \frac{LA_{mature}}{\tau_{mature}}$

689    $\Delta LA_{old} = \frac{LA_{mature}}{\tau_{mature}} - \frac{LA_{old}}{\tau_{old}}$ (56)

690   where τ_{young}, τ_{mature}, τ_{old} are the residence times in each class (in yr), so that LL= τ_{young}+τ_{mature}+τ_{old} with LL the maximal tree

691   leaf lifespan (in yr). LL is inferred from the tree LMA, using the following empirical relationships (Schmitt, 2017):

692    $LL = \frac{1}{12} \max(3, 12.755 \times \exp(0.007 \times LMA - 0.565 \times N))$ (57)

693   τ_{young} was fixed to min(LL/3, 1/12) yr (Doughty and Goulden, 2008; Wu et al., 2016), and τ_{mature} as a third of total leaf lifespan.

694   The loss term LA_{old}/τ_{old} corresponds to the rate of leaf litterfall at each timestep. In the previous TROLL version,

695   litterfall resulted from the dynamics of leaf biomass with τ_{old}= LL - τ_{young}- τ_{mature}. This leaf shedding scheme is passive and

696   does not simulate the observed seasonality in leaf litterfall. Here we propose a new approach to simulate leaf shedding. We

697   first observed that within species and sites, canopy trees can shed their leaves at different times, suggesting that causal

698   environmental drivers should display fine-scale heterogeneity in space (unlike atmospheric shortwave radiation and vapor

699   pressure deficit). In addition, old leaves display nutrient resorption before abscission (Albert et al., 2018; Kitajima et al., 1997a;

700   Urbina et al., 2021); similarly, solute translocation from older to younger leaves can lower osmotic potential and leaf water

701   potential at turgor loss point, thus increasing the drought tolerance of younger leaves to the detriment of older leaves (Pantin

702   et al., 2012). We therefore used predawn leaf water potential as a trigger of leaf shedding as in Xu et al., (2016), but with

703   different thresholds for leaves of different ages, older leaves being more susceptible to a small decrease in tree water

704   availability, while younger leaves can maintain turgor and grow at the same time. More specifically, we defined the following

705   threshold:

706    $\psi_{T,o} = \min(a_{T,o} \times \pi_{tlp}, -0.01 \times h - b_{T,o})$ (58)

707   The first term in $\psi_{T,o}$ with $a_{T,o} < 1$ represents old leaves' lower ability to maintain turgor as soil dries. The second term

708   modulates this susceptibility to drought depending on tree height (Bennett et al., 2015): it induces a susceptibility to a (small)

709   decrease $b_{T,o} > 0$ in soil water availability for large trees, while preventing them from constantly shedding their old leaves at

710   fast pace (see Eq. (37)). τ_{old} is then updated using a multiplying factor f_o (0.001 $\leq f_o \leq$ 1). Initially, $\tau'_{old} = f_o \tau_{old}$ with $f_o =$

711   1 , which is updated daily as follows: $f'_o = f_o - \delta_o$ when $\psi_{pd} < \psi_{T,o}$ and $f'_o = f_o + \delta_o$ when $\psi_{pd} > \psi_{T,o}$, always assuming that

712   f_o has 0.001 as a lower bound, and 1 as an upper bound.

713   We assumed no variation of π_{tlp} with tree height (Maréchaux et al., 2016). The threshold $\psi_{T,o}$ jointly depends on

714   π_{tlp} and tree height h to account for drought tolerance and tree height on leaf-level water stress. Practically, the tree height

715   above which old leaves becomes susceptible to a small decrease in soil water availability is $H_{T,o} = -100 \times (a_{T,o}\pi_{tlp} + b_{T,o})$

716   in m: 28 m at π_{tlp}=-1.5 MPa and 58m at π_{tlp}=-3 MPa (when $a_{T,o}$= 0.2 and $b_{T,o}$ = 0.02). While this scheme is based on

717   process-based observations, parameters $a_{T,o}$, $b_{T,o}$, and δ_o are currently calibrated (see Schmitt et al., submitted companion

718   paper).

2.6.3 Carbon storage

719

720 In TROLL 4.0, trees can store carbon explicitly in non-structural carbohydrates. The maximal amount of carbon a tree can

721 store and remobilize is determined as follows:

722 $$NSC_r = 1000 \times 0.5 \times 0.05 \times 1.25 \times AGB \tag{59}$$

723 where NSC_r stands for non-structural carbohydrates (in gC), AGB is the tree aboveground biomass (in kg), and 1000×0.5

724 converts biomass in kg into C in g (Elias and Potvin, 2003). It is assumed that NSC can account for 10% of the tree biomass,

725 half of which is mobilizable (Martínez-Vilalta et al., 2016), hence the factor 0.05. The other half of NSC supports critical

726 metabolic functions or is no longer accessible. The factor 1.25 accounts for an additional 25% biomass storage in coarse roots,

727 so $1.25 \times AGB$ is total tree biomass (Ledo et al., 2018). AGB is computed following (Chave et al., 2014; Eq. (5) therein):

728 $$AGB = 0.0559 \times wsg \times dbh^2 \times h \tag{60}$$

729 where dbh is in cm, h in m and wsg in g cm^{-3}. The NSC storage compartment is filled by the potential carbon surplus resulting

730 from the allocation to leaf production, i.e. $f_{leaves} \times NPP_{ind} - NPP_{leaves}$, if positive. If the storage compartment has reached

731 its maximal capacity NSC_r, then the surplus is allocated to woody growth.

2.6.4 Growth

732

733 The net primary production allocated to woody growth, NPP_{wood}, depends on the outcome of allocation to leaf

734 production and carbon reserves (see sections 2.6.2 and 2.6.3; Fig. 3). In TROLL 4.0, hydraulic control on carbon assimilation

735 and leaf phenology both influence carbon allocation to trunk growth (e.g. Doughty et al., 2014; Farrior et al., 2013;

736 Friedlingstein et al., 1999), but turgor-mediated processes are not explicitly modeled (Coussement et al., 2018; Peters et al.,

737 2023; Muller et al., 2011; Körner, 2015). NPP_{wood} is converted into an increment of stem volume, ΔV in m^3, as follows:

738 $$\Delta V = 10^{-6} \times \frac{NPP_{wood}}{0.5 \times wsg} \times Senesc(dbh) \tag{61}$$

739 where the factor 0.5 converts dry biomass units into carbon units (Elias and Potvin, 2003). The function $Senesc(dbh)$ is

740 designed so that the largest trees cannot allocate carbon as efficiently into growth, reflecting empirical evidence of a size-

741 related relative growth decline in trees (Yoda et al., 1965; Ryan et al., 1997; Mencuccini et al., 2005; Woodruff and Meinzer,

742 2011; Stephenson et al., 2014). We assumed that trees cannot exceed a trunk diameter of $dbh_{max} = \frac{3}{2} dbh_{thresh}$, where

743 dbh_{thresh} depends on species-specific information provided by the user (see section 2.4.1), so that:

744 $$\begin{aligned} Senesc(dbh) &= 1 & when\ dbh \leq dbh_{thresh} \\ Senesc(dbh) &= \max\left(0;\ 3 - 2\frac{dbh}{dbh_{thresh}}\right) & when\ dbh > dbh_{thresh} \end{aligned} \tag{62}$$

745 Trunk diameter growth increment Δdbh (in m), is computed from ΔV as follows. $V = C\ \pi(\frac{dbh}{2})^2 h$, where C is a form

746 factor (Chave et al. 2014, Eq. (5) therein). The term h (in m) is total tree height inferred from the dbh following Eq. (16), this

747 leads to an expression of V as a function of dbh only. This function can be inverted to estimate Δdbh as a function of ΔV,

748 which is known from Eq. (61). Tree height and crown dimensions are then updated using Eqs (16), (17) and (18).

2.7 Tree demography

2.7.1 Seed production, dispersal and recruitment

The starting point for a tree life cycle, as represented in TROLL 4.0 is an event of seed dispersal into the seed bank. On each 1x1 m ground site and for each species s, a 'seed' bank stores all the seeds dispersed from the mature trees as well as from an external seed rain. The seed bank is updated once a year. Here, our conceptual 'seeds' represent opportunities of seedling recruitment rather than as true seeds, since not all seed dispersal events are modeled explicitly, and the seed-to-seedling transition is implicit.

In TROLL 4.0 trees are assumed to become fertile above a diameter threshold dbh_{mature} that depends on the tree maximal size (Visser et al., 2016) as follows:

$$dbh_{mature} = 0.5 \times dbh_{thresh} \tag{63}$$

This relationship is drawn from direct observations of reproductive status of tree species in the tropical forest of Barro Colorado Island, Panama, with maximal tree dbh spanning a range of 0.05 to 2 m (see Fig. S9 in Visser et al., 2016; R^2=0.81, n= 60 species). The number of reproduction opportunities per mature tree, n_s, is assumed fixed and equal for all individuals, and its value is user-defined. This assumption of a fixed reproductive opportunity per tree is predicated on the fact that there is a trade-off between seed number and seed size, itself related to seed and seedling survival. Thus, the probability of germination does not depend strongly on seed size or on the number of produced seeds and can be assumed a zero-sum game (Coomes and Grubb, 2003; Moles et al., 2004; Moles and Westoby, 2006). Each of the n_s events is scattered away from the tree in a random direction and at a distance randomly drawn from a Rayleigh distribution, thus allowing for potential long-dispersal events. Although seed dispersal distance is known to vary depending on dispersal syndrome and plant traits (Tamme et al., 2014; Seidler and Plotkin, 2006; Muller-Landau et al., 2008), the scale parameter σ_{disp} of the distribution is here fixed across species and individuals.

The intensity of the external seed rain is quantified by N_{tot} (in number of incoming seeds per hectare) and its species composition is defined by the relative abundances of species $f_{reg,s}$, both being user-defined. Hence, for each species s, $n_{ext,s}$ events of dispersal due to seeds immigrating from the outside occurred, with:

$$n_{ext,s} = N_{tot} \times f_{reg,s} \times n_{ha} \tag{64}$$

with n_{ha} the number of hectares of the simulated plot. These reproduction opportunities are uniformly distributed within the simulated area.

If several species are competing for recruitment in a local seed bank, one of the species is picked at random as the winner out of all the seeds present, as in a lottery model (Chesson and Warner, 1981). The recruitment event occurs only if ground-level light availability is sufficiently high. To test if this condition is met, the seedling is first attributed individual trait values depending on the species-specific averages (see section 2.4.1). These traits values are then used to determine the maximum LAI (LAI_{max}) the seedling would support under average environmental conditions, with LAI_{max} defined as the

781   threshold beyond which the seedling leaf assimilation would be less than respiration (see section 2.6.2). The seedling can be
782   recruited if the site LAI at ground level is lower than LAI$_{max}$.

783   Water availability is also key to seedling performance (Engelbrecht et al., 2006; Johnson et al., 2017; Kupers et al.,
784   2019), hence TROLL 4.0 now implements an additional water-dependent dependence on seedling establishment (Craine et al.,
785   2012; Paine et al., 2018). Seedling recruitment is possible only if top-layer soil water potential is less negative than half the
786   turgor loss point ($\pi_{tlp}/2$). Such parameterization is motivated by the fact that, at turgor loss point, the seedlings would not
787   germinate, and a certain level of turgor is needed for germination and growth (Bradford, 1990; Daws et al., 2008; Coussement
788   et al., 2018; Hsiao, 1973; Fatichi et al., 2016).

789   If both conditions on light and water availability are met, the newly recruited tree is initialized with a dbh=0.01m, a
790   total leaf area $LA_t = 0.25 \times LA_{opt}$ distributed across the three leaf age pools in proportion to their relative span (τ_{young}/LL,
791   τ_{mature}/LL, τ_{old}/LL; see section 2.6.2), and a carbon storage compartment filled at half its maximum NSC$_r$ (see section 2.6.3).

792   The assumptions here made on tree reproduction largely reflect limited knowledge on these processes, which remains
793   major sources of uncertainty in current models (König et al., 2022; Hanbury-Brown et al., 2022; Díaz-Yáñez et al., 2024).

794   **2.7.2 Mortality**

795   Mortality processes also play a key role in forest structure and carbon balance (Sevanto et al., 2014; Friend et al., 2014; Johnson
796   et al., 2016; Esquivel-Muelbert et al., 2020; McDowell et al., 2022). TROLL 4.0 explicitly represents several important
797   mechanisms of tree mortality. At each timestep, individual tree death rate (in events yr^{-1}; Sheil et al. 1995) is:

798    $d = d_b + d_{starv} + d_{treefall} + d_{drought}$ (65)

799   where d_b is a background death rate, d_{starv} represents death due to carbohydrate shortage (carbon starvation), $d_{treefall}$
800   represents death due to treefall (including trees indirectly killed by neighboring fallen trees), and $d_{drought}$ the drought-induced
801   tree mortality.

802   Background mortality d_b encapsulates death events that are not attributed to any specific mechanism in the model.
803   Mortality rate is known to vary greatly among species, and we here assume that it is negatively correlated with tree wood
804   density, as observed pan-tropically (King et al., 2006; Kraft et al., 2010; Poorter et al., 2008; Wright et al., 2010). This
805   dependence illustrates a trade-off between investment into construction costs and risk of mortality (Chave et al., 2009). We
806   assumed the following relationship:

807    $d_b = m \times \left(1 - \frac{wsg}{wsg_{lim}}\right)$ (66)

808   where m (in events yr^{-1}) is the reference background mortality rate for a species with low wood density and is user-specified.
809   wsg_{lim} is a value large enough so that d_b always remains positive (here set at 1 g cm^{-3}).

810   A tree can also die because of carbohydrate shortage in case of prolonged stress (d_{starv} in Eq. (65)). In TROLL 4.0

811   that includes an explicit carbohydrate storage compartment, the tree dies of carbon starvation when this compartment is empty

812   and $NPP_{ind} \leq 0$ (Eq. (51)).

813   Tree death may be caused by treefalls (term $d_{treefall}$ in Eq. (65)). To simulate this process, we first define a stochastic

814   threshold Θ, depending on the tree maximal height, and prescribed at tree birth. Then, the tree can fall with a probability equal

815   to $1 - \frac{\Theta}{h}$ (Chave, 1999) each month. As TROLL 4.0 uses a daily timestep, this probability is uniformly distributed across the

816   days of one month. The parameter Θ is computed for each tree, as follows:

817   $\Theta = h_{max} \times (1 - v_T \times |\zeta|)$ (67)

818   where h_{max} is maximal tree height (i.e. the tree height computed using Eq. (16) at dbh_{max}), v_T is a variance term, $|\zeta|$ is the

819   absolute value of a random Gaussian variable with zero mean and unit standard deviation. v_T is modified at tree level so that

820   high risks of treefall (> 99.5th percentile of the Gaussian variable) occur at the same height for all individuals of the same

821   species. This implicitly introduces a growth-mortality trade-off, as more slender trees (larger ratio of height to trunk diameter)

822   should reach this height threshold quicker. The orientation of tree falls is random. Trees on the trajectory of the falling tree can

823   be damaged, especially if they are smaller than the fallen tree (van der Meer and Bongers, 1996). To model this effect, an

824   individual variable *hurt* is defined. If a tree is within the trajectory of the fallen stem or of the fallen crown, its variable *hurt* is

825   updated to h and $\frac{h-CR}{2}$, respectively, if it was lower, where h and CR are the tree height and crown radius of the fallen tree,

826   respectively. The probability to die due to another treefall is then $1 - \frac{1}{2}\frac{h}{hurt \times e^{\varepsilon_{h,j}}}$, where h is the height of the focal tree and

827   $e^{\varepsilon_{h,j}}$ (see Eq. (16)) accounts for the fact that slender individuals (higher tree height deviation) would be more vulnerable to

828   treefall. Such tree can either fall and itself damage other trees or dies standing, depending on the user choice. The *hurt* variable

829   is reset to zero at each timestep.

830   Finally, prolonged drought is also a source of mortality. Drought-induced mortality is triggered when the leaf predawn

831   water potential ψ_{pd} is below a lethal level (ψ_{lethal}), and ψ_{lethal} is computed from the leaf water potential at turgor loss point,

832   using the relationship provided by the global meta-analysis of Bartlett et al. (2016; P=0.03, R²=0.31, n=15 species from tropical

833   dry and moist biomes), as follows:

834   $\psi_{lethal} = -0.9842 + 3.1795 \times \pi_{tlp}$ (68)

835   **3 Modelling protocol**

836   **3.1 Model inputs**

837   TROLL 4.0 requires five input files to run a simulation: (i) global parameters, (ii) species parameters, (iii) soil characteristics,

838   and finally, meteorological drivers varying at (iv) half-hour and (v) daily step.

839   The global input file contains parameters that define the simulation set-up (e.g. the number of timesteps, size of the
840   simulated plot and of the belowground voxels), and values for biophysical parameters that remain constant throughout the
841   simulation and are not species- or tree-specific. These include the light attenuation coefficient, allocation parameters, minimal
842   death rate, and more (see Table A1). Parameter values can be varied across simulations, to test model sensitivity, transfer
843   across sites, or any other reason. The species input file contains mean functional traits for at least one species and with no
844   upper bound (see Table A1). Functional trait values can be prescribed from local field measurements, or retrieved from global
845   trait databases (e.g. Kattge et al., 2020; Díaz et al., 2022).

846   The soil input file contains the soil variables needed for the pedotransfer functions, i.e. soil texture (proportion of silt,
847   clay and sand), soil organic matter content, dry bulk density, soil pH, and cation exchange capacity, for each soil layer, with
848   thickness of each layer. The number of soil layers is at least one, and is not theoretically limited. Lacking local soil data, model
849   users may retrieve soil parameters from online databases (e.g. Poggio et al., 2021), bearing in mind the uncertainties of such
850   products, especially in tropical areas (Khan et al., 2024).

851   Meteorological drivers are provided in two files, depending on their temporal resolution in the model. Daytime
852   temperature, vapor pressure deficit, incident irradiance and wind speed at a reference height above the canopy are provided
853   for every half-hour, while average nighttime temperature and cumulative rainfall are provided at a daily timestep. Such data
854   can typically be retrieved from meteorological stations embedded in eddy-flux towers, or from global products (Muñoz-Sabater
855   et al., 2021), as in Schmitt et al. (2023).

3.2 Initial conditions

857   Two types of initial conditions are useful in most practical settings, and are implemented in TROLL 4.0. First, the user can
858   simulate forest regeneration from bare ground. In this case, forest succession is initiated by the external seed rain, the
859   composition and intensity of which are user-defined (see above). The steady-state forest composition and structure are thus
860   emergent properties of the community assembly mechanisms embedded in the model, and the user-specified seed rain. The
861   second option is to prescribe an initial forest state. This requires that an initial forest state be provided as an additional input
862   file. The code is designed to adapt to the level of information provided by the inventory file, from a minimal requirement of
863   tree *dbh* to the full list of individual variables for each tree. For individual variables missing in the input file, these are either
864   computed from the model relationships or drawn at random. This second initial condition matches a real site forest state given
865   the available data, but will require careful calibration to maintain the forest state over a longer time period (e.g. Fischer et al.,
866   2019). A more common use case is to restart new simulations from an output of a previous simulation, e.g., to perform virtual
867   experiments controlling the initial state.

3.3 Standard outputs

869   TROLL 4.0 provides a range of outputs related to forest structure, forest composition and diversity, and ecosystem functioning
870   (e.g., carbon and water fluxes; Fig. 4). It simulates forest structure and composition and provides outputs comparable to those

871   measured in the field: tree size distribution, tree spatial distribution, biomass accumulation curve, functional trait distribution,

872   canopy height and leaf area index maps (Maréchaux and Chave, 2017), and more generally all information that can be retrieved

873   from a detailed field inventory or a meter-scale airborne laser scanning survey (Fischer et al., 2019). In TROLL 4.0, other

874   outputs are also available: litterfall fluxes, carbon and water fluxes comparable to the one provided by eddy-flux towers, soil

875   water state (content and water potential). An evaluation of these outputs for two Amazonian forest sites is provided in a

876   companion paper (Schmitt et al., submitted companion paper).

877
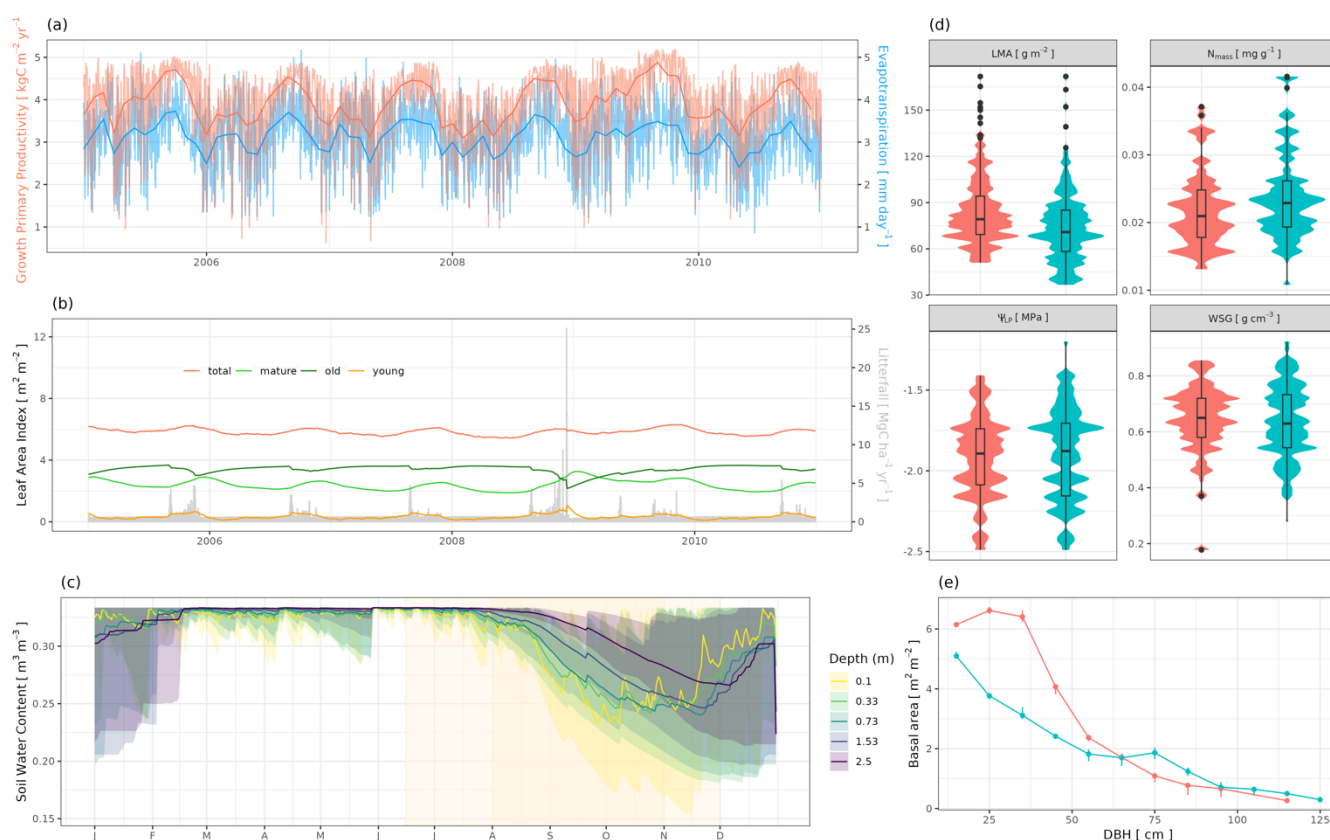
879   **Figure 4: Examples of outputs provided by TROLL 4.0 and related to ecosystem functioning, diversity and structure. (a) Temporal**

880   **variations of gross primary productivity (red) and evapotranspiration (blue) within and across years. (b) Variation in total leaf area**

881   **index (red line) and leaf area index per leaf age cohort (young, mature, old; yellow, light green and dark green lines, respectively),**

882   **together with litterfall (grey bars), within and across years. (c) Mean seasonal variations of water content in soil layers of different**

883   **depths, with the vertical yellow band in the background depicting the dry season. (d) Distribution of functional traits. (e)**

884   **Distributions of basal area per diameter class. Panels (a), (b) and (c) show outputs for an Amazonian forest site (Paracou), panels**

885   **(d) and (e) show outputs for two Amazonian sites (Paracou, red; Tapajos, blue), see Schmitt et al., submitted companion paper. for**

886   **details on similation set-ups.**

4 Discussion

TROLL 4.0 is a novel generation of forest growth models designed to bridge the gap between traditional forest growth models and process-based models informed by ecophysiology. It includes an integration of processes underlying ecosystem fluxes closer to a modern DGVM than most other forest growth simulators. It also includes representation of plant community structure and diversity at a resolution similar to that used by ecologists in the field. This enables a direct comparison with a range of field data, including forest inventories, trait distribution, fine- and large-scale remote-sensing products, or eddy-covariance data. Here we discuss the assumptions of the water cycle newly included in the model, as well as transferability and limitations of the current model version.

4.1 Simulating water fluxes and forest responses to water availability

Previous versions of TROLL assume that water availability does not limit ecosystem fluxes and dynamics, a strong but reasonable assumption in a light-limited forest like in Eastern Amazonia (Guan et al., 2015; Wagner et al., 2016; Maréchaux and Chave, 2017). However, such a simplification does not allow to account for drought-induced inter-annual variability in forest dynamics (Bonal et al., 2008; Aguilos et al., 2018; Leitold et al., 2018) or to transfer the model to sites where water availability is limiting. As droughts will be important drivers for tropical ecosystems in the future (Duffy et al., 2015), such a simplification does not allow to project future states of forest under climate change.

In TROLL 4.0, we implemented a full water cycle. We introduced a belowground field with a hydraulic state coupled to the vegetation, and a representation of the response of leaf gas exchanges to local atmospheric conditions and their control by the leaf boundary layer. This detailed representation is commonplace DGVMs (Prentice et al., 2007) but to our knowledge, it is new for an individual-based spatially explicit forest dynamic simulator. This paves the way for explorations and projections of the independent effects of soil water availability and atmospheric demand on ecosystem functioning (Novick et al., 2016; Santos et al., 2018), community composition and structure (Esquivel-Muelbert et al., 2019; Fauset et al., 2012; Slik, 2004; Feeley et al., 2011).

These developments have striven to follow the parsimonious principle: more complex representations do not systematically result in increased model reliability and robustness, especially if the additional parameters are poorly constrained (Mahnken et al., 2022; Prentice et al., 2015). The soil hydraulic state is simulated using a bucket model (Budyko, 1961; Manabe1969; Vargas Godoy et al., 2021). In the future, more complex representations of soil water dynamics could be implemented at finer temporal and spatial resolutions, such as the implementation of Richards' equation (Richards, 1931), and integration of lateral flows, but this would be at a serious computational cost. These could be compared with the current simpler representation to assess the relevance of increasing complexity in various contexts and soil data availability (Van Nes and Scheffer, 2005). However, two aspects were considered to be needed in the current version, based on biological considerations. First, we implemented a multi-layer soil model, a more detailed representation compared with other models using a bucket model approach (e.g. Fischer et al., 2014; Laio et al., 2001). This was motivated by the need to account for contrasting rooting

919   strategies and access to water among coexisting plants, which is an under-explored, but likely key, aspect of community

920   dynamics in forests (Brum et al., 2019; De Deurwaerder et al., 2018; Ivanov et al., 2012). Second, we assumed that the depth

921   of tree water uptake is not only controlled by the distribution of root biomass (as in Naudts et al., 2015; Sakschewski et al.,

922   2021; Paschalis et al., 2024), but also by soil water state and its vertical variation (as in Williams et al., 1996; Duursma and

923   Medlyn, 2012). These improvements are relevant to the temporal variation of water retrieval depth (Bruno et al., 2006) and

924   the sustained dry-season productivity in rainforest ecosystems (Restrepo-Coupe et al., 2017).

925   The control of leaf gas exchange by water availability has been implemented by means of multiplicative soil water

926   stress factors. Although the use of such factors has been debated (Powell et al., 2013; Joetzjer et al., 2014), it has been preferred

927   over a more explicit representation of the water flow through the plant column (e.g. Yao et al., 2022; Christoffersen et al.,

928   2016; Cochard et al., 2021; De Cáceres et al., 2023). Although the stem hydraulic traits that would be needed for parameterizing

929   an explicit plant water flow module have been increasingly measured over the past decades, data availability for tropical tree

930   species remains low in regards to the actual number of species coexisting in these communities. Alternatively, correlative

931   relationships have been used to infer these traits from more easily measured traits (Christoffersen et al., 2016; Xu et al., 2016).

932   However, these are context dependent (Brodribb, 2017; Rosas et al., 2019) and have at best low statistical support in rainforest

933   communities that are loosely constrained by water availability (Dwyer and Laughlin, 2017; Delhaye et al., 2020; Maréchaux

934   et al., 2020). Innovative methods alleviate the difficulties of robustly measuring the vulnerability of tropical trees to embolism

935   (Cochard et al., 2016; Sergent et al., 2020; Garcia et al., 2023), and this could provide a key motivation for a more explicit

936   module of plant water flow in TROLL (Kennedy et al., 2019; Paschalis et al., 2024). Such developments could be necessary

937   to correctly represent the legacy of drought in forest ecosystems (Paschalis et al., 2024; Anderegg et al., 2015). However, two

938   important aspects were taken into account in the implementation of the multiplicative water stress factors in TROLL 4.0. These

939   factors were parameterized based on soil water potential as independent variable, and not soil water content, the former directly

940   controlling water availability for plants, while the effect of soil water content is strongly mediated by soil properties (Novick

941   et al., 2022). Also, different water stress factors were used for stomatal and non-stomatal limitations, in order to capture the

942   sequence of effects of decreasing water availability on plant function (Trueba et al., 2019; Fatichi et al., 2016; Hsiao, 1973).

943   The effects of water availability on plant function and tree demography were implemented through trait-based

944   parameterization, which allows a range of responses between trees and species. This was made possible through the use of leaf

945   water potential at turgor loss point (π_{tlp}), a leaf-level trait that is mechanistically linked to plant responses to water availability

946   (Bartlett et al., 2016b) and that is measurable at the community scale in diverse systems through a well-validated method

947   (Maréchaux et al., 2016; Griffin-Nolan et al., 2019; Sun et al., 2020; Bartlett et al., 2012a). Leaf water potential at turgor loss

948   point varies greatly across species within Amazonian forest communities (Maréchaux et al., 2015; Ziegler et al., 2019), and

949   this diversity explains contrasting responses to water availability at the leaf and plant levels (Martin-StPaul et al., 2017;

950   Maréchaux et al., 2018; Powell et al., 2017), and species distribution at local, regional and global scales (Bartlett et al., 2016a;

951   Baltzer et al., 2008; Lenz et al., 2006; Bartlett et al., 2012b). The relationships implemented here involving π_{tlp} have a

952   mechanistic basis, as discussed above. However, the relationships controlling the effect of water availability on (1) leaf

953 shedding, (2) seed germination and seedling recruitment, and (3) drought-induced mortality would deserve in-depth
954 exploration. More generally, these three processes remain key aspects of community dynamics and ecosystem functioning in
955 high need of sustained empirical investigation (Albert et al., 2019; Díaz-Yáñez et al., 2024; McDowell et al., 2022).

956 **4.2   Model-data integration, transferability and limitations**

957 TROLL 4.0 simulates forest structure and diversity, while expanding the types of data with which its results can be compared
958 (Schmitt et al., submitted companion paper). The individual-based species-specific representation of forest yields virtual forest
959 inventories, including the location of each individual, their botanical identity, and their dimensions, and virtual airborne laser
960 scanning point clouds (Fischer et al., 2019; Schmitt et al., 2023). TROLL 4.0 additionally provides water, carbon and litter
961 flux dynamics that are directly comparable to eddy-flux tower data and litter trap monitoring at fine temporal resolutions, and
962 this specificity has numerous advantages.

963   Data-driven knowledge can be directly assimilated in TROLL 4.0, offering new perspectives for inference or
964 calibration (Dietze et al., 2013; Fer et al., 2018; Hartig et al., 2012; LeBauer et al., 2013; Fischer et al., 2019). TROLL 4.0 can
965 help inform the development of DGVMs, in which the representation of vegetation does not allow this type of assimilation
966 (Fischer et al., 2019). TROLL 4.0 is also easy to use and test by field ecologists as it simulates trees, not cohorts, PFTs, or gap
967 patches: it can reproduce classical experiments in community or ecosystem ecology (e.g. Crawford et al., 2021; Schmitt et al.,
968 2020) while overcoming known empirical challenges such as low repeatability (Schnitzer and Carson, 2016) or limited spatial
969 footprint (Estes et al., 2018). TROLL 4.0 can be compared with data under the control of different biophysical processes
970 supporting a more robust evaluation, and limiting equifinality issues (Franks et al., 1997; Medlyn et al., 2005). Finally, the
971 model is parameterized based on traits directly measured in the field improving model transferability (Rau et al., 2022a).

972   The individual-scale and spatially-explicit representation of TROLL 4.0 comes with a computational burden. For a
973 reference 4-ha area starting from bare ground, and 600 years of simulation, the computational cost of TROLL 4.0 is about
974 1820 min, compared with version TROLL2.3 (Maréchaux and Chave 2017) about 12 min. While the shift from a monthly to
975 a daily timestep explains the multiplication by a factor of 30 between the two versions, the addition of a belowground field
976 and of an iterative scheme to simulate leaf gas exchanges explains for a great part the remaining factor of five. Several
977 developments should reduce this computational cost: tree demographic processes do not need to be simulated at the daily
978 timestep and could be represented at a monthly resolution; vegetation models already implement such nested time scales
979 (Moorcroft, 2006). We are also confident that further computer time reduction will be brought about by code optimization.
980 Finally, several strategies can be implemented to up-scale the outputs of individual-based models at reduced computational
981 costs, especially by leveraging large scale remote sensing products (Rödig et al., 2017; Sato et al., 2007; Shugart et al., 2015).

982 **4.3   Current and future developments**

983 TROLL 4.0 is a reflection on the state of the art and knowledge gaps in plant physiology and ecology, resulting in an
984 unbalanced representation across processes. TROLL is being continuously developed, as knowledge and data availability

progress, specific questions to address with the model emerge, or important limitations are identified. In a companion paper (Schmitt et al., submitted companion paper), we use data from forest inventories, litter traps, eddy-flux towers and remote sensing products to evaluate and discuss the performance and limitations of TROLL 4.0 at two forest sites. We here mention several on-going or future developments.

Empirical findings suggest that the contribution of undisturbed tropical forests to the global carbon sink is declining (Hubau et al., 2020; Qie et al., 2017), pointing to the need of integrated modelling to understand and predict such trends (Yao et al., 2023, 2024; Koch et al., 2021). Among the possible steps forward with TROLL 4.0 are an improved representation of stomatal conductance and its coupling with photosynthesis (Lamour et al., 2022, 2023; Dewar et al., 2018), as well as respiration response and acclimation to climatic drivers (Smith and Dukes, 2013; Collalti et al., 2020; Slot et al., 2013; Rowland et al., 2015). Improvements on the carbon budget would also be important, with more explicit carbon allocation to reproductive organs and belowground structures, under the control of environmental drivers (Fig. 3). However, such developments would rely on limited empirical or experimental knowledge belowground (Cusack et al., 2024) and scarce information on tree reproductive strategies (Igarashi et al., 2024; Vacchiano et al., 2018; Norden et al., 2007). An improved representation and evaluation of drought-induced tree mortality would be another important step forward as it might play a key role in the observed changing dynamics and functional and floristic turnover (Esquivel-Muelbert et al., 2019; Feeley et al., 2011; Hubau et al., 2020; Qie et al., 2017). Information provided by long-term through fall exclusion experiments would offer interesting opportunities for model development and evaluation (Powell et al., 2013; Yao et al., 2022).

Tropical forest disturbance by land use change, fire regimes, and other degradations are an important source of C emissions (Lapola et al., 2023), and they must be represented in models. For instance, it is important to understand how edge effects affect the forest microclimate, and consequently forest dynamics, functioning and composition (Camargo and Kapos, 1995; Nunes et al., 2022). To this end, micro-climate models could be coupled to or embedded within TROLL (Gril et al., 2023a; Maclean and Klinges, 2021). Fragmentation also impacts seed dispersal, and thus seed rain and seed bank intensity and composition (Warneke et al., 2022; Cubiña and Aide, 2001). Improving TROLL's representation of seed dispersal ability and germination as a function of plant trait and dispersal mode is key to capture the effect of forest loss and fragmentation on forest functioning and biodiversity (Seidler and Plotkin, 2006; Muller-Landau et al., 2008; Tamme et al., 2014; Chase et al., 2020; Riva and Fahrig, 2023). More generally, one overarching objective is to improve model's representation of processes involved in forest regeneration, to simulate secondary forest dynamics and resilience to disturbances (Hanbury-Brown et al., 2022; Díaz-Yáñez et al., 2024; Poorter et al., 2023; Albrich et al., 2020).

Finally, TROLL 4.0 includes major developments that should facilitate its transferability across sites. The explicit integration of the ecosystem water balance and vegetation responses to soil water availability now allows to consider spatio-temporal extrapolation along water stress gradients. The integration of soil topography and heterogeneity would also be an important advance for improved genericity. As nutrient availability is being altered by human activities (Peñuelas et al., 2013), the explicit integration of a nutrient cycle with nitrogen and phosphorous colimitation will be a useful advance in the future

1018   (Fernández-Martínez et al., 2014; Turner et al., 2018). Similarly, the extension of tree functioning responses to a broader range
1019   of temperatures, should support the transferability of TROLL to temperate and boreal forests.

1020   **5. Conclusion**

1021   TROLL 4.0 represents an advance over previous versions as it bridges across forest model types, while maintaining a
1022   representation consistent with field ecology and ecosystem science. TROLL 4.0 simulates the responses of tropical forests to
1023   water availability through the explicit representation of water dynamics belowground and its coupling with leaf-level gas
1024   exchanges and demographic processes. This comes at a computational cost, and a future task is to conduct code optimization
1025   and parallelization, and up-scaling in combination with remote-sensing products. The representation of processes in TROLL
1026   4.0 mirrors an unbalanced state of the art, but its ability to dialogue with a range of data of various nature, makes it a valuable
1027   tool to take up the fundamental and applied research challenges on tropical forests. TROLL 4.0 has benefited from observations
1028   and field experiments that feed the development of models (Medlyn et al., 2015; Paschalis et al., 2020), while modeling
1029   exercises inform and guide empirical approaches (Medlyn et al., 2016; Norby et al., 2016; Pacala and Rees, 1998). This is
1030   possible because of the fine scale representation of forest structure and diversity and the trait-based parameterization of
1031   processes in the model.

1034   *Code and data availability.* The code of TROLL 4.0 is available at https://github.com/TROLL-code/TROLL, a DOI will be
1035   linked to this repository upon publication. Additionally, TROLL 4.0 can be set-up and run, and its outputs can be analyzed
1036   with an updated version of the R package rcontroll: https://github.com/sylvainschmitt/rcontroll/tree/TROLLV4, also available
1037   in R through the command devtools::install_github("sylvainschmitt/rcontroll", ref = "TROLLV4").

1039   *Supplement.* The supplement related to this article will be available online upon publication acceptance.

1041   *Author contributions.* IM led TROLL 4.0, and designed the implementation of the water cycle and its coupling to vegetation.
1042   FJF co-led TROLL 4.0 and designed the new implementation of intra-specific variability and crown shapes. SS and JC
1043   contributed ideas and discussions. IM wrote the paper with contributions from all authors.

1045   *Competing interests.* The authors declare that they have no conflict of interest.
1046

1047   *Acknowledgements.* We acknowledge Nicolas Martin-StPaul and Rémi Vezy for useful discussions on the representation of
1048   gas exchanges and water fluxes in models; Nicolas Barbier, Gregoire Vincent, and James Ball for sharing data and useful

1049   discussions on leaf phenology; Philippe Verley and Thomas Arsouze for IT support; and Marie Boscher for help in designing

1050   figure 1. This work was carried out with the support of MESO@LR-Platform at the University of Montpellier.

1051

1052   *Financial support.* This research has been supported by fundings from ANR (the French National Research Agency) under the

1053   "Investissements d'avenir" program with the references ANR-16-IDEX-0006, ANR-10-LABX-25-01, ANR-10-LABX-0041,

1054   the Amazonian Landscapes in Transition ANR project (ALT), CNES Biomass-Valo project, and ESA CCI-BIOMASS.

References

1056   Aguilos, M., Hérault, B., Burban, B., Wagner, F., and Bonal, D.: What drives long-term variations in carbon flux and balance

1057   in a tropical rainforest in French Guiana?, Agricultural and Forest Meteorology, 253–254, 114–123,

1058   https://doi.org/10.1016/j.agrformet.2018.02.009, 2018.

1059   Albert, L. P., Restrepo-Coupe, N., Smith, M. N., Wu, J., Chavana-Bryant, C., Prohaska, N., Taylor, T. C., Martins, G. A.,

1060   Ciais, P., Mao, J., Arain, M. A., Li, W., Shi, X., Ricciuto, D. M., Huxman, T. E., McMahon, S. M., and Saleska, S. R.:

1061   Cryptic phenology in plants: Case studies, implications, and recommendations, Global Change Biology, 25, 3591–3608,

1062   https://doi.org/10.1111/gcb.14759, 2019.

1063   Albert, L. P., Wu, J., Prohaska, N., de Camargo, P. B., Huxman, T. E., Tribuzy, E. S., Ivanov, V. Y., Oliveira, R. S., Garcia,

1064   S., Smith, M. N., Oliveira Junior, R. C., Restrepo-Coupe, N., da Silva, R., Stark, S. C., Martins, G. A., Penha, D. V., and

1065   Saleska, S. R.: Age-dependent leaf physiology and consequences for crown-scale carbon uptake during the dry season in

1066   an Amazon evergreen forest, New Phytologist, 218, https://doi.org/10.1111/nph.15056, 2018.

1067   Albrich, K., Rammer, W., Turner, M. G., Ratajczak, Z., Braziunas, K. H., Hansen, W. D., and Seidl, R.: Simulating forest

1068   resilience: A review, Global Ecology and Biogeography, 29, 2082–2096, https://doi.org/10.1111/geb.13197, 2020.

1069   Amthor, J. S.: The role of maintenance respiration in plant growth, Plant, Cell & Environment, 7, 561–569,

1070   https://doi.org/10.1111/1365-3040.ep11591833, 1984.

1071   Anderegg, W. R. L., Schwalm, C., Biondi, F., Camarero, J. J., Koch, G., Litvak, M., Ogle, K., Shaw, J. D., Shevliakova, E.,

1072   Williams, A. P., Wolf, A., Ziaco, E., and Pacala, S.: Pervasive drought legacies in forest ecosystems and their implications

1073   for carbon cycle models, Science, 349, 528–532, https://doi.org/10.1126/science.aab1833, 2015.

1074   Anderegg, W. R. L., Wolf, A., Arango-Velez, A., Choat, B., Chmura, D. J., Jansen, S., Kolb, T., Li, S., Meinzer, F., Pita, P.,

1075   Dios, V. R. de, Sperry, J. S., Wolfe, B. T., and Pacala, S.: Plant water potential improves prediction of empirical stomatal

1076   models, PLOS ONE, 12, e0185481, https://doi.org/10.1371/journal.pone.0185481, 2017.

1077   Anderegg, W. R. L., Wolf, A., Arango-Velez, A., Choat, B., Chmura, D. J., Jansen, S., Kolb, T., Li, S., Meinzer, F. C., Pita,

1078   P., Dios, V. R. de, Sperry, J. S., Wolfe, B. T., and Pacala, S.: Woody plants optimise stomatal behaviour relative to hydraulic

1079   risk, Ecology Letters, 21, 968–977, https://doi.org/10.1111/ele.12962, 2018.

Arora, V. K. and Boer, G. J.: A Representation of Variable Root Distribution in Dynamic Vegetation Models, Earth Interact., 7, 1–19, https://doi.org/10.1175/1087-3562(2003)007<0001:AROVRD>2.0.CO;2, 2003.

Asao, S., Bedoya-Arrieta, R., and Ryan, M. G.: Variation in foliar respiration and wood CO2 efflux rates among species and canopy layers in a wet tropical forest, Tree Physiol, 35, 148–159, https://doi.org/10.1093/treephys/tpu107, 2015.

Atkin, O. K., Evans, J. R., Ball, M. C., Lambers, H., and Pons, T. L.: Leaf respiration of snow gum in the light and dark. Interactions between temperature and irradiance., Plant Physiol., 122, 915–924, https://doi.org/10.1104/pp.122.3.915, 2000.

Atkin, O. K., Meir, P., and Turnbull, M. H.: Improving representation of leaf respiration in large-scale predictive climate–vegetation models, New Phytol, 202, 743–748, https://doi.org/10.1111/nph.12686, 2014.

Atkin, O. K., Bloomfield, K. J., Reich, P. B., Tjoelker, M. G., Asner, G. P., Bonal, D., Bönisch, G., Bradford, M. G., Cernusak, L. A., Cosio, E. G., Creek, D., Crous, K. Y., Domingues, T. F., Dukes, J. S., Egerton, J. J. G., Evans, J. R., Farquhar, G. D., Fyllas, N. M., Gauthier, P. P. G., Gloor, E., Gimeno, T. E., Griffin, K. L., Guerrieri, R., Heskel, M. A., Huntingford, C., Ishida, F. Y., Kattge, J., Lambers, H., Liddell, M. J., Lloyd, J., Lusk, C. H., Martin, R. E., Maksimov, A. P., Maximov, T. C., Malhi, Y., Medlyn, B. E., Meir, P., Mercado, L. M., Mirotchnick, N., Ng, D., Niinemets, Ü., O'Sullivan, O. S., Phillips, O. L., Poorter, L., Poot, P., Prentice, I. C., Salinas, N., Rowland, L. M., Ryan, M. G., Sitch, S., Slot, M., Smith, N. G., Turnbull, M. H., VanderWel, M. C., Valladares, F., Veneklaas, E. J., Weerasinghe, L. K., Wirth, C., Wright, I. J., Wythers, K. R., Xiang, J., Xiang, S., and Zaragoza-Castells, J.: Global variability in leaf respiration in relation to climate, plant functional types and leaf traits, New Phytol, 206, 614–636, https://doi.org/10.1111/nph.13253, 2015.

Baltzer, J. L., Davies, S. J., Bunyavejchewin, S., and Noor, N. S. M.: The role of desiccation tolerance in determining tree species distributions along the Malay–Thai Peninsula, Functional Ecology, 22, 221–231, https://doi.org/10.1111/j.1365-2435.2007.01374.x, 2008.

Baraloto, C., Paine, C. E. T., Patiño, S., Bonal, D., Hérault, B., and Chave, J.: Functional trait variation and sampling strategies in species-rich plant communities, Functional Ecology, 24, 208–216, https://doi.org/10.1111/j.1365-2435.2009.01600.x, 2010a.

Baraloto, C., Timothy Paine, C. E., Poorter, L., Beauchene, J., Bonal, D., Domenach, A.-M., Hérault, B., Patiño, S., Roggy, J.-C., and Chave, J.: Decoupled leaf and stem economics in rain forest trees, Ecology Letters, 13, 1338–1347, https://doi.org/10.1111/j.1461-0248.2010.01517.x, 2010b.

Bartlett, M. K., Scoffoni, C., Ardy, R., Zhang, Y., Sun, S., Cao, K., and Sack, L.: Rapid determination of comparative drought tolerance traits: using an osmometer to predict turgor loss point, Methods Ecol. Evol., 3, 880–888, https://doi.org/10.1111/j.2041-210X.2012.00230.x, 2012a.

Bartlett, M. K., Scoffoni, C., and Sack, L.: The determinants of leaf turgor loss point and prediction of drought tolerance of species and biomes: a global meta-analysis, Ecology Letters, 15, 393–405, https://doi.org/10.1111/j.1461-0248.2012.01751.x, 2012b.

Bartlett, M. K., Zhang, Y., Yang, J., Kreidler, N., Sun, S.-W., Lin, L., Hu, Y.-H., Cao, K.-F., and Sack, L.: Drought tolerance as a driver of tropical forest assembly: resolving spatial signatures for multiple processes, Ecology, 97, 503–514, https://doi.org/10.1890/15-0468.1, 2016a.

Bartlett, M. K., Klein, T., Jansen, S., Choat, B., and Sack, L.: The correlations and sequence of plant stomatal, hydraulic, and wilting responses to drought, PNAS, 113, 13098–13103, https://doi.org/10.1073/pnas.1604088113, 2016b.

Beer, C., Reichstein, M., Tomelleri, E., Ciais, P., Jung, M., Carvalhais, N., Rödenbeck, C., Arain, M. A., Baldocchi, D., Bonan, G. B., Bondeau, A., Cescatti, A., Lasslop, G., Lindroth, A., Lomas, M., Luyssaert, S., Margolis, H., Oleson, K. W., Roupsard, O., Veenendaal, E., Viovy, N., Williams, C., Woodward, F. I., and Papale, D.: Terrestrial gross carbon dioxide uptake: global distribution and covariation with climate, Science, 329, 834–838, https://doi.org/10.1126/science.1184984, 2010.

Bennett, A. C., McDowell, N. G., Allen, C. D., and Anderson-Teixeira, K. J.: Larger trees suffer most during drought in forests worldwide, Nature Plants, 1, https://doi.org/10.1038/nplants.2015.139, 2015.

Bernacchi, C. J., Pimentel, C., and Long, S. P.: In vivo temperature response functions of parameters required to model RuBP-limited photosynthesis, Plant, Cell & Environment, 26, 1419–1430, https://doi.org/10.1046/j.0016-8025.2003.01050.x, 2003.

Berzaghi, F., Wright, I. J., Kramer, K., Oddou-Muratorio, S., Bohn, F. J., Reyer, C. P. O., Sabaté, S., Sanders, T. G. M., and Hartig, F.: Towards a New Generation of Trait-Flexible Vegetation Models, Trends in Ecology & Evolution, 35, 191–205, https://doi.org/10.1016/j.tree.2019.11.006, 2020.

Blanchard, G., Barbier, N., Vieilledent, G., Ibanez, T., Hequet, V., McCoy, S., and Birnbaum, P.: UAV-Lidar reveals that canopy structure mediates the influence of edge effects on forest diversity, function and microclimate, Journal of Ecology, 111, 1411–1427, https://doi.org/10.1111/1365-2745.14105, 2023.

Bohlman, S. and O'Brien, S.: Allometry, adult stature and regeneration requirement of 65 tree species on Barro Colorado Island, Panama, Journal of Tropical Ecology, 22, 123–136, https://doi.org/10.1017/S0266467405003019, 2006.

Bonal, D., Bosc, A., Ponton, S., Goret, J.-Y., Burban, B., Gross, P., Bonnefond, J.-M., Elbers, J., Longdoz, B., Epron, D., Guehl, J.-M., and Granier, A.: Impact of severe dry season on net ecosystem exchange in the Neotropical rainforest of French Guiana, Global Change Biology, 14, 1917–1933, https://doi.org/10.1111/j.1365-2486.2008.01610.x, 2008.

Bonan, G. B.: Forests and Climate Change: Forcings, Feedbacks, and the Climate Benefits of Forests, Science, 320, 1444–1449, https://doi.org/10.1126/science.1155121, 2008.

Bonan, G. B., Williams, M., Fisher, R. A., and Oleson, K. W.: Modeling stomatal conductance in the earth system: linking leaf water-use efficiency and water transport along the soil–plant–atmosphere continuum, Geosci. Model Dev., 7, 2193–2222, https://doi.org/10.5194/gmd-7-2193-2014, 2014.

Botkin, D. B.: Functional groups of organisms in model ecosystems, Ecosystem Analysis and Prediction, 98–102, 1975.

Botkin, D. B., Janak, J. F., and Wallis, J. R.: Some Ecological Consequences of a Computer Model of Forest Growth, Journal of Ecology, 60, 849–872, https://doi.org/10.2307/2258570, 1972.

1147 Bradford, K. J.: A Water Relations Analysis of Seed Germination Rates, Plant Physiol., 94, 840–849,
1148   https://doi.org/10.1104/pp.94.2.840, 1990.

1149 Braghiere, R. K., Quaife, T., Black, E., He, L., and Chen, J. M.: Underestimation of Global Photosynthesis in Earth System
1150   Models Due to Representation of Vegetation Structure, Global Biogeochemical Cycles, 33, 1358–1369,
1151   https://doi.org/10.1029/2018GB006135, 2019.

1152 Braghiere, R. K., Wang, Y., Doughty, R., Sousa, D., Magney, T., Widlowski, J.-L., Longo, M., Bloom, A. A., Worden, J.,
1153   Gentine, P., and Frankenberg, C.: Accounting for canopy structure improves hyperspectral radiative transfer and sun-
1154   induced chlorophyll fluorescence representations in a new generation Earth System model, Remote Sensing of
1155   Environment, 261, 112497, https://doi.org/10.1016/j.rse.2021.112497, 2021.

1156 Brodribb, T. J.: Progressing from 'functional' to mechanistic traits, New Phytol, 215, 9–11, https://doi.org/10.1111/nph.14620,
1157   2017.

1158 Brodribb, T. J., Holbrook, N. M., and Gutiérrez, M. V.: Hydraulic and photosynthetic co-ordination in seasonally dry tropical
1159   forest trees, Plant, Cell & Environment, 25, 1435–1444, https://doi.org/10.1046/j.1365-3040.2002.00919.x, 2002.

1160 Brodribb, T. J., Holbrook, N. M., Edwards, E. J., and Gutiérrez, M. V.: Relations between stomatal closure, leaf turgor and
1161   xylem vulnerability in eight tropical dry forest trees, Plant, Cell & Environment, 26, 443–450,
1162   https://doi.org/10.1046/j.1365-3040.2003.00975.x, 2003.

1163 Brooks, R. H. and Corey, A. T.: Hydraulic properties of porous media. Hydrology Paper No. 3, Civil Engineering Department,
1164   Colorado State University., Fort Collins, 1964.

1165 Brum, M., Vadeboncoeur, M. A., Ivanov, V., Asbjornsen, H., Saleska, S., Alves, L. F., Penha, D., Dias, J. D., Aragão, L. E.
1166   O. C., Barros, F., Bittencourt, P., Pereira, L., and Oliveira, R. S.: Hydrological niche segregation defines forest structure
1167   and drought tolerance strategies in a seasonal Amazon forest, Journal of Ecology, 107, 318–333,
1168   https://doi.org/10.1111/1365-2745.13022, 2019.

1169 Bruno, R. D., da Rocha, H. R., de Freitas, H. C., Goulden, M. L., and Miller, S. D.: Soil moisture dynamics in an eastern
1170   Amazonian tropical forest, Hydrol. Process., 20, 2477–2489, https://doi.org/10.1002/hyp.6211, 2006.

1171 Bucci, S., Scholz, F. G., Goldstein, G., Meinzer, F. C., Hinojosa, J. A., Hoffman, W. A., and Franco, A. C.; Processes
1172   preventing nocturnal equilibration between leaf and soil water potential in tropical savanna woody species., Tree
1173   Physiology, 24, 1119–1127, 2004.

1174 Budyko, M. I.: The Heat Balance of the Earth's Surface, Soviet Geography, 1961.

1175 Bugmann, H.: A review of forest gap models, Climatic Change, 51, 259–305, https://doi.org/10.1023/A:1012525626267, 2001.

1176 Burgess, S. S. O., Adams, M. A., Turner, N. C., and Ong, C. K.: The redistribution of soil water by tree root systems, Oecologia,
1177   115, 306–311, https://doi.org/10.1007/s004420050521, 1998.

1178 von Caemmerer, S.: Biochemical models of leaf photosynthesis, Csiro Publishing, 184 pp., 2000.

1179 Camargo, J. L. C. and Kapos, V.: Complex edge effects on soil moisture and microclimate in central Amazonian forest, Journal
1180   of Tropical Ecology, 11, 205–221, 1995.

1181 Canadell, J., Jackson, R. B., Ehleringer, J. R., Mooney, H. A., Sala, O. E., and Schulze, E. D.: Maximum rooting depth of
1182   vegetation types at the global scale, Oecologia, 108, 583–595, https://doi.org/10.1007/BF00329030, 1996.

1183 Cannell, M. G. R. and Thornley, J. H. M.: Modelling the components of plant respiration: some guiding principles, Ann Bot,
1184   85, 45–54, https://doi.org/10.1006/anbo.1999.0996, 2000.

1185 Cavaleri, M. A., Oberbauer, S. F., and Ryan, M. G.: Wood CO2 efflux in a primary tropical rain forest, Global Change Biology,
1186   12, 2442–2458, https://doi.org/10.1111/j.1365-2486.2006.01269.x, 2006.

1187 Cavaleri, M. A., Oberbauer, S. F., and Ryan, M. G.: Foliar and ecosystem respiration in an old-growth tropical rain forest,
1188   Plant, Cell & Environment, 31, 473–483, https://doi.org/10.1111/j.1365-3040.2008.01775.x, 2008.

1189 Charney, J. G.: Dynamics of deserts and drought in the Sahel, Q.J.R. Meteorol. Soc., 101, 193–202,
1190   https://doi.org/10.1002/qj.49710142802, 1975.

1191 Chase, J. M., Blowes, S. A., Knight, T. M., Gerstner, K., and May, F.: Ecosystem decay exacerbates biodiversity loss with
1192   habitat loss, Nature, 584, 238–243, https://doi.org/10.1038/s41586-020-2531-2, 2020.

1193 Chave: Study of structural, successional and spatial patterns in tropical rain forests using TROLL, a spatially explicit forest
1194   model, Ecological Modelling, 124, 233–254, https://doi.org/10.1016/S0304-3800(99)00171-4, 1999.

1195 Chave, J., Olivier, J., Bongers, F., Châtelet, P., Forget, P.-M., van der Meer, P., Norden, N., Riéra, B., and Charles-Dominique,
1196   P.: Above-ground biomass and productivity in a rain forest of eastern South America, Journal of Tropical Ecology, 24,
1197   355–366, https://doi.org/10.1017/S0266467408005075, 2008.

1198 Chave, J., Coomes, D., Jansen, S., Lewis, S. L., Swenson, N. G., and Zanne, A. E.: Towards a worldwide wood economics
1199   spectrum, Ecology Letters, 12, 351–366, https://doi.org/10.1111/j.1461-0248.2009.01285.x, 2009.

1200 Chave, J., Navarrete, D., Almeida, S., Álvarez, E., Aragão, L. E. O. C., Bonal, D., Châtelet, P., Silva-Espejo, J. E., Goret, J.-
1201   Y., von Hildebrand, P., Jiménez, E., Patiño, S., Peñuela, M. C., Phillips, O. L., Stevenson, P., and Malhi, Y.: Regional and
1202   seasonal patterns of litterfall in tropical South America, Biogeosciences, 7, 43–55, https://doi.org/10.5194/bg-7-43-2010,
1203   2010.

1204 Chave, J., Réjou-Méchain, M., Búrquez, A., Chidumayo, E., Colgan, M. S., Delitti, W. B. C., Duque, A., Eid, T., Fearnside,
1205   P. M., Goodman, R. C., Henry, M., Martínez-Yrízar, A., Mugasha, W. A., Muller-Landau, H. C., Mencuccini, M., Nelson,
1206   B. W., Ngomanda, A., Nogueira, E. M., Ortiz-Malavassi, E., Pélissier, R., Ploton, P., Ryan, C. M., Saldarriaga, J. G., and
1207   Vieilledent, G.: Improved allometric models to estimate the aboveground biomass of tropical trees, Glob Change Biol, 20,
1208   3177–3190, https://doi.org/10.1111/gcb.12629, 2014.

1209 Chen, X., Maignan, F., Viovy, N., Bastos, A., Goll, D., Wu, J., Liu, L., Yue, C., Peng, S., Yuan, W., Conceição, A. C. da,
1210   O'Sullivan, M., and Ciais, P.: Novel Representation of Leaf Phenology Improves Simulation of Amazonian Evergreen
1211   Forest Photosynthesis in a Land Surface Model, Journal of Advances in Modeling Earth Systems, 12, e2018MS001565,
1212   https://doi.org/10.1029/2018MS001565, 2020.

1213 Chen, X., Ciais, P., Maignan, F., Zhang, Y., Bastos, A., Liu, L., Bacour, C., Fan, L., Gentine, P., Goll, D., Green, J., Kim, H.,
1214   Li, L., Liu, Y., Peng, S., Tang, H., Viovy, N., Wigneron, J.-P., Wu, J., Yuan, W., and Zhang, H.: Vapor Pressure Deficit

1215   and Sunlight Explain Seasonality of Leaf Phenology and Photosynthesis Across Amazonian Evergreen Broadleaved Forest,

1216   Global Biogeochemical Cycles, 35, e2020GB006893, https://doi.org/10.1029/2020GB006893, 2021.

1217 Chen, Y., Ryder, J., Bastrikov, V., McGrath, M. J., Naudts, K., Otto, J., Ottlé, C., Peylin, P., Polcher, J., Valade, A., Black,

1218   A., Elbers, J. A., Moors, E., Foken, T., van Gorsel, E., Haverd, V., Heinesch, B., Tiedemann, F., Knohl, A., Launiainen,

1219   S., Loustau, D., Ogée, J., Vessala, T., and Luyssaert, S.: Evaluating the performance of land surface model ORCHIDEE-

1220   CAN v1.0 on water and energy flux estimation with a single- and multi-layer energy budget scheme, Geoscientific Model

1221   Development, 9, 2951–2972, https://doi.org/10.5194/gmd-9-2951-2016, 2016.

1222 Chesson, P. L. and Warner, R. R.: Environmental variability promotes coexistence in lottery competitive systems, The

1223   American Naturalist, 117, 923–943, 1981.

1224 Christoffersen, B. O., Gloor, M., Fauset, S., Fyllas, N. M., Galbraith, D. R., Baker, T. R., Rowland, L., Fisher, R. A., Binks,

1225   O. J., Sevanto, S. A., Xu, C., Jansen, S., Choat, B., Mencuccini, M., McDowell, N. G., and Meir, P.: Linking hydraulic

1226   traits to tropical forest function in a size-structured and trait-driven model (TFS v.1-Hydro), Geoscientific Model

1227   Development Discussions, 0, 1–60, https://doi.org/10.5194/gmd-2016-128, 2016.

1228 Chuine, I. and Beaubien, E. G.: Phenology is a major determinant of tree species range, Ecology Letters, 4, 500–510,

1229   https://doi.org/10.1046/j.1461-0248.2001.00261.x, 2001.

1230 Clark, D. B., Mercado, L. M., Sitch, S., Jones, C. D., Gedney, N., Best, M. J., Pryor, M., Rooney, G. G., Essery, R. L. H.,

1231   Blyth, E., Boucher, O., Harding, R. J., Huntingford, C., and Cox, P. M.: The Joint UK Land Environment Simulator

1232   (JULES), model description – Part 2: Carbon fluxes and vegetation dynamics, Geosci. Model Dev., 4, 701–722,

1233   https://doi.org/10.5194/gmd-4-701-2011, 2011.

1234 Cochard, H.: A new mechanism for tree mortality due to drought and heatwaves, Peer Community Journal, 1,

1235   https://doi.org/10.24072/pcjournal.45, 2021.

1236 Cochard, H., Torres-Ruiz, J. M., and Delzon, S.: Let plant hydraulics catch the wave, Journal of Plant Hydraulics, 3, 002,

1237   2016.

1238 Cochard, H., Pimont, F., Ruffault, J., and Martin-StPaul, N.: SurEau: a mechanistic model of plant water relations under

1239   extreme drought, Annals of Forest Science, 78, 55, https://doi.org/10.1007/s13595-021-01067-y, 2021.

1240 Collalti, A., Tjoelker, M. G., Hoch, G., Mäkelä, A., Guidolotti, G., Heskel, M., Petit, G., Ryan, M. G., Battipaglia, G.,

1241   Matteucci, G., and Prentice, I. C.: Plant respiration: Controlled by photosynthesis or biomass?, Global Change Biology,

1242   26, 1739–1753, https://doi.org/10.1111/gcb.14857, 2020.

1243 Coomes, D. A. and Grubb, P. J.: Colonization, tolerance, competition and seed-size variation within functional groups, Trends

1244   in Ecology & Evolution, 18, 283–291, https://doi.org/10.1016/S0169-5347(03)00072-7, 2003.

1245 Cosby, B. J., Hornberger, G. M., Clapp, R. B., and Ginn, T. R.: A Statistical Exploration of the Relationships of Soil Moisture

1246   Characteristics to the Physical Properties of Soils, Water Resources Research, 20, 682–690,

1247   https://doi.org/10.1029/WR020i006p00682, 1984.

1248 Costa, F. R. C., Schietti, J., Stark, S. C., and Smith, M. N.: The other side of tropical forest drought: do shallow water table
1249   regions of Amazonia act as large-scale hydrological refugia from drought?, New Phytologist, 237, 714–733,
1250   https://doi.org/10.1111/nph.17914, 2023.

1251 Coussement, J. R., De Swaef, T., Lootens, P., Roldán-Ruiz, I., and Steppe, K.: Introducing turgor-driven growth dynamics
1252   into functional–structural plant models, Ann Bot, 121, 849–861, https://doi.org/10.1093/aob/mcx144, 2018.

1253 Cox, P. M., Betts, R. A., Jones, C. D., Spall, S. A., and Totterdell, I. J.: Acceleration of global warming due to carbon-cycle
1254   feedbacks in a coupled climate model, Nature, 408, 184–187, https://doi.org/10.1038/35041539, 2000.

1255 Craine, J. M., Engelbrecht, B. M. J., Lusk, C. H., McDowell, N. G., and Poorter, H.: Resource limitation, tolerance, and the
1256   future of ecological plant classification, Frontiers in Plant Science, 3, https://doi.org/10.3389/fpls.2012.00246, 2012.

1257 Crawford, M. S., Barry, K. E., Clark, A. T., Farrior, C. E., Hines, J., Ladouceur, E., Lichstein, J. W., Maréchaux, I., May, F.,
1258   Mori, A. S., Reineking, B., Turnbull, L. A., Wirth, C., and Rüger, N.: The function-dominance correlation drives the
1259   direction and strength of biodiversity–ecosystem functioning relationships, Ecology Letters, 24, 1762–1775,
1260   https://doi.org/10.1111/ele.13776, 2021.

1261 Cubiña, A. and Aide, T. M.: The Effect of Distance from Forest Edge on Seed Rain and Soil Seed Bank in a Tropical Pasture,
1262   BIOTROPICA, 33, 260–267, https://doi.org/10.1646/0006-3606(2001)033[0260:TEODFF]2.0.CO;2, 2001.

1263 Cusack, D. F., Christoffersen, B., Smith-Martin, C. M., Andersen, K. M., Cordeiro, A. L., Fleischer, K., Wright, S. J., Guerrero-
1264   Ramírez, N. R., Lugli, L. F., McCulloch, L. A., Sanchez-Julia, M., Batterman, S. A., Dallstream, C., Fortunel, C., Toro,
1265   L., Fuchslueger, L., Wong, M. Y., Yaffar, D., Fisher, J. B., Arnaud, M., Dietterich, L. H., Addo-Danso, S. D., Valverde-
1266   Barrantes, O. J., Weemstra, M., Ng, J. C., and Norby, R. J.: Toward a coordinated understanding of hydro-biogeochemical
1267   root functions in tropical forests for application in vegetation models, New Phytologist, n/a,
1268   https://doi.org/10.1111/nph.19561, 2024.

1269 Damour, G., Simonneau, T., Cochard, H., and Urban, L.: An overview of models of stomatal conductance at the leaf level,
1270   Plant, Cell & Environment, 33, 1419–1438, https://doi.org/10.1111/j.1365-3040.2010.02181.x, 2010.

1271 Daws, M. I., Crabtree, L. M., Dalling, J. W., Mullins, C. E., and Burslem, D. F. R. P.: Germination Responses to Water
1272   Potential in Neotropical Pioneers Suggest Large-seeded Species Take More Risks, Ann Bot, 102, 945–951,
1273   https://doi.org/10.1093/aob/mcn186, 2008.

1274 Dawson, T. E.: Hydraulic lift and water use by plants: implications for water balance, performance and plant-plant interactions,
1275   Oecologia, 95, 565–574, https://doi.org/10.1007/BF00317442, 1993.

1276 De Cáceres, M., Molowny-Horas, R., Cabon, A., Martínez-Vilalta, J., Mencuccini, M., García-Valdés, R., Nadal-Sala, D.,
1277   Sabaté, S., Martin-StPaul, N., Morin, X., D'Adamo, F., Batllori, E., and Améztegui, A.: MEDFATE 2.9.3: a trait-enabled
1278   model to simulate Mediterranean forest function and dynamics at regional scales, Geoscientific Model Development, 16,
1279   3165–3201, https://doi.org/10.5194/gmd-16-3165-2023, 2023.

1280 De Deurwaerder, H., Hervé-Fernández, P., Stahl, C., Burban, B., Petronelli, P., Hoffman, B., Bonal, D., Boeckx, P., and
1281   Verbeeck, H.: Liana and tree below-ground water competition—evidence for water resource partitioning during the dry
1282   season, Tree Physiol, 38, 1071–1083, https://doi.org/10.1093/treephys/tpy002, 2018.

1283 De Frenne, P., Zellweger, F., Rodríguez-Sánchez, F., Scheffers, B. R., Hylander, K., Luoto, M., Vellend, M., Verheyen, K.,
1284   and Lenoir, J.: Global buffering of temperatures under forest canopies, Nat Ecol Evol, 3, 744–749,
1285   https://doi.org/10.1038/s41559-019-0842-1, 2019.

1286 De Kauwe, M. G., Zhou, S.-X., Medlyn, B. E., Pitman, A. J., Wang, Y.-P., Duursma, R. A., and Prentice, I. C.: Do land surface
1287   models need to include differential plant species responses to drought? Examining model predictions across a mesic-xeric
1288   gradient in Europe, Biogeosciences, 12, 7503–7518, https://doi.org/10.5194/bg-12-7503-2015, 2015.

1289 De Kauwe, M. G., Medlyn, B. E., Knauer, J., and Williams, C. A.: Ideas and perspectives: how coupled is the vegetation to
1290   the boundary layer?, Biogeosciences, 14, 4435–4453, http://dx.doi.org/10.5194/bg-14-4435-2017, 2017.

1291 Delhaye, G., Bauman, D., Séleck, M., Ilunga wa Ilunga, E., Mahy, G., and Meerts, P.: Interspecific trait integration increases
1292   with environmental harshness: A case study along a metal toxicity gradient, Functional Ecology, 34, 1428–1437,
1293   https://doi.org/10.1111/1365-2435.13570, 2020.

1294 Dewar, R., Mauranen, A., Mäkelä, A., Hölttä, T., Medlyn, B., and Vesala, T.: New insights into the covariation of stomatal,
1295   mesophyll and hydraulic conductances from optimization models incorporating nonstomatal limitations to photosynthesis,
1296   New Phytologist, 217, 571–585, https://doi.org/10.1111/nph.14848, 2018.

1297 Díaz, S., Kattge, J., Cornelissen, J. H. C., Wright, I. J., Lavorel, S., Dray, S., Reu, B., Kleyer, M., Wirth, C., Colin Prentice, I.,
1298   Garnier, E., Bönisch, G., Westoby, M., Poorter, H., Reich, P. B., Moles, A. T., Dickie, J., Gillison, A. N., Zanne, A. E.,
1299   Chave, J., Joseph Wright, S., Sheremet'ev, S. N., Jactel, H., Baraloto, C., Cerabolini, B., Pierce, S., Shipley, B., Kirkup,
1300   D., Casanoves, F., Joswig, J. S., Günther, A., Falczuk, V., Rüger, N., Mahecha, M. D., and Gorné, L. D.: The global
1301   spectrum of plant form and function, Nature, 529, 167–171, https://doi.org/10.1038/nature16489, 2016.

1302 Díaz, S., Kattge, J., Cornelissen, J. H. C., Wright, I. J., Lavorel, S., Dray, S., Reu, B., Kleyer, M., Wirth, C., Prentice, I. C.,
1303   Garnier, E., Bönisch, G., Westoby, M., Poorter, H., Reich, P. B., Moles, A. T., Dickie, J., Zanne, A. E., Chave, J., Wright,
1304   S. J., Sheremetiev, S. N., Jactel, H., Baraloto, C., Cerabolini, B. E. L., Pierce, S., Shipley, B., Casanoves, F., Joswig, J. S.,
1305   Günther, A., Falczuk, V., Rüger, N., Mahecha, M. D., Gorné, L. D., Amiaud, B., Atkin, O. K., Bahn, M., Baldocchi, D.,
1306   Beckmann, M., Blonder, B., Bond, W., Bond-Lamberty, B., Brown, K., Burrascano, S., Byun, C., Campetella, G.,
1307   Cavender-Bares, J., Chapin, F. S., Choat, B., Coomes, D. A., Cornwell, W. K., Craine, J., Craven, D., Dainese, M., de
1308   Araujo, A. C., de Vries, F. T., Domingues, T. F., Enquist, B. J., Fagúndez, J., Fang, J., Fernández-Méndez, F., Fernandez-
1309   Piedade, M. T., Ford, H., Forey, E., Freschet, G. T., Gachet, S., Gallagher, R., Green, W., Guerin, G. R., Gutiérrez, A. G.,
1310   Harrison, S. P., Hattingh, W. N., He, T., Hickler, T., Higgins, S. I., Higuchi, P., Ilic, J., Jackson, R. B., Jalili, A., Jansen,
1311   S., Koike, F., König, C., Kraft, N., Kramer, K., Kreft, H., Kühn, I., Kurokawa, H., Lamb, E. G., Laughlin, D. C., Leishman,
1312   M., Lewis, S., Louault, F., Malhado, A. C. M., Manning, P., Meir, P., Mencuccini, M., Messier, J., Miller, R., Minden, V.,

1313   Molofsky, J., et al.: The global spectrum of plant form and function: enhanced species-level trait dataset, Sci Data, 9, 755,
1314   https://doi.org/10.1038/s41597-022-01774-9, 2022.

1315 Díaz-Yáñez, O., Käber, Y., Anders, T., Bohn, F., Braziunas, K. H., Brůna, J., Fischer, R., Fischer, S. M., Hetzer, J., Hickler,
1316   T., Hochauer, C., Lexer, M. J., Lischke, H., Mairota, P., Merganič, J., Merganičová, K., Mette, T., Mina, M., Morin, X.,
1317   Nieberg, M., Rammer, W., Reyer, C. P. O., Scheiter, S., Scherrer, D., and Bugmann, H.: Tree regeneration in models of
1318   forest dynamics: A key priority for further research, Ecosphere, 15, e4807, https://doi.org/10.1002/ecs2.4807, 2024.

1319 Dietze, M. C., Lebauer, D. S., and Kooper, R.: On improving the communication between models and data, Plant, Cell &
1320   Environment, 36, 1575–1585, https://doi.org/10.1111/pce.12043, 2013.

1321 Dilley, A. C. and O'brien, D. M.: Estimating downward clear sky long-wave irradiance at the surface from screen temperature
1322   and precipitable water, Quarterly Journal of the Royal Meteorological Society, 124, 1391–1401,
1323   https://doi.org/10.1002/qj.49712454903, 1998.

1324 Domingues, T. F., Meir, P., Feldpausch, T. R., Saiz, G., Veenendaal, E. M., Schrodt, F., Bird, M., Djagbletey, G., Hien, F.,
1325   Compaore, H., Diallo, A., Grace, J., and Lloyd, J.: Co-limitation of photosynthetic capacity by nitrogen and phosphorus in
1326   West Africa woodlands, Plant, Cell & Environment, 33, 959–980, https://doi.org/10.1111/j.1365-3040.2010.02119.x,
1327   2010.

1328 Domingues, T. F., Martinelli, L. A., and Ehleringer, J. R.: Seasonal patterns of leaf-level photosynthetic gas exchange in an
1329   eastern Amazonian rain forest, Plant Ecology & Diversity, 7, 189–203, https://doi.org/10.1080/17550874.2012.748849,
1330   2014.

1331 Donovan, L. A., Richards, J. H., and Linton, M. J.: Magnitude and mechanisms of disequilibrium between predawn plant and
1332   soil water potentials, Ecology, 84, 463–470, https://doi.org/10.1890/0012-9658(2003)084[0463:MAMODB]2.0.CO;2,
1333   2003.

1334 Dormann, C. F., Schymanski, S. J., Cabral, J., Chuine, I., Graham, C., Hartig, F., Kearney, M., Morin, X., Römermann, C.,
1335   Schröder, B., and Singer, A.: Correlation and process in species distribution models: bridging a dichotomy, Journal of
1336   Biogeography, 39, 2119–2131, https://doi.org/10.1111/j.1365-2699.2011.02659.x, 2012.

1337 Doughty, C. E. and Goulden, M. L.: Seasonal patterns of tropical forest leaf area index and CO_2 exchange, J. Geophys. Res.,
1338   113, G00B06, https://doi.org/10.1029/2007JG000590, 2008.

1339 Doughty, C. E., Gaillard, C., Burns, P., Keany, J. M., Abraham, A. J., Malhi, Y., Aguirre-Gutierrez, J., Koch, G., Jantz, P.,
1340   Shenkin, A., and Tang, H.: Tropical forests are mainly unstratified especially in Amazonia and regions with lower fertility
1341   or higher temperatures, Environ. Res.: Ecology, 2, 035002, https://doi.org/10.1088/2752-664X/ace723, 2023.

1342 Drake, J. E., Power, S. A., Duursma, R. A., Medlyn, B. E., Aspinwall, M. J., Choat, B., Creek, D., Eamus, D., Maier, C.,
1343   Pfautsch, S., Smith, R. A., Tjoelker, M. G., and Tissue, D. T.: Stomatal and non-stomatal limitations of photosynthesis for
1344   four tree species under drought: A comparison of model formulations, Agricultural and Forest Meteorology, 247, 454–466,
1345   https://doi.org/10.1016/j.agrformet.2017.08.026, 2017.

1346 Drake, P. L., Boer, H. J. de, Schymanski, S. J., and Veneklaas, E. J.: Two sides to every leaf: water and CO2 transport in
1347   hypostomatous and amphistomatous leaves, New Phytologist, 222, 1179–1187, https://doi.org/10.1111/nph.15652, 2019.

1348 Duffy, P. B., Brando, P., Asner, G. P., and Field, C. B.: Projections of future meteorological drought and wet periods in the
1349   Amazon, PNAS, 112, 13172–13177, https://doi.org/10.1073/pnas.1421010112, 2015.

1350 Dunne, T. and Black, R. D.: An Experimental Investigation of Runoff Production in Permeable Soils, Water Resources
1351   Research, 6, 478–490, https://doi.org/10.1029/WR006i002p00478, 1970.

1352 Duursma, R. A.: Plantecophys - An R Package for Analysing and Modelling Leaf Gas Exchange Data, PLOS ONE, 10,
1353   e0143346, https://doi.org/10.1371/journal.pone.0143346, 2015.

1354 Duursma, R. A. and Medlyn, B. E.: MAESPA: a model to study interactions between water limitation, environmental drivers
1355   and vegetation function at tree and stand levels, with an example application to [CO_2] × drought interactions, Geoscientific
1356   Model Development, 5, 919–940, https://doi.org/10.5194/gmd-5-919-2012, 2012.

1357 Duursma, R. A., Blackman, C. J., Lopéz, R., Martin-StPaul, N. K., Cochard, H., and Medlyn, B. E.: On the minimum leaf
1358   conductance: its role in models of plant water use, and ecological and environmental controls, New Phytologist, 221, 693–
1359   705, https://doi.org/10.1111/nph.15395, 2019.

1360 Dwyer, J. M. and Laughlin, D. C.: Constraints on trait combinations explain climatic drivers of biodiversity: the importance
1361   of trait covariance in community assembly, Ecol Lett, 20, 872–882, https://doi.org/10.1111/ele.12781, 2017.

1362 Egea, G., Verhoef, A., and Vidale, P. L.: Towards an improved and more flexible representation of water stress in coupled
1363   photosynthesis–stomatal conductance models, Agricultural and Forest Meteorology, 151, 1370–1384,
1364   https://doi.org/10.1016/j.agrformet.2011.05.019, 2011.

1365 Elias, M. and Potvin, C.: Assessing inter- and intra-specific variation in trunk carbon concentration for 32 neotropical tree
1366   species, Can. J. For. Res., 33, 1039–1045, https://doi.org/10.1139/x03-018, 2003.

1367 Elith, J. and Leathwick, J. R.: Species Distribution Models: Ecological Explanation and Prediction Across Space and Time,
1368   Annual Review of Ecology, Evolution, and Systematics, 40, 677–697,
1369   https://doi.org/10.1146/annurev.ecolsys.110308.120159, 2009.

1370 Engelbrecht, B. M. J., Dalling, J. W., Pearson, T. R. H., Wolf, R. L., Galvez, D. A., Koehler, T., Tyree, M. T., and Kursar, T.
1371   A.: Short dry spells in the wet season increase mortality of tropical pioneer seedlings, Oecologia, 148, 258–269,
1372   https://doi.org/10.1007/s00442-006-0368-5, 2006.

1373 Esquivel-Muelbert, A., Baker, T. R., Dexter, K. G., Lewis, S. L., Brienen, R. J. W., Feldpausch, T. R., Lloyd, J., Monteagudo-
1374   Mendoza, A., Arroyo, L., Álvarez-Dávila, E., Higuchi, N., Marimon, B. S., Marimon-Junior, B. H., Silveira, M., Vilanova,
1375   E., Gloor, E., Malhi, Y., Chave, J., Barlow, J., Bonal, D., Cardozo, N. D., Erwin, T., Fauset, S., Hérault, B., Laurance, S.,
1376   Poorter, L., Qie, L., Stahl, C., Sullivan, M. J. P., Steege, H. ter, Vos, V. A., Zuidema, P. A., Almeida, E., Oliveira, E. A.
1377   de, Andrade, A., Vieira, S. A., Aragão, L., Araujo-Murakami, A., Arets, E., C, G. A. A., Baraloto, C., Camargo, P. B.,
1378   Barroso, J. G., Bongers, F., Boot, R., Camargo, J. L., Castro, W., Moscoso, V. C., Comiskey, J., Valverde, F. C., Costa, A.
1379   C. L. da, Pasquel, J. del A., Fiore, A. D., Duque, L. F., Elias, F., Engel, J., Llampazo, G. F., Galbraith, D., Fernández, R.

1380   H., Coronado, E. H., Hubau, W., Jimenez-Rojas, E., Lima, A. J. N., Umetsu, R. K., Laurance, W., Lopez-Gonzalez, G.,
1381   Lovejoy, T., Cruz, O. A. M., Morandi, P. S., Neill, D., Vargas, P. N., Camacho, N. C. P., Gutierrez, A. P., Pardo, G.,
1382   Peacock, J., Peña-Claros, M., Peñuela-Mora, M. C., Petronelli, P., Pickavance, G. C., Pitman, N., Prieto, A., Quesada, C.,
1383   Ramírez-Angulo, H., Réjou-Méchain, M., Correa, Z. R., Roopsind, A., Rudas, A., Salomão, R., Silva, N., Espejo, J. S.,
1384   Singh, J., Stropp, J., Terborgh, J., Thomas, R., Toledo, M., Torres-Lezama, A., Gamarra, L. V., Meer, P. J. van de, Heijden,
1385   G. van der, et al.: Compositional response of Amazon forests to climate change, Global Change Biology, 25, 39–56,
1386   https://doi.org/10.1111/gcb.14413, 2019.

1387 Esquivel-Muelbert, A., Phillips, O. L., Brienen, R. J. W., Fauset, S., Sullivan, M. J. P., Baker, T. R., Chao, K.-J., Feldpausch,
1388   T. R., Gloor, E., Higuchi, N., Houwing-Duistermaat, J., Lloyd, J., Liu, H., Malhi, Y., Marimon, B., Marimon Junior, B. H.,
1389   Monteagudo-Mendoza, A., Poorter, L., Silveira, M., Torre, E. V., Dávila, E. A., del Aguila Pasquel, J., Almeida, E., Loayza,
1390   P. A., Andrade, A., Aragão, L. E. O. C., Araujo-Murakami, A., Arets, E., Arroyo, L., C, G. A. A., Baisie, M., Baraloto, C.,
1391   Camargo, P. B., Barroso, J., Blanc, L., Bonal, D., Bongers, F., Boot, R., Brown, F., Burban, B., Camargo, J. L., Castro,
1392   W., Moscoso, V. C., Chave, J., Comiskey, J., Valverde, F. C., da Costa, A. L., Cardozo, N. D., Di Fiore, A., Dourdain, A.,
1393   Erwin, T., Llampazo, G. F., Vieira, I. C. G., Herrera, R., Honorio Coronado, E., Huamantupa-Chuquimaco, I., Jimenez-
1394   Rojas, E., Killeen, T., Laurance, S., Laurance, W., Levesley, A., Lewis, S. L., Ladvocat, K. L. L. M., Lopez-Gonzalez, G.,
1395   Lovejoy, T., Meir, P., Mendoza, C., Morandi, P., Neill, D., Nogueira Lima, A. J., Vargas, P. N., de Oliveira, E. A.,
1396   Camacho, N. P., Pardo, G., Peacock, J., Peña-Claros, M., Peñuela-Mora, M. C., Pickavance, G., Pipoly, J., Pitman, N.,
1397   Prieto, A., Pugh, T. A. M., Quesada, C., Ramirez-Angulo, H., de Almeida Reis, S. M., Rejou-Machain, M., Correa, Z. R.,
1398   Bayona, L. R., Rudas, A., Salomão, R., Serrano, J., Espejo, J. S., Silva, N., Singh, J., Stahl, C., Stropp, J., Swamy, V.,
1399   Talbot, J., ter Steege, H., et al.: Tree mode of death and mortality risk factors across Amazon forests, Nature
1400   Communications, 11, 5515, https://doi.org/10.1038/s41467-020-18996-3, 2020.

1401 Estes, L., Elsen, P. R., Treuer, T., Ahmed, L., Caylor, K., Chang, J., Choi, J. J., and Ellis, E. C.: The spatial and temporal
1402   domains of modern ecology, Nature Ecology & Evolution, 1, https://doi.org/10.1038/s41559-018-0524-4, 2018.

1403 Evans, M. R.: Modelling ecological systems in a changing world, Phil. Trans. R. Soc. B, 367, 181–190,
1404   https://doi.org/10.1098/rstb.2011.0172, 2012.

1405 Farquhar, G. D., Caemmerer, S. von, and Berry, J. A.: A biochemical model of photosynthetic CO_2 assimilation in leaves of
1406   C3 species, Planta, 149, 78–90, 1980.

1407 Farrell, C., Szota, C., and Arndt, S. K.: Does the turgor loss point characterize drought response in dryland plants?, Plant, Cell
1408   & Environment, 40, 1500–1511, https://doi.org/10.1111/pce.12948, 2017.

1409 Fatichi, S., Pappas, C., and Ivanov, V. Y.: Modeling plant–water interactions: an ecohydrological overview from the cell to
1410   the global scale, WIREs Water, 3, 327–368, https://doi.org/10.1002/wat2.1125, 2016.

1411 Fauset, S., Baker, T. R., Lewis, S. L., Feldpausch, T. R., Affum-Baffoe, K., Foli, E. G., Hamer, K. C., and Swaine, M. D.:
1412   Drought-induced shifts in the floristic and functional composition of tropical forests in Ghana, Ecol Lett, 15, 1120–1129,
1413   https://doi.org/10.1111/j.1461-0248.2012.01834.x, 2012.

Feeley, K. J., Davies, S. J., Perez, R., Hubbell, S. P., and Foster, R. B.: Directional changes in the species composition of a tropical forest, Ecology, 92, 871–882, 2011.

Fer, I., Kelly, R., Moorcroft, P. R., Richardson, A. D., Cowdery, E. M., and Dietze, M. C.: Linking big models to big data: efficient ecosystem model calibration through Bayesian model emulation, Biogeosciences, 15, 5801–5830, https://doi.org/10.5194/bg-15-5801-2018, 2018.

Fernández-Martínez, M., Vicca, S., Janssens, I. A., Sardans, J., Luyssaert, S., Campioli, M., Chapin Iii, F. S., Ciais, P., Malhi, Y., Obersteiner, M., Papale, D., Piao, S. L., Reichstein, M., Rodà, F., and Peñuelas, J.: Nutrient availability as the key regulator of global forest carbon balance, Nature Clim. Change, 4, 471–476, https://doi.org/10.1038/nclimate2177, 2014.

Ferrier, S. and Guisan, A.: Spatial modelling of biodiversity at the community level, Journal of Applied Ecology, 43, 393–404, https://doi.org/10.1111/j.1365-2664.2006.01149.x, 2006.

Fichtner, A., Härdtle, W., Bruelheide, H., Kunz, M., Li, Y., and Oheimb, G.: Neighbourhood interactions drive overyielding in mixed-species tree communities, Nature Communications, 9, 1144, https://doi.org/10.1038/s41467-018-03529-w, 2018.

Fischer, F. J.: Inferring the structure and dynamics of tropical rain forests with individual-based forest growth models, Doctoral Dissertation, Université Paul Sabatier-Toulouse III., 2019.

Fischer, F. J., Maréchaux, I., and Chave, J.: Improving plant allometry by fusing forest models and remote sensing, New Phytologist, 223, 1159–1165, https://doi.org/10.1111/nph.15810, 2019.

Fischer, F. J., Labrière, N., Vincent, G., Hérault, B., Alonso, A., Memiaghe, H., Bissiengou, P., Kenfack, D., Saatchi, S., and Chave, J.: A simulation method to infer tree allometry and forest structure from airborne laser scanning and forest inventories, Remote Sensing of Environment, 251, 112056, https://doi.org/10.1016/j.rse.2020.112056, 2020.

Fischer, R., Armstrong, A., Shugart, H. H., and Huth, A.: Simulating the impacts of reduced rainfall on carbon stocks and net ecosystem exchange in a tropical forest, Environmental Modelling & Software, 52, 200–206, https://doi.org/10.1016/j.envsoft.2013.10.026, 2014.

Fisher, J. B., Huntzinger, D. N., Schwalm, C. R., and Sitch, S.: Modeling the Terrestrial Biosphere, Annual Review of Environment and Resources, 39, 91–123, https://doi.org/10.1146/annurev-environ-012913-093456, 2014.

Fisher, R. A., Williams, M., Do Vale, R. L., Da Costa, A. L., and Meir, P.: Evidence from Amazonian forests is consistent with isohydric control of leaf water potential, Plant, Cell & Environment, 29, 151–165, https://doi.org/10.1111/j.1365-3040.2005.01407.x, 2006.

Fisher, R. A., Williams, M., Da Costa, A. L., Malhi, Y., Da Costa, R. F., Almeida, S., and Meir, P.: The response of an Eastern Amazonian rain forest to drought stress: results and modelling analyses from a throughfall exclusion experiment, Global Change Biology, 13, 2361–2378, https://doi.org/10.1111/j.1365-2486.2007.01417.x, 2007.

Fisher, R. A., Muszala, S., Verteinstein, M., Lawrence, P., Xu, C., McDowell, N. G., Knox, R. G., Koven, C., Holm, J., Rogers, B. M., Spessa, A., Lawrence, D., and Bonan, G.: Taking off the training wheels: the properties of a dynamic vegetation model without climate envelopes, CLM4.5(ED), Geosci. Model Dev., 8, 3593–3619, https://doi.org/10.5194/gmd-8-3593-2015, 2015.

Fisher, R. A., Koven, C. D., Anderegg, W. R. L., Christoffersen, B. O., Dietze, M. C., Farrior, C. E., Holm, J. A., Hurtt, G. C., Knox, R. G., Lawrence, P. J., Lichstein, J. W., Longo, M., Matheny, A. M., Medvigy, D., Muller-Landau, H. C., Powell, T. L., Serbin, S. P., Sato, H., Shuman, J. K., Smith, B., Trugman, A. T., Viskari, T., Verbeeck, H., Weng, E., Xu, C., Xu, X., Zhang, T., and Moorcroft, P. R.: Vegetation demographics in Earth System Models: A review of progress and priorities, Global Change Biology, 24, 35–54, https://doi.org/10.1111/gcb.13910, 2018.

Flexas, J., Bota, J., Loreto, F., Cornic, G., and Sharkey, T. D.: Diffusive and Metabolic Limitations to Photosynthesis under Drought and Salinity in C3 Plants, Plant biol (Stuttg), 6, 269–279, https://doi.org/10.1055/s-2004-820867, 2004.

Flexas, J., Galmes, J., Ribas-Carbo, M., and Medrano, H.: The Effects of Water Stress on Plant Respiration, in: Plant Respiration, Springer, Dordrecht, 85–94, https://doi.org/10.1007/1-4020-3589-6_6, 2005.

Flexas, J., Bota, J., Galmés, J., Medrano, H., and Ribas-Carbó, M.: Keeping a positive carbon balance under adverse conditions: responses of photosynthesis and respiration to water stress, Physiologia Plantarum, 127, 343–352, https://doi.org/10.1111/j.1399-3054.2006.00621.x, 2006.

Flexas, J., Barbour, M. M., Brendel, O., Cabrera, H. M., Carriquí, M., Díaz-Espejo, A., Douthe, C., Dreyer, E., Ferrio, J. P., Gago, J., Gallé, A., Galmés, J., Kodama, N., Medrano, H., Niinemets, Ü., Peguero-Pina, J. J., Pou, A., Ribas-Carbó, M., Tomás, M., Tosens, T., and Warren, C. R.: Mesophyll diffusion conductance to CO2: An unappreciated central player in photosynthesis, Plant Science, 193–194, 70–84, https://doi.org/10.1016/j.plantsci.2012.05.009, 2012.

Franks, P. J., Bonan, G. B., Berry, J. A., Lombardozzi, D. L., Holbrook, N. M., Herold, N., and Oleson, K. W.: Comparing optimal and empirical stomatal conductance models for application in Earth system models, Global Change Biology, 24, 5708–5723, https://doi.org/10.1111/gcb.14445, 2018.

Franks, S. W., Beven, K. J., Quinn, P. F., and Wright, I. R.: On the sensitivity of soil-vegetation-atmosphere transfer (SVAT) schemes: equifinality and the problem of robust calibration, Agricultural and Forest Meteorology, 86, 63–75, https://doi.org/10.1016/S0168-1923(96)02421-5, 1997.

Friend, A. D., Lucht, W., Rademacher, T. T., Keribin, R., Betts, R., Cadule, P., Ciais, P., Clark, D. B., Dankers, R., Falloon, P. D., Ito, A., Kahana, R., Kleidon, A., Lomas, M. R., Nishina, K., Ostberg, S., Pavlick, R., Peylin, P., Schaphoff, S., Vuichard, N., Warszawski, L., Wiltshire, A., and Woodward, F. I.: Carbon residence time dominates uncertainty in terrestrial vegetation responses to future climate and atmospheric CO2, Proc. Natl. Acad. Sci. U. S. A., 111, 3280–3285, https://doi.org/10.1073/pnas.1222477110, 2014.

Fyllas, N. M., Gloor, E., Mercado, L. M., Sitch, S., Quesada, C. A., Domingues, T. F., Galbraith, D. R., Torre-Lezama, A., Vilanova, E., Ramírez-Angulo, H., Higuchi, N., Neill, D. A., Silveira, M., Ferreira, L., Aymard C., G. A., Malhi, Y., Phillips, O. L., and Lloyd, J.: Analysing Amazonian forest productivity using a new individual and trait-based model (TFS v.1), Geosci. Model Dev., 7, 1251–1269, https://doi.org/10.5194/gmd-7-1251-2014, 2014.

Garcia, M. N., Domingues, T. F., Oliveira, R. S., and Costa, F. R. C.: The biogeography of embolism resistance across resource gradients in the Amazon, Global Ecology and Biogeography, 32, 2199–2211, https://doi.org/10.1111/geb.13765, 2023.

Gardner, W. R.: Relation of Root Distribution to Water Uptake and Availability, Agronomy Journal, 56, 41–45, https://doi.org/10.2134/agronj1964.00021962005600010013x, 1964.

Gash, J. H. C.: An analytical model of rainfall interception by forests, Q.J.R. Meteorol. Soc., 105, 43–55, https://doi.org/10.1002/qj.49710544304, 1979.

Gash, J. H. C., Lloyd, C. R., and Lachaud, G.: Estimating sparse forest rainfall interception with an analytical model, Journal of Hydrology, 170, 79–86, https://doi.org/10.1016/0022-1694(95)02697-N, 1995.

van Genuchten, M. Th.: A Closed-form Equation for Predicting the Hydraulic Conductivity of Unsaturated Soils1, Soil Science Society of America Journal, 44, 892–898, https://doi.org/10.2136/sssaj1980.03615995004400050002x, 1980.

Girard-Tercieux, C., Maréchaux, I., Clark, A. T., Clark, J. S., Courbaud, B., Fortunel, C., Guillemot, J., Künstler, G., le Maire, G., Pélissier, R., Rüger, N., and Vieilledent, G.: Rethinking the nature of intraspecific variability and its consequences on species coexistence, Ecology and Evolution, 13, e9860, https://doi.org/10.1002/ece3.9860, 2023.

Girard-Tercieux, C., Vieilledent, G., Clark, A., Clark, J. S., Courbaud, B., Fortunel, C., Kunstler, G., Pélissier, R., Rüger, N., and Maréchaux, I.: Beyond variance: simple random distributions are not a good proxy for intraspecific variability in systems with environmental structure, Peer Community Journal, 4, https://doi.org/10.24072/pcjournal.360, 2024.

Gourlet-Fleury, S., Blanc, L., Picard, N., Sist, P., Dick, J., Nasi, R., Swaine, M. D., and Forni, E.: Grouping species for predicting mixed tropical forest dynamics: looking for a strategy, Annals of Forest Science, 62, 12, https://doi.org/10.1051/forest:2005084, 2005.

Griffin-Nolan, R. J., Ocheltree, T. W., Mueller, K. E., Blumenthal, D. M., Kray, J. A., and Knapp, A. K.: Extending the osmometer method for assessing drought tolerance in herbaceous species, Oecologia, 189, 353–363, https://doi.org/10.1007/s00442-019-04336-w, 2019.

Gril, E., Spicher, F., Greiser, C., Ashcroft, M. B., Pincebourde, S., Durrieu, S., Nicolas, M., Richard, B., Decocq, G., Marrec, R., and Lenoir, J.: Slope and equilibrium: A parsimonious and flexible approach to model microclimate, Methods in Ecology and Evolution, 14, 885–897, https://doi.org/10.1111/2041-210X.14048, 2023a.

Gril, E., Laslier, M., Gallet-Moron, E., Durrieu, S., Spicher, F., Le Roux, V., Brasseur, B., Haesen, S., Van Meerbeek, K., Decocq, G., Marrec, R., and Lenoir, J.: Using airborne LiDAR to map forest microclimate temperature buffering or amplification, Remote Sensing of Environment, 298, 113820, https://doi.org/10.1016/j.rse.2023.113820, 2023b.

Grisebach, A.: Die Vegetation der Erde nach ihrer klimatischen Anordnung: Ein Abriss der vergleichenden Geographie der Pflanzen. Bd. I und II., Verlag von Wilhelm Engelmann, Leipzig, 1872.

Gu, L., Shugart, H. H., Fuentes, J. D., Black, T. A., and Shewchuk, S. R.: Micrometeorology, biophysical exchanges and NEE decomposition in a two-story boreal forest — development and test of an integrated model, Agricultural and Forest Meteorology, 94, 123–148, https://doi.org/10.1016/S0168-1923(99)00006-4, 1999.

Guan, K., Pan, M., Li, H., Wolf, A., Wu, J., Medvigy, D., Caylor, K. K., Sheffield, J., Wood, E. F., Malhi, Y., Liang, M., Kimball, J. S., Saleska, S. R., Berry, J., Joiner, J., and Lyapustin, A. I.: Photosynthetic seasonality of global tropical forests constrained by hydroclimate, Nature Geosci, 8, 284–289, https://doi.org/10.1038/ngeo2382, 2015.

1515 Guerrero-Ramírez, N. R., Mommer, L., Freschet, G. T., Iversen, C. M., McCormack, M. L., Kattge, J., Poorter, H., van der
1516   Plas, F., Bergmann, J., Kuyper, T. W., York, L. M., Bruelheide, H., Laughlin, D. C., Meier, I. C., Roumet, C., Semchenko,
1517   M., Sweeney, C. J., van Ruijven, J., Valverde-Barrantes, O. J., Aubin, I., Catford, J. A., Manning, P., Martin, A., Milla, R.,
1518   Minden, V., Pausas, J. G., Smith, S. W., Soudzilovskaia, N. A., Ammer, C., Butterfield, B., Craine, J., Cornelissen, J. H.
1519   C., de Vries, F. T., Isaac, M. E., Kramer, K., König, C., Lamb, E. G., Onipchenko, V. G., Peñuelas, J., Reich, P. B., Rillig,
1520   M. C., Sack, L., Shipley, B., Tedersoo, L., Valladares, F., van Bodegom, P., Weigelt, P., Wright, J. P., and Weigelt, A.:
1521   Global root traits (GRooT) database, Global Ecology and Biogeography, 30, 25–37, https://doi.org/10.1111/geb.13179,
1522   2021.

1523 Guillemot, J., Kunz, M., Schnabel, F., Fichtner, A., Madsen, C. P., Gebauer, T., Härdtle, W., von Oheimb, G., and Potvin, C.:
1524   Neighbourhood-mediated shifts in tree biomass allocation drive overyielding in tropical species mixtures, New Phytologist,
1525   228, 1256–1268, https://doi.org/10.1111/nph.16722, 2020.

1526 Guimberteau, M., Ducharne, A., Ciais, P., Boisier, J.-P., Peng, S., De Weirdt, M., and Verbeeck, H.: Testing conceptual and
1527   physically based soil hydrology schemes against observations for the Amazon Basin, Geoscientific Model Development,
1528   7, 1115–1136, https://doi.org/10.5194/gmd-7-1115-2014, 2014.

1529 Guisan, A. and Thuiller, W.: Predicting species distribution: offering more than simple habitat models, Ecology Letters, 8,
1530   993–1009, https://doi.org/10.1111/j.1461-0248.2005.00792.x, 2005.

1531 Guisan, A., Thuiller, W., and Zimmermann, N. E.: Habitat Suitability and Distribution Models: with Applications in R,
1532   Cambridge University Press, 513 pp., 2017.

1533 Gutiérrez, A. G., Armesto, J. J., Díaz, M. F., and Huth, A.: Increased Drought Impacts on Temperate Rainforests from Southern
1534   South America: Results of a Process-Based, Dynamic Forest Model, PLOS ONE, 9, e103226,
1535   https://doi.org/10.1371/journal.pone.0103226, 2014.

1536 Hanbury-Brown, A. R., Ward, R. E., and Kueppers, L. M.: Forest regeneration within Earth system models: current process
1537   representations and ways forward, New Phytologist, 235, 20–40, https://doi.org/10.1111/nph.18131, 2022.

1538 Harper, A., Baker, I. T., Denning, A. S., Randall, D. A., Dazlich, D., and Branson, M.: Impact of evapotranspiration on dry
1539   season climate in the Amazon forest, Journal of Climate, 27, 574–591, https://doi.org/10.1175/JCLI-D-13-00074.1, 2013.

1540 Hartig, F., Dyke, J., Hickler, T., Higgins, S. I., O'Hara, R. B., Scheiter, S., and Huth, A.: Connecting dynamic vegetation
1541   models to data – an inverse perspective, Journal of Biogeography, 39, 2240–2252, https://doi.org/10.1111/j.1365-
1542   2699.2012.02745.x, 2012.

1543 Hasselquist, N. J., Allen, M. F., and Santiago, L. S.: Water relations of evergreen and drought-deciduous trees along a
1544   seasonally dry tropical forest chronosequence, Oecologia, 164, 881–890, https://doi.org/10.1007/s00442-010-1725-y,
1545   2010.

1546 Hengl, T., Jesus, J. M. de, Heuvelink, G. B. M., Gonzalez, M. R., Kilibarda, M., Blagotić, A., Shangguan, W., Wright, M. N.,
1547   Geng, X., Bauer-Marschallinger, B., Guevara, M. A., Vargas, R., MacMillan, R. A., Batjes, N. H., Leenaars, J. G. B.,

1548   Ribeiro, E., Wheeler, I., Mantel, S., and Kempen, B.: SoilGrids250m: Global gridded soil information based on machine
1549   learning, PLOS ONE, 12, e0169748, https://doi.org/10.1371/journal.pone.0169748, 2017.

1550   Héroult, A., Lin, Y.-S., Bourne, A., Medlyn, B. E., and Ellsworth, D. S.: Optimal stomatal conductance in relation to
1551   photosynthesis in climatically contrasting Eucalyptus species under drought, Plant, Cell & Environment, 36, 262–274,
1552   https://doi.org/10.1111/j.1365-3040.2012.02570.x, 2013.

1553   Heskel, M. A., O'Sullivan, O. S., Reich, P. B., Tjoelker, M. G., Weerasinghe, L. K., Penillard, A., Egerton, J. J. G., Creek, D.,
1554   Bloomfield, K. J., Xiang, J., Sinca, F., Stangl, Z. R., Torre, A. M. la, Griffin, K. L., Huntingford, C., Hurry, V., Meir, P.,
1555   Turnbull, M. H., and Atkin, O. K.: Convergence in the temperature response of leaf respiration across biomes and plant
1556   functional types, PNAS, 201520282, https://doi.org/10.1073/pnas.1520282113, 2016.

1557   Hodnett, M. G. and Tomasella, J.: Marked differences between van Genuchten soil water-retention parameters for temperate
1558   and tropical soils: a new water-retention pedo-transfer functions developed for tropical soils, Geoderma, 108, 155–180,
1559   https://doi.org/10.1016/S0016-7061(02)00105-2, 2002.

1560   Horton, R. E.: The role of infiltration in the hydrologic cycle, Eos, Transactions American Geophysical Union, 14, 446–460,
1561   https://doi.org/10.1029/TR014i001p00446, 1933.

1562   Hsiao, T. C.: Plant Responses to Water Stress, Annual Review of Plant Physiology, 24, 519–570,
1563   https://doi.org/10.1146/annurev.pp.24.060173.002511, 1973.

1564   Huaraca Huasco, W., Riutta, T., Girardin, C. A. J., Hancco Pacha, F., Puma Vilca, B. L., Moore, S., Rifai, S. W., del Aguila-
1565   Pasquel, J., Araujo Murakami, A., Freitag, R., Morel, A. C., Demissie, S., Doughty, C. E., Oliveras, I., Galiano Cabrera,
1566   D. F., Durand Baca, L., Farfán Amézquita, F., Silva Espejo, J. E., da Costa, A. C. L., Oblitas Mendoza, E., Quesada, C. A.,
1567   Evouna Ondo, F., Edzang Ndong, J., Jeffery, K. J., Mihindou, V., White, L. J. T., N'ssi Bengone, N., Ibrahim, F., Addo-
1568   Danso, S. D., Duah-Gyamfi, A., Djaney Djagbletey, G., Owusu-Afriyie, K., Amissah, L., Mbou, A. T., Marthews, T. R.,
1569   Metcalfe, D. B., Aragão, L. E. O., Marimon-Junior, B. H., Marimon, B. S., Majalap, N., Adu-Bredu, S., Abernethy, K. A.,
1570   Silman, M., Ewers, R. M., Meir, P., and Malhi, Y.: Fine root dynamics across pantropical rainforest ecosystems, Global
1571   Change Biology, 27, 3657–3680, https://doi.org/10.1111/gcb.15677, 2021.

1572   Hubau, W., Lewis, S. L., Phillips, O. L., Affum-Baffoe, K., Beeckman, H., Cuní-Sanchez, A., Daniels, A. K., Ewango, C. E.
1573   N., Fauset, S., Mukinzi, J. M., Sheil, D., Sonké, B., Sullivan, M. J. P., Sunderland, T. C. H., Taedoumg, H., Thomas, S. C.,
1574   White, L. J. T., Abernethy, K. A., Adu-Bredu, S., Amani, C. A., Baker, T. R., Banin, L. F., Baya, F., Begne, S. K., Bennett,
1575   A. C., Benedet, F., Bitariho, R., Bocko, Y. E., Boeckx, P., Boundja, P., Brienen, R. J. W., Brncic, T., Chezeaux, E.,
1576   Chuyong, G. B., Clark, C. J., Collins, M., Comiskey, J. A., Coomes, D. A., Dargie, G. C., de Haulleville, T., Kamdem, M.
1577   N. D., Doucet, J.-L., Esquivel-Muelbert, A., Feldpausch, T. R., Fofanah, A., Foli, E. G., Gilpin, M., Gloor, E., Gonmadje,
1578   C., Gourlet-Fleury, S., Hall, J. S., Hamilton, A. C., Harris, D. J., Hart, T. B., Hockemba, M. B. N., Hladik, A., Ifo, S. A.,
1579   Jeffery, K. J., Jucker, T., Yakusu, E. K., Kearsley, E., Kenfack, D., Koch, A., Leal, M. E., Levesley, A., Lindsell, J. A.,
1580   Lisingo, J., Lopez-Gonzalez, G., Lovett, J. C., Makana, J.-R., Malhi, Y., Marshall, A. R., Martin, J., Martin, E. H., Mbayu,
1581   F. M., Medjibe, V. P., Mihindou, V., Mitchard, E. T. A., Moore, S., Munishi, P. K. T., Bengone, N. N., Ojo, L., Ondo, F.

E., Peh, K. S.-H., Pickavance, G. C., Poulsen, A. D., Poulsen, J. R., Qie, L., Reitsma, J., Rovero, F., Swaine, M. D., Talbot, J., Taplin, J., Taylor, D. M., Thomas, D. W., Toirambe, B., Mukendi, J. T., Tuagben, D., Umunay, P. M., et al.: Asynchronous carbon sink saturation in African and Amazonian tropical forests, Nature, 579, 80–87, https://doi.org/10.1038/s41586-020-2035-0, 2020.

Humbel, F.-X.: Caractérisation, par des mesures physiques, hydriques et d'enracinement, de sols de Guyane francaise à dynamique de l'eau superficielle, Sciences du sol, 2, 83–94, 1978.

Humboldt, A. von: Aspects of nature, in different lands and different climates; with scientific elucidations, Lea and Blanchard, 512 pp., 1849.

Huntingford, C., Zelazowski, P., Galbraith, D., Mercado, L. M., Sitch, S., Fisher, R., Lomas, M., Walker, A. P., Jones, C. D., Booth, B. B. B., Malhi, Y., Hemming, D., Kay, G., Good, P., Lewis, S. L., Phillips, O. L., Atkin, O. K., Lloyd, J., Gloor, E., Zaragoza-Castells, J., Meir, P., Betts, R., Harris, P. P., Nobre, C., Marengo, J., and Cox, P. M.: Simulated resilience of tropical rainforests to CO_2-induced climate change, Nature Geosci, 6, 268–273, https://doi.org/10.1038/ngeo1741, 2013.

Hutchinson, G. E.: Concluding remarks, Cold Spring Harbor Symposia on Quantitative Biology, 22, 415–427, 1957.

Igarashi, S., Yoshida, S., Kenzo, T., Sakai, S., Nagamasu, H., Hyodo, F., Tayasu, I., Mohamad, M., and Ichie, T.: No evidence of carbon storage usage for seed production in 18 dipterocarp masting species in a tropical rain forest, Oecologia, https://doi.org/10.1007/s00442-024-05527-w, 2024.

Iida, Y., Poorter, L., Sterck, F. J., Kassim, A. R., Kubo, T., Potts, M. D., and Kohyama, T. S.: Wood density explains architectural differentiation across 145 co-occurring tropical tree species, Funct. Ecol., 26, 274–282, https://doi.org/10.1111/j.1365-2435.2011.01921.x, 2012.

Ivanov, V. Y., Hutyra, L. R., Wofsy, S. C., Munger, J. W., Saleska, S. R., Oliveira, R. C. de, and Camargo, P. B. de: Root niche separation can explain avoidance of seasonal drought stress and vulnerability of overstory trees to extended drought in a mature Amazonian forest, Water Resources Research, 48, https://doi.org/10.1029/2012WR011972, 2012.

Jackson, R. B., Canadell, J., Ehleringer, J. R., Mooney, H. A., Sala, O. E., and Schulze, E. D.: A global analysis of root distributions for terrestrial biomes, Oecologia, 108, 389–411, https://doi.org/10.1007/BF00333714, 1996.

Jackson, R. B., Moore, L. A., Hoffmann, W. A., Pockman, W. T., and Linder, C. R.: Ecosystem rooting depth determined with caves and DNA, PNAS, 96, 11387–11392, https://doi.org/10.1073/pnas.96.20.11387, 1999.

Jarvis, P. G. and McNaughton, K. G.: Stomatal Control of Transpiration: Scaling Up from Leaf to Region, Advances in Ecological Research, 15, 1–49, https://doi.org/10.1016/S0065-2504(08)60119-1, 1986.

Joetzjer, E., Delire, C., Douville, H., Ciais, P., Decharme, B., Fisher, R., Christoffersen, B., Calvet, J. C., da Costa, A. C. L., Ferreira, L. V., and Meir, P.: Predicting the response of the Amazon rainforest to persistent drought conditions under current and future climates: a major challenge for global land surface models, Geosci. Model Dev., 7, 2933–2950, https://doi.org/10.5194/gmd-7-2933-2014, 2014.

1614 Joetzjer, E., Maignan, F., Chave, J., Goll, D., Poulter, B., Barichivich, J., Maréchaux, I., Luyssaert, S., Guimberteau, M.,
1615   Naudts, K., Bonal, D., and Ciais, P.: Effect of tree demography and flexible root water uptake for modeling the carbon and
1616   water cycles of Amazonia, Ecological Modelling, 469, 109969, https://doi.org/10.1016/j.ecolmodel.2022.109969, 2022.

1617 Johnson, D. J., Condit, R., Hubbell, S. P., and Comita, L. S.: Abiotic niche partitioning and negative density dependence drive
1618   tree seedling survival in a tropical forest, Proc. R. Soc. B, 284, 20172210, https://doi.org/10.1098/rspb.2017.2210, 2017.

1619 Johnson, M. O., Galbraith, D., Gloor, M., De Deurwaerder, H., Guimberteau, M., Rammig, A., Thonicke, K., Verbeeck, H.,
1620   von Randow, C., Monteagudo, A., Phillips, O. L., Brienen, R. J. W., Feldpausch, T. R., Lopez Gonzalez, G., Fauset, S.,
1621   Quesada, C. A., Christoffersen, B., Ciais, P., Sampaio, G., Kruijt, B., Meir, P., Moorcroft, P., Zhang, K., Alvarez-Davila,
1622   E., Alves de Oliveira, A., Amaral, I., Andrade, A., Aragao, L. E. O. C., Araujo-Murakami, A., Arets, E. J. M. M., Arroyo,
1623   L., Aymard, G. A., Baraloto, C., Barroso, J., Bonal, D., Boot, R., Camargo, J., Chave, J., Cogollo, A., Cornejo Valverde,
1624   F., Lola da Costa, A. C., Di Fiore, A., Ferreira, L., Higuchi, N., Honorio, E. N., Killeen, T. J., Laurance, S. G., Laurance,
1625   W. F., Licona, J., Lovejoy, T., Malhi, Y., Marimon, B., Marimon, B. H., Matos, D. C. L., Mendoza, C., Neill, D. A., Pardo,
1626   G., Peña-Claros, M., Pitman, N. C. A., Poorter, L., Prieto, A., Ramirez-Angulo, H., Roopsind, A., Rudas, A., Salomao, R.
1627   P., Silveira, M., Stropp, J., ter Steege, H., Terborgh, J., Thomas, R., Toledo, M., Torres-Lezama, A., van der Heijden, G.
1628   M. F., Vasquez, R., Guimarães Vieira, I. C., Vilanova, E., Vos, V. A., and Baker, T. R.: Variation in stem mortality rates
1629   determines patterns of above-ground biomass in Amazonian forests: implications for dynamic global vegetation models,
1630   Glob Change Biol, 22, 3996–4013, https://doi.org/10.1111/gcb.13315, 2016.

1631 Jones, H. G.: Plants and Microclimate: A Quantitative Approach to Environmental Plant Physiology, 3rd ed., Cambridge
1632   University Press, Cambridge, https://doi.org/10.1017/CBO9780511845727, 2013.

1633 Jourdan, M., Kunstler, G., and Morin, X.: How neighbourhood interactions control the temporal stability and resilience to
1634   drought of trees in mountain forests, Journal of Ecology, 108, 666–677, https://doi.org/10.1111/1365-2745.13294, 2020.

1635 Journé, V., Barnagaud, J.-Y., Bernard, C., Crochet, P.-A., and Morin, X.: Correlative climatic niche models predict real and
1636   virtual species distributions equally well, Ecology, 101, e02912, https://doi.org/10.1002/ecy.2912, 2020.

1637 Jucker, T., Caspersen, J., Chave, J., Antin, C., Barbier, N., Bongers, F., Dalponte, M., van Ewijk, K. Y., Forrester, D. I., Haeni,
1638   M., Higgins, S. I., Holdaway, R. J., Iida, Y., Lorimer, C., Marshall, P. L., Momo, S., Moncrieff, G. R., Ploton, P., Poorter,
1639   L., Rahman, K. A., Schlund, M., Sonké, B., Sterck, F. J., Trugman, A. T., Usoltsev, V. A., Vanderwel, M. C., Waldner, P.,
1640   Wedeux, B. M. M., Wirth, C., Wöll, H., Woods, M., Xiang, W., Zimmermann, N. E., and Coomes, D. A.: Allometric
1641   equations for integrating remote sensing imagery into forest monitoring programmes, Glob Change Biol, 23, 177–190,
1642   https://doi.org/10.1111/gcb.13388, 2017.

1643 Jucker, T., Hardwick, S. R., Both, S., Elias, D. M. O., Ewers, R. M., Milodowski, D. T., Swinfield, T., and Coomes, D. A.:
1644   Canopy structure and topography jointly constrain the microclimate of human-modified tropical landscapes, Global Change
1645   Biology, 24, 5243–5258, https://doi.org/10.1111/gcb.14415, 2018.

1646 Jucker, T., Fischer, F. J., Chave, J., Coomes, D. A., Caspersen, J., Ali, A., Loubota Panzou, G. J., Feldpausch, T. R., Falster,
1647   D., Usoltsev, V. A., Adu-Bredu, S., Alves, L. F., Aminpour, M., Angoboy, I. B., Anten, N. P. R., Antin, C., Askari, Y.,

Muñoz, R., Ayyappan, N., Balvanera, P., Banin, L., Barbier, N., Battles, J. J., Beeckman, H., Bocko, Y. E., Bond-Lamberty, B., Bongers, F., Bowers, S., Brade, T., van Breugel, M., Chantrain, A., Chaudhary, R., Dai, J., Dalponte, M., Dimobe, K., Domec, J.-C., Doucet, J.-L., Duursma, R. A., Enríquez, M., van Ewijk, K. Y., Farfán-Rios, W., Fayolle, A., Forni, E., Forrester, D. I., Gilani, H., Godlee, J. L., Gourlet-Fleury, S., Haeni, M., Hall, J. S., He, J.-K., Hemp, A., Hernández-Stefanoni, J. L., Higgins, S. I., Holdaway, R. J., Hussain, K., Hutley, L. B., Ichie, T., Iida, Y., Jiang, H., Joshi, P. R., Kaboli, H., Larsary, M. K., Kenzo, T., Kloeppel, B. D., Kohyama, T., Kunwar, S., Kuyah, S., Kvasnica, J., Lin, S., Lines, E. R., Liu, H., Lorimer, C., Loumeto, J.-J., Malhi, Y., Marshall, P. L., Mattsson, E., Matula, R., Meave, J. A., Mensah, S., Mi, X., Momo, S., Moncrieff, G. R., Mora, F., Nissanka, S. P., O'Hara, K. L., Pearce, S., Pelissier, R., Peri, P. L., Ploton, P., Poorter, L., Pour, M. J., Pourbabaei, H., Dupuy-Rada, J. M., Ribeiro, S. C., Ryan, C., Sanaei, A., Sanger, J., Schlund, M., Sellan, G., et al.: Tallo: A global tree allometry and crown architecture database, Global Change Biology, 28, 5254–5268, https://doi.org/10.1111/gcb.16302, 2022.

Kattge, J. and Knorr, W.: Temperature acclimation in a biochemical model of photosynthesis: a reanalysis of data from 36 species, Plant, Cell & Environment, 30, 1176–1190, https://doi.org/10.1111/j.1365-3040.2007.01690.x, 2007.

Kattge, J., Díaz, S., Lavorel, S., Prentice, I. C., Leadley, P., Bönisch, G., Garnier, E., Westoby, M., Reich, P. B., Wright, I. J., Cornelissen, J. H. C., Violle, C., Harrison, S. P., Van Bodegom, P. M., Reichstein, M., Enquist, B. J., Soudzilovskaia, N. A., Ackerly, D. D., Anand, M., Atkin, O., Bahn, M., Baker, T. R., Baldocchi, D., Bekker, R., Blanco, C. C., Blonder, B., Bond, W. J., Bradstock, R., Bunker, D. E., Casanoves, F., Cavender-bares, J., Chambers, J. Q., Chapin Iii, F. S., Chave, J., Coomes, D., Cornwell, W. K., Craine, J. M., Dobrin, B. H., Duarte, L., Durka, W., Elser, J., Esser, G., Estiarte, M., Fagan, W. F., Fang, J., Fernández-méndez, F., Fidelis, A., Finegan, B., Flores, O., Ford, H., Frank, D., Freschet, G. T., Fyllas, N. M., Gallagher, R. V., Green, W. A., Gutierrez, A. G., Hickler, T., Higgins, S. I., Hodgson, J. G., Jalili, A., Jansen, S., Joly, C. A., Kerkhoff, A. J., Kirkup, D., Kitajima, K., Kleyer, M., Klotz, S., Knops, J. M. H., Kramer, K., Kühn, I., Kurokawa, H., Laughlin, D., Lee, T. D., Leishman, M., Lens, F., Lenz, T., Lewis, S. L., Lloyd, J., Llusià, J., Louault, F., Ma, S., Mahecha, M. D., Manning, P., Massad, T., Medlyn, B. E., Messier, J., Moles, A. T., Müller, S. C., Nadrowski, K., Naeem, S., Niinemets, Ü., Nöllert, S., Nüske, A., Ogaya, R., Oleksyn, J., Onipchenko, V. G., Onoda, Y., Ordoñez, J., Overbeck, G., et al.: TRY – a global database of plant traits, Global Change Biology, 17, 2905–2935, https://doi.org/10.1111/j.1365-2486.2011.02451.x, 2011.

Kattge, J., Bönisch, G., Díaz, S., Lavorel, S., Prentice, I. C., Leadley, P., Tautenhahn, S., Werner, G. D. A., Aakala, T., Abedi, M., Acosta, A. T. R., Adamidis, G. C., Adamson, K., Aiba, M., Albert, C. H., Alcántara, J. M., C, C. A., Aleixo, I., Ali, H., Amiaud, B., Ammer, C., Amoroso, M. M., Anand, M., Anderson, C., Anten, N., Antos, J., Apgaua, D. M. G., Ashman, T.-L., Asmara, D. H., Asner, G. P., Aspinwall, M., Atkin, O., Aubin, I., Baastrup-Spohr, L., Bahalkeh, K., Bahn, M., Baker, T., Baker, W. J., Bakker, J. P., Baldocchi, D., Baltzer, J., Banerjee, A., Baranger, A., Barlow, J., Barneche, D. R., Baruch, Z., Bastianelli, D., Battles, J., Bauerle, W., Bauters, M., Bazzato, E., Beckmann, M., Beeckman, H., Beierkuhnlein, C., Bekker, R., Belfry, G., Belluau, M., Beloiu, M., Benavides, R., Benomar, L., Berdugo-Lattke, M. L., Berenguer, E., Bergamin, R., Bergmann, J., Carlucci, M. B., Berner, L., Bernhardt-Römermann, M., Bigler, C., Bjorkman, A. D.,

1682 Blackman, C., Blanco, C., Blonder, B., Blumenthal, D., Bocanegra-González, K. T., Boeckx, P., Bohlman, S., Böhning-
1683 Gaese, K., Boisvert-Marsh, L., Bond, W., Bond-Lamberty, B., Boom, A., Boonman, C. C. F., Bordin, K., Boughton, E. H.,
1684 Boukili, V., Bowman, D. M. J. S., Bravo, S., Brendel, M. R., Broadley, M. R., Brown, K. A., Bruelheide, H., Brumnich,
1685 F., Bruun, H. H., Bruy, D., Buchanan, S. W., Bucher, S. F., Buchmann, N., Buitenwerf, R., Bunker, D. E., et al.: TRY plant
1686 trait database – enhanced coverage and open access, Global Change Biology, 26, 119–188,
1687 https://doi.org/10.1111/gcb.14904, 2020.

1688 Kazmierczak, M., Wiegand, T., and Huth, A.: A neutral vs. non-neutral parametrizations of a physiological forest gap model,
1689 Ecological Modelling, 288, 94–102, https://doi.org/10.1016/j.ecolmodel.2014.05.002, 2014.

1690 Kearney, M. and Porter, W.: Mechanistic niche modelling: combining physiological and spatial data to predict species' ranges,
1691 Ecology Letters, 12, 334–350, https://doi.org/10.1111/j.1461-0248.2008.01277.x, 2009.

1692 Keenan, T., Sabate, S., and Gracia, C.: Soil water stress and coupled photosynthesis–conductance models: Bridging the gap
1693 between conflicting reports on the relative roles of stomatal, mesophyll conductance and biochemical limitations to
1694 photosynthesis, Agricultural and Forest Meteorology, 150, 443–453, https://doi.org/10.1016/j.agrformet.2010.01.008,
1695 2010.

1696 Kennedy, D., Swenson, S., Oleson, K. W., Lawrence, D. M., Fisher, R., Costa, A. C. L. da, and Gentine, P.: Implementing
1697 Plant Hydraulics in the Community Land Model, Version 5, Journal of Advances in Modeling Earth Systems, 11, 485–
1698 513, https://doi.org/10.1029/2018MS001500, 2019.

1699 Kenzo, T., Ichie, T., Hattori, D., Itioka, T., Handa, C., Ohkubo, T., Kendawang, J. J., Nakamura, M., Sakaguchi, M., Takahashi,
1700 N., Okamoto, M., Tanaka-Oda, A., Sakurai, K., and Ninomiya, I.: Development of allometric relationships for accurate
1701 estimation of above- and below-ground biomass in tropical secondary forests in Sarawak, Malaysia, Journal of Tropical
1702 Ecology, 25, 371–386, https://doi.org/10.1017/S0266467409006129, 2009.

1703 Khan, S., Maréchaux, I., Vieilledent, G., Guitet, S., Brunaux, O., Ferry, B., Soulard, F., Stahl, C., Baraloto, C., Fortunel, C.,
1704 and Freycon, V.: Regional Soil Profile Data Reveals the Predominant Role of Geomorphology and Geology in Accurately
1705 Deriving Digital Soil Texture Maps in a Tropical Area, https://doi.org/10.2139/ssrn.4789279, 9 April 2024.

1706 King, D. A., Davies, S. J., Tan, S., and Noor, N. S. Md.: The role of wood density and stem support costs in the growth and
1707 mortality of tropical trees, Journal of Ecology, 94, 670–680, https://doi.org/10.1111/j.1365-2745.2006.01112.x, 2006.

1708 Kitajima, K., Mulkey, S., and Wright, S.: Decline of photosynthetic capacity with leaf age in relation to leaf longevities for
1709 five tropical canopy tree species., Am. J. Bot., 84, 702–702, 1997a.

1710 Kitajima, K., Mulkey, S. S., and Wright, S. J.: Seasonal leaf phenotypes in the canopy of a tropical dry forest: photosynthetic
1711 characteristics and associated traits, Oecologia, 109, 490–498, https://doi.org/10.1007/s004420050109, 1997b.

1712 Kitajima, K., Mulkey, S. S., Samaniego, M., and Wright, S. J.: Decline of photosynthetic capacity with leaf age and position
1713 in two tropical pioneer tree species, Am. J. Bot., 89, 1925–1932, https://doi.org/10.3732/ajb.89.12.1925, 2002.

1714 Kitajima, K., Mulkey, S. S., and Wright, S. J.: Variation in crown light utilization characteristics among tropical canopy trees,
1715 Ann Bot, 95, 535–547, https://doi.org/10.1093/aob/mci051, 2005.

1716 Koch, A., Hubau, W., and Lewis, S. L.: Earth System Models Are Not Capturing Present-Day Tropical Forest Carbon
1717   Dynamics, Earth's Future, 9, e2020EF001874, https://doi.org/10.1029/2020EF001874, 2021.

1718 Köhler, P. and Huth, A.: The effects of tree species grouping in tropical rainforest modelling: simulations with the individual-
1719   based model Formind, Ecological Modelling, 109, 301–321, https://doi.org/10.1016/S0304-3800(98)00066-0, 1998.

1720 Köhler, P., Ditzer, T., and Huth, A.: Concepts for the aggregation of tropical tree species into functional types and the
1721   application to Sabah's lowland rain forests, Journal of Tropical Ecology, 16, 591–602, https://doi.org/null, 2000.

1722 König, L. A., Mohren, F., Schelhaas, M.-J., Bugmann, H., and Nabuurs, G.-J.: Tree regeneration in models of forest dynamics
1723   – Suitability to assess climate change impacts on European forests, Forest Ecology and Management, 520, 120390,
1724   https://doi.org/10.1016/j.foreco.2022.120390, 2022.

1725 Körner, C.: Paradigm shift in plant growth control, Current Opinion in Plant Biology, 25, 107–114,
1726   https://doi.org/10.1016/j.pbi.2015.05.003, 2015.

1727 Kraft, N. J. B., Metz, M. R., Condit, R. S., and Chave, J.: The relationship between wood density and mortality in a global
1728   tropical forest data set, New Phytologist, 188, 1124–1136, https://doi.org/10.1111/j.1469-8137.2010.03444.x, 2010.

1729 Krinner, G., Viovy, N., de Noblet-Ducoudré, N., Ogée, J., Polcher, J., Friedlingstein, P., Ciais, P., Sitch, S., and Prentice, I.
1730   C.: A dynamic global vegetation model for studies of the coupled atmosphere-biosphere system, Global Biogeochem.
1731   Cycles, 19, GB1015, https://doi.org/10.1029/2003GB002199, 2005.

1732 Kume, A., Nasahara, K. N., Nagai, S., and Muraoka, H.: The ratio of transmitted near-infrared radiation to photosynthetically
1733   active radiation (PAR) increases in proportion to the adsorbed PAR in the canopy, J Plant Res, 124, 99–106,
1734   https://doi.org/10.1007/s10265-010-0346-1, 2011.

1735 Kupers, S. J., Engelbrecht, B. M. J., Hernández, A., Wright, S. J., Wirth, C., and Rüger, N.: Growth responses to soil water
1736   potential indirectly shape local species distributions of tropical forest seedlings, Journal of Ecology, 107, 860–874,
1737   https://doi.org/10.1111/1365-2745.13096, 2019.

1738 Kursar, T. A., Engelbrecht, B. M. J., Burke, A., Tyree, M. T., EI Omari, B., and Giraldo, J. P.: Tolerance to low leaf water
1739   status of tropical tree seedlings is related to drought performance and distribution, Functional Ecology, 23, 93–102,
1740   https://doi.org/10.1111/j.1365-2435.2008.01483.x, 2009.

1741 Lagarrigues, G., Jabot, F., Lafond, V., and Courbaud, B.: Approximate Bayesian computation to recalibrate individual-based
1742   models with population data: illustration with a forest simulation model, Ecological Modelling, 306, 278–286,
1743   https://doi.org/10.1016/j.ecolmodel.2014.09.023, 2015.

1744 Laio, F., Porporato, A., Ridolfi, L., and Rodriguez-Iturbe, I.: Plants in water-controlled ecosystems: active role in hydrologic
1745   processes and response to water stress: II. Probabilistic soil moisture dynamics, Advances in Water Resources, 24, 707–
1746   723, https://doi.org/10.1016/S0309-1708(01)00005-7, 2001.

1747 Lamour, J., Davidson, K. J., Ely, K. S., Le Moguédec, G., Leakey, A. D. B., Li, Q., Serbin, S. P., and Rogers, A.: An improved
1748   representation of the relationship between photosynthesis and stomatal conductance leads to more stable estimation of

1749   conductance parameters and improves the goodness-of-fit across diverse data sets, Global Change Biology, 28, 3537–3556,
1750   https://doi.org/10.1111/gcb.16103, 2022.

1751 Lamour, J., Souza, D. C., Gimenez, B. O., Higuchi, N., Chave, J., Chambers, J., and Rogers, A.: Wood-density has no effect
1752   on stomatal control of leaf-level water use efficiency in an Amazonian forest, Plant, Cell & Environment, 46, 3806–3821,
1753   https://doi.org/10.1111/pce.14704, 2023.

1754 Lapola, D. M., Pinho, P., Barlow, J., Aragão, L. E. O. C., Berenguer, E., Carmenta, R., Liddy, H. M., Seixas, H., Silva, C. V.
1755   J., Silva-Junior, C. H. L., Alencar, A. A. C., Anderson, L. O., Armenteras, D., Brovkin, V., Calders, K., Chambers, J.,
1756   Chini, L., Costa, M. H., Faria, B. L., Fearnside, P. M., Ferreira, J., Gatti, L., Gutierrez-Velez, V. H., Han, Z., Hibbard, K.,
1757   Koven, C., Lawrence, P., Pongratz, J., Portela, B. T. T., Rounsevell, M., Ruane, A. C., Schaldach, R., da Silva, S. S., von
1758   Randow, C., and Walker, W. S.: The drivers and impacts of Amazon forest degradation, Science, 379, eabp8622,
1759   https://doi.org/10.1126/science.abp8622, 2023.

1760 Laurans, M., Munoz, F., Charles-Dominique, T., Heuret, P., Fortunel, C., Isnard, S., Sabatier, S.-A., Caraglio, Y., and Violle,
1761   C.: Why incorporate plant architecture into trait-based ecology?, Trends in Ecology & Evolution, 0,
1762   https://doi.org/10.1016/j.tree.2023.11.011, 2024.

1763 LeBauer, D. S., Wang, D., Richter, K. T., Davidson, C. C., and Dietze, M. C.: Facilitating feedbacks between field
1764   measurements and ecosystem models, Ecological Monographs, 83, 133–154, https://doi.org/10.1890/12-0137.1, 2013.

1765 Ledo, A., Paul, K. I., Burslem, D. F. R. P., Ewel, J. J., Barton, C., Battaglia, M., Brooksbank, K., Carter, J., Eid, T. H., England,
1766   J. R., Fitzgerald, A., Jonson, J., Mencuccini, M., Montagu, K. D., Montero, G., Mugasha, W. A., Pinkard, E., Roxburgh,
1767   S., Ryan, C. M., Ruiz-Peinado, R., Sochacki, S., Specht, A., Wildy, D., Wirth, C., Zerihun, A., and Chave, J.: Tree size
1768   and climatic water deficit control root to shoot ratio in individual trees globally, New Phytologist, 217, 8–11,
1769   https://doi.org/10.1111/nph.14863, 2018.

1770 Leitold, V., Morton, D. C., Longo, M., dos-Santos, M. N., Keller, M., and Scaranello, M.: El Niño drought increased canopy
1771   turnover in Amazon forests, New Phytologist, 219, 959–971, https://doi.org/10.1111/nph.15110, 2018.

1772 Lenz, T. I., Wright, I. J., and Westoby, M.: Interrelations among pressure–volume curve traits across species and water
1773   availability gradients, Physiologia Plantarum, 127, 423–433, https://doi.org/10.1111/j.1399-3054.2006.00680.x, 2006.

1774 Leuning, R., Kelliher, F. M., Pury, D. G. G., and Schulze, E. -d: Leaf nitrogen, photosynthesis, conductance and transpiration:
1775   scaling from leaves to canopies, Plant, Cell & Environment, 18, 1183–1200, https://doi.org/10.1111/j.1365-
1776   3040.1995.tb00628.x, 1995.

1777 Li, Q., Serbin, S. P., Lamour, J., Davidson, K. J., Ely, K. S., and Rogers, A.: Implementation and evaluation of the unified
1778   stomatal optimization approach in the Functionally Assembled Terrestrial Ecosystem Simulator (FATES), Geoscientific
1779   Model Development, 15, 4313–4329, https://doi.org/10.5194/gmd-15-4313-2022, 2022.

1780 Liang, J. and Picard, N.: Matrix Model of Forest Dynamics: An Overview and Outlook, Forest Science, 59, 359–378,
1781   https://doi.org/10.5849/forsci.11-123, 2013.

1782   Liang, X., Lettenmaier, D. P., Wood, E. F., and Burges, S. J.: A simple hydrologically based model of land surface water and
1783   energy fluxes for general circulation models, J. Geophys. Res., 99, 14415–14428, https://doi.org/10.1029/94JD00483,
1784   1994.

1785   Lin, Y.-S., Medlyn, B. E., Duursma, R. A., Prentice, I. C., Wang, H., Baig, S., Eamus, D., de Dios, V. R., Mitchell, P.,
1786   Ellsworth, D. S., de Beeck, M. O., Wallin, G., Uddling, J., Tarvainen, L., Linderson, M.-L., Cernusak, L. A., Nippert, J.
1787   B., Ocheltree, T. W., Tissue, D. T., Martin-StPaul, N. K., Rogers, A., Warren, J. M., De Angelis, P., Hikosaka, K., Han,
1788   Q., Onoda, Y., Gimeno, T. E., Barton, C. V. M., Bennie, J., Bonal, D., Bosc, A., Löw, M., Macinins-Ng, C., Rey, A.,
1789   Rowland, L., Setterfield, S. A., Tausz-Posch, S., Zaragoza-Castells, J., Broadmeadow, M. S. J., Drake, J. E., Freeman, M.,
1790   Ghannoum, O., Hutley, L. B., Kelly, J. W., Kikuzawa, K., Kolari, P., Koyama, K., Limousin, J.-M., Meir, P., Lola da
1791   Costa, A. C., Mikkelsen, T. N., Salinas, N., Sun, W., and Wingate, L.: Optimal stomatal behaviour around the world, Nature
1792   Clim. Change, 5, 459–464, https://doi.org/10.1038/nclimate2550, 2015.

1793   Liu, Y., Parolari, A. J., Kumar, M., Huang, C.-W., Katul, G. G., and Porporato, A.: Increasing atmospheric humidity and CO2
1794   concentration alleviate forest mortality risk, PNAS, 114, 9918–9923, https://doi.org/10.1073/pnas.1704811114, 2017.

1795   Long, S. P., Postl, W. F., and Bolhár-Nordenkampf, H. R.: Quantum yields for uptake of carbon dioxide in C3 vascular
1796   plants of contrasting habitats and taxonomic groupings, Planta, 189, 226–234, https://doi.org/10.1007/BF00195081,
1797   1993.

1798   Longo, M., Knox, R. G., Medvigy, D. M., Levine, N. M., Dietze, M. C., Kim, Y., Swann, A. L. S., Zhang, K., Rollinson, C.
1799   R., Bras, R. L., Wofsy, S. C., and Moorcroft, P. R.: The biophysics, ecology, and biogeochemistry of functionally diverse,
1800   vertically and horizontally heterogeneous ecosystems: the Ecosystem Demography model, version 2.2 – Part 1: Model
1801   description, Geoscientific Model Development, 12, 4309–4346, https://doi.org/10.5194/gmd-12-4309-2019, 2019.

1802   Loubry, D.: La phénologie des arbres caducifoliés en forêt guyanaise (5° de latitude nord) : illustration d'un déterminisme à
1803   composantes endogène et exogène, Can. J. Bot., 72, 1843–1857, https://doi.org/10.1139/b94-226, 1994.

1804   Maclean, I. M. D. and Klinges, D. H.: Microclimc: A mechanistic model of above, below and within-canopy microclimate,
1805   Ecological Modelling, 451, 109567, https://doi.org/10.1016/j.ecolmodel.2021.109567, 2021.

1806   Mahnken, M., Cailleret, M., Collalti, A., Trotta, C., Biondo, C., D'Andrea, E., Dalmonech, D., Marano, G., Mäkelä, A.,
1807   Minunno, F., Peltoniemi, M., Trotsiuk, V., Nadal-Sala, D., Sabaté, S., Vallet, P., Aussenac, R., Cameron, D. R., Bohn, F.
1808   J., Grote, R., Augustynczik, A. L. D., Yousefpour, R., Huber, N., Bugmann, H., Merganičová, K., Merganic, J., Valent, P.,
1809   Lasch-Born, P., Hartig, F., Vega del Valle, I. D., Volkholz, J., Gutsch, M., Matteucci, G., Krejza, J., Ibrom, A., Meesenburg,
1810   H., Rötzer, T., van der Maaten-Theunissen, M., van der Maaten, E., and Reyer, C. P. O.: Accuracy, realism and general
1811   applicability of European forest models, Global Change Biology, 28, 6921–6943, https://doi.org/10.1111/gcb.16384, 2022.

1812   Malhi, Y.: The productivity, metabolism and carbon cycle of tropical forest vegetation, Journal of Ecology, 100, 65–75,
1813   https://doi.org/10.1111/j.1365-2745.2011.01916.x, 2012.

1814   Malhi, Y., Doughty, C., and Galbraith, D.: The allocation of ecosystem net primary productivity in tropical forests,
1815   Philosophical Transactions of the Royal Society of London B: Biological Sciences, 366, 3225–3245,
1816   https://doi.org/10.1098/rstb.2011.0062, 2011.

1817   Manabe, S.: Climate and the ocean circulation: I. The atmospheric circulation and the hydrology of the earth's surface, Mon.
1818   Wea. Rev., 97, 739–774, https://doi.org/10.1175/1520-0493(1969)097<0739:CATOC>2.3.CO;2, 1969.

1819   Manoli, G., Ivanov, V. Y., and Fatichi, S.: Dry-Season Greening and Water Stress in Amazonia: The Role of Modeling Leaf
1820   Phenology, Journal of Geophysical Research: Biogeosciences, 123, 1909–1926, https://doi.org/10.1029/2017JG004282,
1821   2018.

1822   Manzoni, S.: Integrating plant hydraulics and gas exchange along the drought-response trait spectrum, Tree Physiol, tpu088,
1823   https://doi.org/10.1093/treephys/tpu088, 2014.

1824   Maréchaux, I. and Chave, J.: An individual-based forest model to jointly simulate carbon and tree diversity in Amazonia:
1825   description and applications, Ecol Monogr, 87, 632–664, https://doi.org/10.1002/ecm.1271, 2017.

1826   Maréchaux, I., Bartlett, M. K., Sack, L., Baraloto, C., Engel, J., Joetzjer, E., and Chave, J.: Drought tolerance as predicted by
1827   leaf water potential at turgor loss point varies strongly across species within an Amazonian forest, Funct Ecol, 29, 1268–
1828   1277, https://doi.org/10.1111/1365-2435.12452, 2015.

1829   Maréchaux, I., Bartlett, M. K., Gaucher, P., Sack, L., and Chave, J.: Causes of variation in leaf-level drought tolerance within
1830   an Amazonian forest, Journal of Plant Hydraulics, 3, e004, 2016.

1831   Maréchaux, I., Bonal, D., Bartlett, M. K., Burban, B., Coste, S., Courtois, E. A., Dulormne, M., Goret, J.-Y., Mira, E., Mirabel,
1832   A., Sack, L., Stahl, C., and Chave, J.: Dry-season decline in tree sapflux is correlated with leaf turgor loss point in a tropical
1833   rainforest, Functional Ecology, 32, 2285–2297, https://doi.org/10.1111/1365-2435.13188, 2018.

1834   Maréchaux, I., Saint-André, L., Bartlett, M. K., Sack, L., and Chave, J.: Leaf drought tolerance cannot be inferred from classic
1835   leaf traits in a tropical rainforest, Journal of Ecology, 108, 1030–1045, https://doi.org/10.1111/1365-2745.13321, 2020.

1836   Maréchaux, I., Langerwisch, F., Huth, A., Bugmann, H., Morin, X., Reyer, C. P. O., Seidl, R., Collalti, A., Paula, M. D. de,
1837   Fischer, R., Gutsch, M., Lexer, M. J., Lischke, H., Rammig, A., Rödig, E., Sakschewski, B., Taubert, F., Thonicke, K.,
1838   Vacchiano, G., and Bohn, F. J.: Tackling unresolved questions in forest ecology: The past and future role of simulation
1839   models, Ecology and Evolution, 11, 3746–3770, https://doi.org/10.1002/ece3.7391, 2021.

1840   Marthews, T. R., Malhi, Y., and Iwata, H.: Calculating downward longwave radiation under clear and cloudy conditions over
1841   a tropical lowland forest site: an evaluation of model schemes for hourly data, Theor Appl Climatol, 107, 461–477,
1842   https://doi.org/10.1007/s00704-011-0486-9, 2012.

1843   Marthews, T. R., Quesada, C. A., Galbraith, D. R., Malhi, Y., Mullins, C. E., Hodnett, M. G., and Dharssi, I.: High-resolution
1844   hydraulic parameter maps for surface soils in tropical South America, Geoscientific Model Development, 7, 711, 2014.

1845   Martínez-Vilalta, J., Sala, A., Asensio, D., Galiano, L., Hoch, G., Palacio, S., Piper, F. I., and Lloret, F.: Dynamics of non-
1846   structural carbohydrates in terrestrial plants: a global synthesis, Ecol Monogr, 86, 495–516,
1847   https://doi.org/10.1002/ecm.1231, 2016.

Martin-StPaul, N., Delzon, S., and Cochard, H.: Plant resistance to drought depends on timely stomatal closure, Ecol Lett, 20, 1437–1447, https://doi.org/10.1111/ele.12851, 2017.

McDowell, N. G., Sapes, G., Pivovaroff, A., Adams, H. D., Allen, C. D., Anderegg, W. R. L., Arend, M., Breshears, D. D., Brodribb, T., Choat, B., Cochard, H., De Cáceres, M., De Kauwe, M. G., Grossiord, C., Hammond, W. M., Hartmann, H., Hoch, G., Kahmen, A., Klein, T., Mackay, D. S., Mantova, M., Martínez-Vilalta, J., Medlyn, B. E., Mencuccini, M., Nardini, A., Oliveira, R. S., Sala, A., Tissue, D. T., Torres-Ruiz, J. M., Trowbridge, A. M., Trugman, A. T., Wiley, E., and Xu, C.: Mechanisms of woody-plant mortality under rising drought, CO2 and vapour pressure deficit, Nat Rev Earth Environ, 1–15, https://doi.org/10.1038/s43017-022-00272-1, 2022.

McMahon, S. M., Harrison, S. P., Armbruster, W. S., Bartlein, P. J., Beale, C. M., Edwards, M. E., Kattge, J., Midgley, G., Morin, X., and Prentice, I. C.: Improving assessment and modelling of climate change impacts on global terrestrial biodiversity, Trends in Ecology & Evolution, 26, 249–259, https://doi.org/10.1016/j.tree.2011.02.012, 2011.

Medlyn, B. E., Robinson, A. P., Clement, R., and McMurtrie, R. E.: On the validation of models of forest CO2 exchange using eddy covariance data: some perils and pitfalls, Tree Physiol, 25, 839–857, https://doi.org/10.1093/treephys/25.7.839, 2005.

Medlyn, B. E., Pepper, D. A., O'Grady, A. P., and Keith, H.: Linking leaf and tree water use with an individual-tree model, Tree Physiol, 27, 1687–1699, https://doi.org/10.1093/treephys/27.12.1687, 2007.

Medlyn, B. E., Duursma, R. A., Eamus, D., Ellsworth, D. S., Prentice, I. C., Barton, C. V. M., Crous, K. Y., De Angelis, P., Freeman, M., and Wingate, L.: Reconciling the optimal and empirical approaches to modelling stomatal conductance, Global Change Biology, 17, 2134–2144, https://doi.org/10.1111/j.1365-2486.2010.02375.x, 2011.

Medlyn, B. E., Zaehle, S., De Kauwe, M. G., Walker, A. P., Dietze, M. C., Hanson, P. J., Hickler, T., Jain, A. K., Luo, Y., Parton, W., Prentice, I. C., Thornton, P. E., Wang, S., Wang, Y.-P., Weng, E., Iversen, C. M., McCarthy, H. R., Warren, J. M., Oren, R., and Norby, R. J.: Using ecosystem experiments to improve vegetation models, Nature Clim. Change, 5, 528–534, https://doi.org/10.1038/nclimate2621, 2015.

Medlyn, B. E., De Kauwe, M. G., Zaehle, S., Walker, A. P., Duursma, R. A., Luus, K., Mishurov, M., Pak, B., Smith, B., Wang, Y.-P., Yang, X., Crous, K. Y., Drake, J. E., Gimeno, T. E., Macdonald, C. A., Norby, R. J., Power, S. A., Tjoelker, M. G., and Ellsworth, D. S.: Using models to guide field experiments: a priori predictions for the CO2 response of a nutrient- and water-limited native Eucalypt woodland, Glob Change Biol, 22, 2834–2851, https://doi.org/10.1111/gcb.13268, 2016.

van der Meer, P. J. and Bongers, F.: Patterns of tree-fall and branch-fall in a tropical rain forest in French Guiana, Journal of Ecology, 84, 19–29, https://doi.org/10.2307/2261696, 1996.

Meinzer, F. C., Andrade, J. L., Goldstein, G., Holbrook, N. M., Cavelier, J., and Jackson, P.: Control of transpiration from the upper canopy of a tropical forest: the role of stomatal, boundary layer and hydraulic architecture components, Plant, Cell & Environment, 20, 1242–1252, https://doi.org/10.1046/j.1365-3040.1997.d01-26.x, 1997.

1880   Meinzer, F. C., Woodruff, D. R., Marias, D. E., Smith, D. D., McCulloh, K. A., Howard, A. R., and Magedman, A. L.: Mapping
1881   'hydroscapes' along the iso- to anisohydric continuum of stomatal regulation of plant water status, Ecol Lett, 19, 1343–
1882   1352, https://doi.org/10.1111/ele.12670, 2016.

1883   Meir, P. and Grace, J.: Scaling relationships for woody tissue respiration in two tropical rain forests, Plant, Cell & Environment,
1884   25, 963–973, https://doi.org/10.1046/j.1365-3040.2002.00877.x, 2002.

1885   Meir, P., Grace, J., and Miranda, A. C.: Leaf respiration in two tropical rainforests: constraints on physiology by phosphorus,
1886   nitrogen and temperature, Functional Ecology, 15, 378–387, https://doi.org/10.1046/j.1365-2435.2001.00534.x, 2001.

1887   Meir, P., Cox, P., and Grace, J.: The influence of terrestrial ecosystems on climate, Trends in Ecology & Evolution, 21, 254–
1888   260, https://doi.org/10.1016/j.tree.2006.03.005, 2006.

1889   Mencuccini, M., Martínez-Vilalta, J., Vanderklein, D., Hamid, H. A., Korakaki, E., Lee, S., and Michiels, B.: Size-mediated
1890   ageing reduces vigour in trees, Ecology Letters, 8, 1183–1190, https://doi.org/10.1111/j.1461-0248.2005.00819.x, 2005.

1891   Menezes, J., Garcia, S., Grandis, A., Nascimento, H., Domingues, T. F., Guedes, A. V., Aleixo, I., Camargo, P., Campos, J.,
1892   Damasceno, A., Dias-Silva, R., Fleischer, K., Kruijt, B., Cordeiro, A. L., Martins, N. P., Meir, P., Norby, R. J., Pereira, I.,
1893   Portela, B., Rammig, A., Ribeiro, A. G., Lapola, D. M., and Quesada, C. A.: Changes in leaf functional traits with leaf age:
1894   when do leaves decrease their photosynthetic capacity in Amazonian trees?, Tree Physiology, tpab042,
1895   https://doi.org/10.1093/treephys/tpab042, 2021.

1896   Mercado, L. M., Lloyd, J., Dolman, A. J., Sitch, S., and Patiño, S.: Modelling basin-wide variations in Amazon forest
1897   productivity – Part 1: model calibration, evaluation and upscaling functions for canopy photosynthesis, Biogeosciences, 6,
1898   1247–1272, https://doi.org/10.5194/bg-6-1247-2009, 2009.

1899   Mercado, L. M., Patiño, S., Domingues, T. F., Fyllas, N. M., Weedon, G. P., Sitch, S., Quesada, C. A., Phillips, O. L., Aragão,
1900   L. E. O. C., Malhi, Y., Dolman, A. J., Restrepo-Coupe, N., Saleska, S. R., Baker, T. R., Almeida, S., Higuchi, N., and
1901   Lloyd, J.: Variations in Amazon forest productivity correlated with foliar nutrients and modelled rates of photosynthetic
1902   carbon supply, Phil. Trans. R. Soc. B, 366, 3316–3329, https://doi.org/10.1098/rstb.2011.0045, 2011.

1903   Merganičová, K., Merganič, J., Lehtonen, A., Vacchiano, G., Zorana, M., Ostrogović, S., Augustynczik, A. L. D., Grote, R.,
1904   Kyselová, I., Mäkelä, A., Yousefpour, R., Krejza, J., Collalti, A., and Reyer, C.: Forest carbon allocation modelling under
1905   climate change, Tree Physiology, https://doi.org/10.1093/treephys/tpz105, 2019.

1906   Merlin, O., Stefan, V. G., Amazirh, A., Chanzy, A., Ceschia, E., Er-Raki, S., Gentine, P., Tallec, T., Ezzahar, J., Bircher, S.,
1907   Beringer, J., and Khabba, S.: Modeling soil evaporation efficiency in a range of soil and atmospheric conditions using a
1908   meta-analysis approach, Water Resources Research, 52, 3663–3684, https://doi.org/10.1002/2015WR018233, 2016.

1909   Metcalfe, D. B., Meir, P., Aragão, L. E. O. C., Costa, A. C. L. da, Braga, A. P., Gonçalves, P. H. L., Junior, J. de A. S.,
1910   Almeida, S. S. de, Dawson, L. A., Malhi, Y., and Williams, M.: The effects of water availability on root growth and
1911   morphology in an Amazon rainforest, Plant and Soil, 311, 189–199, https://doi.org/10.1007/s11104-008-9670-9, 2008.

1912   Mokany, K., Ferrier, S., Connolly, S. R., Dunstan, P. K., Fulton, E. A., Harfoot, M. B., Harwood, T. D., Richardson, A. J.,
1913   Roxburgh, S. H., Scharlemann, J. P. W., Tittensor, D. P., Westcott, D. A., and Wintle, B. A.: Integrating modelling of
1914   biodiversity composition and ecosystem function, Oikos, 125, 10–19, https://doi.org/10.1111/oik.02792, 2016.

1915   Moles, A. T. and Westoby, M.: Seed size and plant strategy across the whole life cycle, Oikos, 113, 91–105,
1916   https://doi.org/10.1111/j.0030-1299.2006.14194.x, 2006.

1917   Moles, A. T., Falster, D. S., Leishman, M. R., and Westoby, M.: Small-seeded species produce more seeds per square metre
1918   of canopy per year, but not per individual per lifetime, Journal of Ecology, 92, 384–396, https://doi.org/10.1111/j.0022-
1919   0477.2004.00880.x, 2004.

1920   Moorcroft, P. R.: Recent advances in ecosystem-atmosphere interactions: an ecological perspective, Proceedings of the Royal
1921   Society of London B: Biological Sciences, 270, 1215–1227, https://doi.org/10.1098/rspb.2002.2251, 2003.

1922   Moorcroft, P. R.: How close are we to a predictive science of the biosphere?, Trends in Ecology & Evolution, 21, 400–407,
1923   https://doi.org/10.1016/j.tree.2006.04.009, 2006.

1924   Moorcroft, P. R., Hurtt, G. C., and Pacala, S. W.: A method for scaling vegetation dynamics: the ecosystem demography model
1925   (ed), Ecological Monographs, 71, 557–586, https://doi.org/10.1890/0012-9615(2001)071[0557:AMFSVD]2.0.CO;2,
1926   2001.

1927   Morin, X. and Lechowicz, M. J.: Contemporary perspectives on the niche that can improve models of species range shifts
1928   under climate change, Biology Letters, 4, 573–576, https://doi.org/10.1098/rsbl.2008.0181, 2008.

1929   Morin, X. and Thuiller, W.: Comparing niche-and process-based models to reduce prediction uncertainty in species range
1930   shifts under climate change, Ecology, 90, 1301–1313, 2009.

1931   Mualem, Y.: A new model for predicting the hydraulic conductivity of unsaturated porous media, Water Resources Research,
1932   12, 513–522, https://doi.org/10.1029/WR012i003p00513, 1976.

1933   Muir, C. D.: Making pore choices: repeated regime shifts in stomatal ratio, Proceedings of the Royal Society B: Biological
1934   Sciences, 282, 20151498, https://doi.org/10.1098/rspb.2015.1498, 2015.

1935   Muller, B., Pantin, F., Génard, M., Turc, O., Freixes, S., Piques, M., and Gibon, Y.: Water deficits uncouple growth from
1936   photosynthesis, increase C content, and modify the relationships between C and growth in sink organs, J. Exp. Bot., erq438,
1937   https://doi.org/10.1093/jxb/erq438, 2011.

1938   Muller-Landau, H. C., Wright, S. J., Calderón, O., Condit, R., and Hubbell, S. P.: Interspecific variation in primary seed
1939   dispersal in a tropical forest, Journal of Ecology, 96, 653–667, https://doi.org/10.1111/j.1365-2745.2008.01399.x, 2008.

1940   Muñoz-Sabater, J., Dutra, E., Agustí-Panareda, A., Albergel, C., Arduini, G., Balsamo, G., Boussetta, S., Choulga, M.,
1941   Harrigan, S., Hersbach, H., Martens, B., Miralles, D. G., Piles, M., Rodríguez-Fernández, N. J., Zsoter, E., Buontempo, C.,
1942   and Thépaut, J.-N.: ERA5-Land: a state-of-the-art global reanalysis dataset for land applications, Earth System Science
1943   Data, 13, 4349–4383, https://doi.org/10.5194/essd-13-4349-2021, 2021.

1944   Naudts, K., Ryder, J., McGrath, M. J., Otto, J., Chen, Y., Valade, A., Bellasen, V., Berhongaray, G., Bönisch, G., Campioli,
1945   M., Ghattas, J., De Groote, T., Haverd, V., Kattge, J., MacBean, N., Maignan, F., Merilä, P., Penuelas, J., Peylin, P., Pinty,

1946   B., Pretzsch, H., Schulze, E. D., Solyga, D., Vuichard, N., Yan, Y., and Luyssaert, S.: A vertically discretised canopy
1947   description for ORCHIDEE (SVN r2290) and the modifications to the energy, water and carbon fluxes, Geosci. Model
1948   Dev., 8, 2035–2065, https://doi.org/10.5194/gmd-8-2035-2015, 2015.

1949   Nemetschek, D., Derroire, G., Marcon, E., Aubry-Kientz, M., Auer, J., Badouard, V., Baraloto, C., Bauman, D., Le Blaye, Q.,
1950   Boisseaux, M., Bonal, D., Coste, S., Dardevet, E., Heuret, P., Hietz, P., Levionnois, S., Maréchaux, I., McMahon, S. M.,
1951   Stahl, C., Vleminckx, J., Wanek, W., Ziegler, C., and Fortunel, C.: Climate anomalies and neighbourhood crowding interact
1952   in shaping tree growth in old-growth and selectively logged tropical forests, Journal of Ecology, 112, 590–612,
1953   https://doi.org/10.1111/1365-2745.14256, 2024.

1954   Nemetschek, D., Fortunel, C., Marcon, E., Auer, J., Badouard, V., Baraloto, C., Boisseaux, M., Bonal, D., Coste, S.,
1955   Dardevette, E., Heuret, P., Hietz, P., Levionnois, S., Maréchaux, I., Stahl, C., Vleminckx, J., Wanek, W., Ziegler, C., and
1956   Derroire, G.: Love thy neighbour? Tropical tree growth and its response to climate anomalies is mediated by neighbourhood
1957   hierarchy and dissimilarity in carbon and water related traits., https://doi.org/10.22541/au.171366417.71658960/v1, 21
1958   April 2024.

1959   Nepstad, D. C., de Carvalho, C. R., Davidson, E. A., Jipp, P. H., Lefebvre, P. A., Negreiros, G. H., da Silva, E. D., Stone, T.
1960   A., Trumbore, S. E., and Vieira, S.: The role of deep roots in the hydrological and carbon cycles of Amazonian forests and
1961   pastures, Nature, 372, 666–669, https://doi.org/10.1038/372666a0, 1994.

1962   Newman, E. I.: Resistance to Water Flow in Soil and Plant. I. Soil Resistance in Relation to Amounts of Root: Theoretical
1963   Estimates, Journal of Applied Ecology, 6, 1–12, https://doi.org/10.2307/2401297, 1969.

1964   Nicolini, E., Beauchêne, J., de la Vallée, B. L., Ruelle, J., Mangenet, T., and Heuret, P.: Dating branch growth units in a
1965   tropical tree using morphological and anatomical markers: the case of Parkia velutina Benoist (Mimosoïdeae), Annals of
1966   Forest Science, 69, 543–555, https://doi.org/10.1007/s13595-011-0172-1, 2012.

1967   Norby, R. J., De Kauwe, M. G., Domingues, T. F., Duursma, R. A., Ellsworth, D. S., Goll, D. S., Lapola, D. M., Luus, K. A.,
1968   MacKenzie, A. R., Medlyn, B. E., Pavlick, R., Rammig, A., Smith, B., Thomas, R., Thonicke, K., Walker, A. P., Yang,
1969   X., and Zaehle, S.: Model–data synthesis for the next generation of forest free-air CO2 enrichment (FACE) experiments,
1970   New Phytol, 209, 17–28, https://doi.org/10.1111/nph.13593, 2016.

1971   Norden, N., Chave, J., Belbenoit, P., Caubère, A., Châtelet, P., Forget, P.-M., and Thébaud, C.: Mast fruiting is a frequent
1972   strategy in woody species of eastern South America, PLOS ONE, 2, e1079, https://doi.org/10.1371/journal.pone.0001079,
1973   2007.

1974   Novick, K. A., Ficklin, D. L., Stoy, P. C., Williams, C. A., Bohrer, G., Oishi, A. C., Papuga, S. A., Blanken, P. D., Noormets,
1975   A., Sulman, B. N., Scott, R. L., Wang, L., and Phillips, R. P.: The increasing importance of atmospheric demand for
1976   ecosystem water and carbon fluxes, Nature Climate Change, 6, 1023–1027, https://doi.org/10.1038/nclimate3114, 2016.

1977   Novick, K. A., Ficklin, D. L., Baldocchi, D., Davis, K. J., Ghezzehei, T. A., Konings, A. G., MacBean, N., Raoult, N., Scott,
1978   R. L., Shi, Y., Sulman, B. N., and Wood, J. D.: Confronting the water potential information gap, Nat. Geosci., 15, 158–
1979   164, https://doi.org/10.1038/s41561-022-00909-2, 2022.

Nunes, M. H., Camargo, J. L. C., Vincent, G., Calders, K., Oliveira, R. S., Huete, A., Mendes de Moura, Y., Nelson, B., Smith, M. N., Stark, S. C., and Maeda, E. E.: Forest fragmentation impacts the seasonality of Amazonian evergreen canopies, Nat Commun, 13, 917, https://doi.org/10.1038/s41467-022-28490-7, 2022.

Ogée, J., Brunet, Y., Loustau, D., Berbigier, P., and Delzon, S.: MuSICA, a CO2, water and energy multilayer, multileaf pine forest model: evaluation from hourly to yearly time scales and sensitivity analysis, Global Change Biology, 9, 697–717, https://doi.org/10.1046/j.1365-2486.2003.00628.x, 2003.

Oleson, K. W., Niu, G.-Y., Yang, Z.-L., Lawrence, D. M., Thornton, P. E., Lawrence, P. J., Stöckli, R., Dickinson, R. E., Bonan, G. B., Levis, S., Dai, A., and Qian, T.: Improvements to the Community Land Model and their impact on the hydrological cycle, J. Geophys. Res., 113, G01021, https://doi.org/10.1029/2007JG000563, 2008.

Oliveira, R. S., Dawson, T. E., Burgess, S. S. O., and Nepstad, D. C.: Hydraulic redistribution in three Amazonian trees, Oecologia, 145, 354–363, https://doi.org/10.1007/s00442-005-0108-2, 2005.

d'Orgeval, T., Polcher, J., and de Rosnay, P.: Sensitivity of the West African hydrological cycle in ORCHIDEE to infiltration processes, Hydrol. Earth Syst. Sci., 12, 1387–1401, https://doi.org/10.5194/hess-12-1387-2008, 2008.

Pacala, S. W. and Rees, M.: Models Suggesting Field Experiments to Test Two Hypotheses Explaining Successional Diversity, The American Naturalist, 152, 729–737, https://doi.org/10.1086/286203, 1998.

Paine, C. E. T., Deasey, A., and Duthie, A. B.: Towards the general mechanistic prediction of community dynamics, Functional Ecology, 32, 1681–1692, https://doi.org/10.1111/1365-2435.13096, 2018.

Pan, Y., Birdsey, R. A., Fang, J., Houghton, R., Kauppi, P. E., Kurz, W. A., Phillips, O. L., Shvidenko, A., Lewis, S. L., Canadell, J. G., Ciais, P., Jackson, R. B., Pacala, S. W., McGuire, A. D., Piao, S., Rautiainen, A., Sitch, S., and Hayes, D.: A Large and Persistent Carbon Sink in the World's Forests, Science, 333, 988–993, https://doi.org/10.1126/science.1201609, 2011.

Pantin, F., Simonneau, T., and Muller, B.: Coming of leaf age: control of growth by hydraulics and metabolics during leaf ontogeny, New Phytologist, 196, 349–366, https://doi.org/10.1111/j.1469-8137.2012.04273.x, 2012.

Paschalis, A., Fatichi, S., Zscheischler, J., Ciais, P., Bahn, M., Boysen, L., Chang, J., De Kauwe, M., Estiarte, M., Goll, D., Hanson, P. J., Harper, A. B., Hou, E., Kigel, J., Knapp, A. K., Larsen, K. S., Li, W., Lienert, S., Luo, Y., Meir, P., Nabel, J. E. M. S., Ogaya, R., Parolari, A. J., Peng, C., Peñuelas, J., Pongratz, J., Rambal, S., Schmidt, I. K., Shi, H., Sternberg, M., Tian, H., Tschumi, E., Ukkola, A., Vicca, S., Viovy, N., Wang, Y.-P., Wang, Z., Williams, K., Wu, D., and Zhu, Q.: Rainfall manipulation experiments as simulated by terrestrial biosphere models: Where do we stand?, Global Change Biology, 26, 3336–3355, https://doi.org/10.1111/gcb.15024, 2020.

Paschalis, A., De Kauwe, M. G., Sabot, M., and Fatichi, S.: When do plant hydraulics matter in terrestrial biosphere modelling?, Global Change Biology, 30, e17022, https://doi.org/10.1111/gcb.17022, 2024.

Pavlick, R., Drewry, D. T., Bohn, K., Reu, B., and Kleidon, A.: The Jena Diversity-Dynamic Global Vegetation Model (JeDi-DGVM): a diverse approach to representing terrestrial biogeography and biogeochemistry based on plant functional trade-offs, Biogeosciences, 10, 4137–4177, https://doi.org/10.5194/bg-10-4137-2013, 2013.

2014   Peters, R. L., Kaewmano, A., Fu, P.-L., Fan, Z.-X., Sterck, F., Steppe, K., and Zuidema, P. A.: High vapour pressure deficit
2015   enhances turgor limitation of stem growth in an Asian tropical rainforest tree, Plant, Cell & Environment, 46, 2747–2762,
2016   https://doi.org/10.1111/pce.14661, 2023.

2017   Picard, N. and Franc, A.: Are ecological groups of species optimal for forest dynamics modelling?, Ecological Modelling, 163,
2018   175–186, https://doi.org/10.1016/S0304-3800(03)00010-3, 2003.

2019   Picard, N., Köhler, P., Mortier, F., and Gourlet-Fleury, S.: A comparison of five classifications of species into functional
2020   groups   in   tropical   forests   of   French   Guiana,   Ecological   Complexity,   11,   75–83,
2021   https://doi.org/10.1016/j.ecocom.2012.03.003, 2012.

2022   Pitman, A. J.: The evolution of, and revolution in, land surface schemes designed for climate models, Int. J. Climatol., 23,
2023   479–510, https://doi.org/10.1002/joc.893, 2003.

2024   Poggio, L., de Sousa, L. M., Batjes, N. H., Heuvelink, G. B. M., Kempen, B., Ribeiro, E., and Rossiter, D.: SoilGrids 2.0:
2025   producing soil information for the globe with quantified spatial uncertainty, SOIL, 7, 217–240, https://doi.org/10.5194/soil-
2026   7-217-2021, 2021.

2027   Poorter, L., Bongers, L., and Bongers, F.: Architecture of 54 moist-forest tree species: traits, trade-offs, and functional groups,
2028   Ecology, 87, 1289–1301, https://doi.org/10.1890/0012-9658(2006)87[1289:AOMTST]2.0.CO;2, 2006.

2029   Poorter, L., Wright, S. J., Paz, H., Ackerly, D. D., Condit, R., Ibarra-Manríquez, G., Harms, K. E., Licona, J. C., Martínez-
2030   Ramos, M., Mazer, S. J., Muller-Landau, H. C., Peña-Claros, M., Webb, C. O., and Wright, I. J.: Are functional traits good
2031   predictors   of   demographic   rates?   Evidence   from   five   Neotropical   forests,   Ecology,   89,   1908–1920,
2032   https://doi.org/10.1890/07-0207.1, 2008.

2033   Poorter, L., Oberbauer, S. F., and Clark, D. B.: Leaf optical properties along a vertical gradient in a tropical rain forest
2034   canopy in Costa Rica, American Journal of Botany, 82, 1257–1263, https://doi.org/10.2307/2446248, 1995.

2035   Poorter, L., van der Sande, M. T., Thompson, J., Arets, E. J. M. M., Alarcón, A., Álvarez-Sánchez, J., Ascarrunz, N., Balvanera,
2036   P., Barajas-Guzmán, G., Boit, A., Bongers, F., Carvalho, F. A., Casanoves, F., Cornejo-Tenorio, G., Costa, F. R. C., de
2037   Castilho, C. V., Duivenvoorden, J. F., Dutrieux, L. P., Enquist, B. J., Fernández-Méndez, F., Finegan, B., Gormley, L. H.
2038   L., Healey, J. R., Hoosbeek, M. R., Ibarra-Manríquez, G., Junqueira, A. B., Levis, C., Licona, J. C., Lisboa, L. S.,
2039   Magnusson, W. E., Martínez-Ramos, M., Martínez-Yrizar, A., Martorano, L. G., Maskell, L. C., Mazzei, L., Meave, J. A.,
2040   Mora, F., Muñoz, R., Nytch, C., Pansonato, M. P., Parr, T. W., Paz, H., Pérez-García, E. A., Rentería, L. Y., Rodríguez-
2041   Velazquez, J., Rozendaal, D. M. A., Ruschel, A. R., Sakschewski, B., Salgado-Negret, B., Schietti, J., Simões, M., Sinclair,
2042   F. L., Souza, P. F., Souza, F. C., Stropp, J., ter Steege, H., Swenson, N. G., Thonicke, K., Toledo, M., Uriarte, M., van der
2043   Hout, P., Walker, P., Zamora, N., and Peña-Claros, M.: Diversity enhances carbon storage in tropical forests, Global
2044   Ecology and Biogeography, 24, 1314–1328, https://doi.org/10.1111/geb.12364, 2015.

2045   Poorter, L., Amissah, L., Bongers, F., Hordijk, I., Kok, J., Laurance, S. G. W., Lohbeck, M., Martínez-Ramos, M., Matsuo,
2046   T., Meave, J. A., Muñoz, R., Peña-Claros, M., and van der Sande, M. T.: Successional theories, Biological Reviews, 98,
2047   2049–2077, https://doi.org/10.1111/brv.12995, 2023.

Porté, A. and Bartelink, H. H.: Modelling mixed forest growth: a review of models for forest management, Ecological Modelling, 150, 141–188, https://doi.org/10.1016/S0304-3800(01)00476-8, 2002.

Poulter, B., Ciais, P., Hodson, E., Lischke, H., Maignan, F., Plummer, S., and Zimmermann, N. E.: Plant functional type mapping for earth system models, Geosci. Model Dev., 4, 993–1010, https://doi.org/10.5194/gmd-4-993-2011, 2011.

Powell, T. L., Galbraith, D. R., Christoffersen, B. O., Harper, A., Imbuzeiro, H. M. A., Rowland, L., Almeida, S., Brando, P. M., da Costa, A. C. L., Costa, M. H., Levine, N. M., Malhi, Y., Saleska, S. R., Sotta, E., Williams, M., Meir, P., and Moorcroft, P. R.: Confronting model predictions of carbon fluxes with measurements of Amazon forests subjected to experimental drought, New Phytologist, 200, 350–365, https://doi.org/10.1111/nph.12390, 2013.

Powell, T. L., Wheeler, J. K., Oliveira, A. A. R. de, Costa, A. C. L. da, Saleska, S. R., Meir, P., and Moorcroft, P. R.: Differences in xylem and leaf hydraulic traits explain differences in drought tolerance among mature Amazon rainforest trees, Global Change Biology, 23, 4280–4293, https://doi.org/10.1111/gcb.13731, 2017.

Prentice, I. C., Bondeau, A., Cramer, W., Harrison, S. P., Hickler, T., Lucht, W., Sitch, S., Smith, B., and Sykes, M. T.: Dynamic Global Vegetation Modeling: Quantifying Terrestrial Ecosystem Responses to Large-Scale Environmental Change, in: Terrestrial ecosystems in a changing world, edited by: Canadell, J. G., Pataki, D. E., and Pitelka, L. F., Springer Berlin Heidelberg, 175–192, 2007.

Prentice, I. C., Liang, X., Medlyn, B. E., and Wang, Y.-P.: Reliable, robust and realistic: the three R's of next-generation land-surface modelling, Atmos. Chem. Phys., 15, 5987–6005, https://doi.org/10.5194/acp-15-5987-2015, 2015.

Purves, D. and Pacala, S.: Predictive models of forest dynamics, Science, 320, 1452–1453, https://doi.org/10.1126/science.1155359, 2008.

Qie, L., Lewis, S. L., Sullivan, M. J. P., Lopez-Gonzalez, G., Pickavance, G. C., Sunderland, T., Ashton, P., Hubau, W., Salim, K. A., Aiba, S.-I., Banin, L. F., Berry, N., Brearley, F. Q., Burslem, D. F. R. P., Dančák, M., Davies, S. J., Fredriksson, G., Hamer, K. C., Hédl, R., Kho, L. K., Kitayama, K., Krisnawati, H., Lhota, S., Malhi, Y., Maycock, C., Metali, F., Mirmanto, E., Nagy, L., Nilus, R., Ong, R., Pendry, C. A., Poulsen, A. D., Primack, R. B., Rutishauser, E., Samsoedin, I., Saragih, B., Sist, P., Slik, J. W. F., Sukri, R. S., Svátek, M., Tan, S., Tjoa, A., Nieuwstadt, M. van, Vernimmen, R. R. E., Yassir, I., Kidd, P. S., Fitriadi, M., Ideris, N. K. H., Serudin, R. M., Lim, L. S. A., Saparudin, M. S., and Phillips, O. L.: Long-term carbon sink in Borneo's forests halted by drought and vulnerable to edge effects, Nature Communications, 8, 1966, https://doi.org/10.1038/s41467-017-01997-0, 2017.

Rau, E.-P., Fischer, F., Joetzjer, É., Maréchaux, I., Sun, I. F., and Chave, J.: Transferability of an individual- and trait-based forest dynamics model: A test case across the tropics, Ecological Modelling, 463, 109801, https://doi.org/10.1016/j.ecolmodel.2021.109801, 2022a.

Rau, E.-P., Gardiner, B. A., Fischer, F. J., Maréchaux, I., Joetzjer, E., Sun, I.-F., and Chave, J.: Wind Speed Controls Forest Structure in a Subtropical Forest Exposed to Cyclones: A Case Study Using an Individual-Based Model, Frontiers in Forests and Global Change, 5, 2022b.

2081 Restrepo-Coupe, N., da Rocha, H. R., Hutyra, L. R., da Araujo, A. C., Borma, L. S., Christoffersen, B., Cabral, O. M. R., de
2082   Camargo, P. B., Cardoso, F. L., da Costa, A. C. L., Fitzjarrald, D. R., Goulden, M. L., Kruijt, B., Maia, J. M. F., Malhi, Y.
2083   S., Manzi, A. O., Miller, S. D., Nobre, A. D., von Randow, C., Sá, L. D. A., Sakai, R. K., Tota, J., Wofsy, S. C., Zanchi,
2084   F. B., and Saleska, S. R.: What drives the seasonality of photosynthesis across the Amazon basin? A cross-site analysis of
2085   eddy flux tower measurements from the Brasil flux network, Agricultural and Forest Meteorology, 182–183, 128–144,
2086   https://doi.org/10.1016/j.agrformet.2013.04.031, 2013.
2087 Restrepo-Coupe, N., Levine, N. M., Christoffersen, B. O., Albert, L. P., Wu, J., Costa, M. H., Galbraith, D., Imbuzeiro, H.,
2088   Martins, G., da Araujo, A. C., Malhi, Y. S., Zeng, X., Moorcroft, P., and Saleska, S. R.: Do dynamic global vegetation
2089   models capture the seasonality of carbon fluxes in the Amazon basin? A data-model intercomparison, Glob Change Biol,
2090   23, 191–208, https://doi.org/10.1111/gcb.13442, 2017.
2091 Richards, L. A.: Capillary conduction of liquids through porous mediums, Physics, 1, 318–333,
2092   https://doi.org/10.1063/1.1745010, 1931.
2093 Riva, F. and Fahrig, L.: Landscape-scale habitat fragmentation is positively related to biodiversity, despite patch-scale
2094   ecosystem decay, Ecology Letters, 26, 268–277, https://doi.org/10.1111/ele.14145, 2023.
2095 Rödig, E., Cuntz, M., Heinke, J., Rammig, A., and Huth, A.: Spatial heterogeneity of biomass and forest structure of the
2096   Amazon rain forest: Linking remote sensing, forest modelling and field inventory, Global Ecology and Biogeography, 26,
2097   1292–1302, https://doi.org/10.1111/geb.12639, 2017.
2098 Rodriguez-Dominguez, C. M., Buckley, T. N., Egea, G., de Cires, A., Hernandez-Santana, V., Martorell, S., and Diaz-Espejo,
2099   A.: Most stomatal closure in woody species under moderate drought can be explained by stomatal responses to leaf turgor,
2100   Plant, Cell & Environment, 39, 2014–2026, https://doi.org/10.1111/pce.12774, 2016.
2101 Rodriguez-Iturbe, I., Porporato, A., Ridolfi, L., Isham, V., and Coxi, D. R.: Probabilistic modelling of water balance at a point:
2102   the role of climate, soil and vegetation, Proceedings of the Royal Society of London A: Mathematical, Physical and
2103   Engineering Sciences, 455, 3789–3805, https://doi.org/10.1098/rspa.1999.0477, 1999.
2104 Rogers, A., Medlyn, B. E., Dukes, J. S., Bonan, G., von Caemmerer, S., Dietze, M. C., Kattge, J., Leakey, A. D. B., Mercado,
2105   L. M., Niinemets, Ü., Prentice, I. C., Serbin, S. P., Sitch, S., Way, D. A., and Zaehle, S.: A roadmap for improving the
2106   representation of photosynthesis in Earth system models, New Phytol, 213, 22–42, https://doi.org/10.1111/nph.14283,
2107   2017.
2108 Rosas, T., Mencuccini, M., Barba, J., Cochard, H., Saura-Mas, S., and Martínez-Vilalta, J.: Adjustments and coordination of
2109   hydraulic, leaf and stem traits along a water availability gradient, New Phytologist, 223, 632–646,
2110   https://doi.org/10.1111/nph.15684, 2019.
2111 Ross, J.: The radiation regime and architecture of plant stands, The Hague, The Netherlands, 1981.
2112 Rowland, L., Lobo-do-Vale, R. L., Christoffersen, B. O., Melém, E. A., Kruijt, B., Vasconcelos, S. S., Domingues, T., Binks,
2113   O. J., Oliveira, A. A. R., Metcalfe, D., da Costa, A. C. L., Mencuccini, M., and Meir, P.: After more than a decade of soil

moisture deficit, tropical rainforest trees maintain photosynthetic capacity, despite increased leaf respiration, Glob Change Biol, 21, 4662–4672, https://doi.org/10.1111/gcb.13035, 2015.

Rowland, L., Costa, A. C. L. da, Oliveira, A. A. R., Oliveira, R. S., Bittencourt, P. L., Costa, P. B., Giles, A. L., Sosa, A. I., Coughlin, I., Godlee, J. L., Vasconcelos, S. S., Junior, J. A. S., Ferreira, L. V., Mencuccini, M., and Meir, P.: Drought stress and tree size determine stem CO2 efflux in a tropical forest, New Phytologist, 218, 1393–1405, https://doi.org/10.1111/nph.15024, 2018.

Rowland, L., Ramírez-Valiente, J.-A., Hartley, I. P., and Mencuccini, M.: How woody plants adjust above- and below-ground traits in response to sustained drought, New Phytologist, 239, 1173–1189, https://doi.org/10.1111/nph.19000, 2023.

Rutter, A. J. and Morton, A. J.: A Predictive Model of Rainfall Interception in Forests. III. Sensitivity of The Model to Stand Parameters and Meteorological Variables, Journal of Applied Ecology, 14, 567–588, https://doi.org/10.2307/2402568, 1977.

Ryan, M. G., Hubbard, R. M., Clark, D. A., and Jr, R. L. S.: Woody-tissue respiration for Simarouba amara and Minquartia guianensis, two tropical wet forest trees with different growth habits, Oecologia, 100, 213–220, https://doi.org/10.1007/BF00316947, 1994.

Ryan, M. G., Binkley, D., and Fownes, J. H.: Age-related decline in forest productivity., Adv. Ecol. Res., 27, 213–262, 1997.

Sabot, M. E. B., Kauwe, M. G. D., Pitman, A. J., Medlyn, B. E., Verhoef, A., Ukkola, A. M., and Abramowitz, G.: Plant profit maximization improves predictions of European forest responses to drought, New Phytologist, 226, 1638–1655, https://doi.org/10.1111/nph.16376, 2020.

Sabot, M. E. B., De Kauwe, M. G., Pitman, A. J., Medlyn, B. E., Ellsworth, D. S., Martin-StPaul, N. K., Wu, J., Choat, B., Limousin, J.-M., Mitchell, P. J., Rogers, A., and Serbin, S. P.: One Stomatal Model to Rule Them All? Toward Improved Representation of Carbon and Water Exchange in Global Models, Journal of Advances in Modeling Earth Systems, 14, e2021MS002761, https://doi.org/10.1029/2021MS002761, 2022.

Sakschewski, B., von Bloh, W., Boit, A., Rammig, A., Kattge, J., Poorter, L., Peñuelas, J., and Thonicke, K.: Leaf and stem economics spectra drive diversity of functional plant traits in a dynamic global vegetation model, Glob Change Biol, 21, 2711–2725, https://doi.org/10.1111/gcb.12870, 2015.

Sakschewski, B., von Bloh, W., Drüke, M., Sörensson, A. A., Ruscica, R., Langerwisch, F., Billing, M., Bereswill, S., Hirota, M., Oliveira, R. S., Heinke, J., and Thonicke, K.: Variable tree rooting strategies are key for modelling the distribution, productivity and evapotranspiration of tropical evergreen forests, Biogeosciences, 18, 4091–4116, https://doi.org/10.5194/bg-18-4091-2021, 2021.

Sander, H.: The porosity of tropical soils and implications for geomorphological and pedogenetic processes and the movement of solutions within the weathering cover, CATENA, 49, 129–137, https://doi.org/10.1016/S0341-8162(02)00021-8, 2002.

2146 Santos, V. A. H. F. dos, Ferreira, M. J., Rodrigues, J. V. F. C., Garcia, M. N., Ceron, J. V. B., Nelson, B. W., and Saleska, S.
2147 R.: Causes of reduced leaf-level photosynthesis during strong El Niño drought in a Central Amazon forest, Global Change
2148 Biology, 24, 4266–4279, https://doi.org/10.1111/gcb.14293, 2018.

2149 Sato, H., Itoh, A., and Kohyama, T.: SEIB-DGVM: a new dynamic global vegetation model using a spatially explicit
2150 individual-based approach, Ecol. Model., 200, 279–307, https://doi.org/10.1016/j.ecolmodel.2006.09.006, 2007.

2151 Schaphoff, S., von Bloh, W., Rammig, A., Thonicke, K., Biemans, H., Forkel, M., Gerten, D., Heinke, J., Jägermeyr, J.,
2152 Knauer, J., Langerwisch, F., Lucht, W., Müller, C., Rolinski, S., and Waha, K.: LPJmL4 – a dynamic global vegetation
2153 model with managed land – Part 1: Model description, Geoscientific Model Development, 11, 1343–1375,
2154 https://doi.org/Schaphoff, Sibyll, von Bloh, Werner, Rammig, Anja, Thonicke, Kirsten, Biemans, Hester, Forkel, Matthias,
2155 Gerten, Dieter, Heinke, Jens, Jägermeyr, Jonas, Knauer, Jürgen, Langerwisch, Fanny, Lucht, Wolfgang, Müller, Christoph,
2156 Rolinski, Susanne and Waha, Katharina (2018) LPJmL4 – a dynamic global vegetation model with managed land – Part
2157 1: Model description. Open Access Geoscientific Model Development, 11 (4). pp. 1343-1375. DOI 10.5194/gmd-11-
2158 1343-2018 <http://dx.doi.org/10.5194/gmd-11-1343-2018>., 2018.

2159 Scheiter, S., Langan, L., and Higgins, S. I.: Next-generation dynamic global vegetation models: learning from community
2160 ecology, New Phytol, 198, 957–969, https://doi.org/10.1111/nph.12210, 2013.

2161 Schimel, D., Pavlick, R., Fisher, J. B., Asner, G. P., Saatchi, S., Townsend, P., Miller, C., Frankenberg, C., Hibbard, K., and
2162 Cox, P.: Observing terrestrial ecosystems and the carbon cycle from space, Global Change Biology, 21, 1762–1776,
2163 https://doi.org/10.1111/gcb.12822, 2015.

2164 Schippers, P., Vlam, M., Zuidema, P. A., and Sterck, F.: Sapwood allocation in tropical trees: a test of hypotheses, Functional
2165 Plant Biol., 42, 697–709, https://doi.org/10.1071/FP14127, 2015.

2166 Schmidhalter, U.: The gradient between pre-dawn rhizoplane and bulk soil matric potentials, and its relation to the pre-dawn
2167 root and leaf water potentials of four species, Plant, Cell & Environment, 20, 953–960, https://doi.org/10.1046/j.1365-
2168 3040.1997.d01-136.x, 1997.

2169 Schmitt, S., Maréchaux, I., Chave, J., Fischer, F. J., Piponiot, C., Traissac, S., and Hérault, B.: Functional diversity improves
2170 tropical forest resilience: Insights from a long-term virtual experiment, Journal of Ecology, 108, 831–843,
2171 https://doi.org/10.1111/1365-2745.13320, 2020.

2172 Schmitt, S.: Rôle de la biodiversité dans la résilience des écosystèmes forestiers tropicaux après perturbations, AgroParisTech,
2173 Université de Montpellier, Kourou, 2017.

2174 Schmitt, S., Salzet, G., Fischer, F. J., Maréchaux, I., and Chave, J.: rcontroll: An R interface for the individual-based forest
2175 dynamics simulator TROLL, Methods in Ecology and Evolution, 14, 2749–2757, https://doi.org/10.1111/2041-
2176 210X.14215, 2023.

2177 Schnabel, F., Schwarz, J. A., Dănescu, A., Fichtner, A., Nock, C. A., Bauhus, J., and Potvin, C.: Drivers of productivity and
2178 its temporal stability in a tropical tree diversity experiment, Global Change Biology, 25, 4257–4272,
2179 https://doi.org/10.1111/gcb.14792, 2019.

Schnitzer, S. A. and Carson, W. P.: Would Ecology Fail the Repeatability Test?, BioScience, 66, 98–99, https://doi.org/10.1093/biosci/biv176, 2016.

Seidl, R., Rammer, W., and Blennow, K.: Simulating wind disturbance impacts on forest landscapes: Tree-level heterogeneity matters, Environmental Modelling & Software, 51, 1–11, https://doi.org/10.1016/j.envsoft.2013.09.018, 2014.

Seidler, T. G. and Plotkin, J. B.: Seed Dispersal and Spatial Pattern in Tropical Trees, PLOS Biology, 4, e344, https://doi.org/10.1371/journal.pbio.0040344, 2006.

Sellers, P. J., Mintz, Y., Sud, Y. C., and Dalcher, A.: A Simple Biosphere Model (SIB) for Use within General Circulation Models, J. Atmos. Sci., 43, 505–531, https://doi.org/10.1175/1520-0469(1986)043<0505:ASBMFU>2.0.CO;2, 1986.

Sellers, P. J., Heiser, M. D., and Hall, F. G.: Relations between surface conductance and spectral vegetation indices at intermediate (100 m2 to 15 km2) length scales, Journal of Geophysical Research: Atmospheres, 97, 19033–19059, https://doi.org/10.1029/92JD01096, 1992.

Sellers, P. J., Dickinson, R. E., Randall, D. A., Betts, A. K., Hall, F. G., Berry, J. A., Collatz, G. J., Denning, A. S., Mooney, H. A., Nobre, C. A., Sato, N., Field, C. B., and Henderson-Sellers, A.: Modeling the Exchanges of Energy, Water, and Carbon Between Continents and the Atmosphere, Science, 275, 502–509, https://doi.org/10.1126/science.275.5299.502, 1997.

Sergent, A. S., Varela, S. A., Barigah, T. S., Badel, E., Cochard, H., Dalla-Salda, G., Delzon, S., Fernández, M. E., Guillemot, J., Gyenge, J., Lamarque, L. J., Martinez-Meier, A., Rozenberg, P., Torres-Ruiz, J. M., and Martin-StPaul, N. K.: A comparison of five methods to assess embolism resistance in trees, Forest Ecology and Management, 468, 118175, https://doi.org/10.1016/j.foreco.2020.118175, 2020.

Sevanto, S., Mcdowell, N. G., Dickman, L. T., Pangle, R., and Pockman, W. T.: How do trees die? A test of the hydraulic failure and carbon starvation hypotheses, Plant Cell Environ, 37, 153–161, https://doi.org/10.1111/pce.12141, 2014.

Sheil, D., Burslem, D. F. R. P., and Alder, D.: The interpretation and misinterpretation of mortality rate measures, Journal of Ecology, 83, 331–333, https://doi.org/10.2307/2261571, 1995.

Shugart, H. H., Asner, G. P., Fischer, R., Huth, A., Knapp, N., Le Toan, T., and Shuman, J. K.: Computer and remote-sensing infrastructure to enhance large-scale testing of individual-based forest models, Frontiers in Ecology and the Environment, 13, 503–511, 2015.

Shuttleworth, W. J.: Daily variations of temperature and humidity within and above Amazonian forest, Weather, 40, 102–108, https://doi.org/10.1002/j.1477-8696.1985.tb07489.x, 1985.

Shuttleworth, W. J., Leuning, R., Black, T. A., Grace, J., Jarvis, P. G., Roberts, J., and Jones, H. G.: Micrometeorology of temperate and tropical forest, Philosophical Transactions of the Royal Society of London B: Biological Sciences, 324, 299–334, https://doi.org/10.1098/rstb.1989.0050, 1989.

Slik, J. W. F.: El Niño droughts and their effects on tree species composition and diversity in tropical rain forests, Oecologia, 141, 114–120, https://doi.org/10.1007/s00442-004-1635-y, 2004.

2213 Slot, M., Wright, S. J., and Kitajima, K.: Foliar respiration and its temperature sensitivity in trees and lianas: in situ
2214   measurements in the upper canopy of a tropical forest, Tree Physiol, 33, 505–515, https://doi.org/10.1093/treephys/tpt026,
2215   2013.

2216 Slot, M., Nardwattanawong, T., Hernández, G. G., Bueno, A., Riederer, M., and Winter, K.: Large differences in leaf cuticle
2217   conductance and its temperature response among 24 tropical tree species from across a rainfall gradient, New Phytologist,
2218   232, 1618–1631, https://doi.org/10.1111/nph.17626, 2021.

2219 Smith, B., Prentice, I. C., and Sykes, M. T.: Representation of vegetation dynamics in the modelling of terrestrial ecosystems:
2220   comparing two contrasting approaches within European climate space, Global Ecology and Biogeography, 10, 621–637,
2221   https://doi.org/10.1046/j.1466-822X.2001.t01-1-00256.x, 2001.

2222 Smith, N. G. and Dukes, J. S.: Plant respiration and photosynthesis in global-scale models: incorporating acclimation to
2223   temperature and CO2, Glob Change Biol, 19, 45–63, https://doi.org/10.1111/j.1365-2486.2012.02797.x, 2013.

2224 Smith-Martin, C. M., Xu, X., Medvigy, D., Schnitzer, S. A., and Powers, J. S.: Allometric scaling laws linking biomass and
2225   rooting depth vary across ontogeny and functional groups in tropical dry forest lianas and trees, New Phytologist, 226,
2226   714–726, https://doi.org/10.1111/nph.16275, 2020.

2227 Soberón, J.: Grinnellian and Eltonian niches and geographic distributions of species, Ecology Letters, 10, 1115–1123,
2228   https://doi.org/10.1111/j.1461-0248.2007.01107.x, 2007.

2229 Sobrado, M. A.: Aspects of tissue water relations and seasonal changes of leaf water potential components of evergreen and
2230   deciduous species coexisting in tropical dry forests, Oecologia, 68, 413–416, https://doi.org/10.1007/BF01036748, 1986.

2231 Song, X., Wang, D.-Y., Li, F., and Zeng, X.-D.: Evaluating the performance of CMIP6 Earth system models in simulating
2232   global vegetation structure and distribution, Advances in Climate Change Research, 12, 584–595,
2233   https://doi.org/10.1016/j.accre.2021.06.008, 2021.

2234 Sousa, T. R., Schietti, J., Ribeiro, I. O., Emílio, T., Fernández, R. H., ter Steege, H., Castilho, C. V., Esquivel-Muelbert, A.,
2235   Baker, T., Pontes-Lopes, A., Silva, C. V. J., Silveira, J. M., Derroire, G., Castro, W., Mendoza, A. M., Ruschel, A., Prieto,
2236   A., Lima, A. J. N., Rudas, A., Araujo-Murakami, A., Gutierrez, A. P., Andrade, A., Roopsind, A., Manzatto, A. G., Di
2237   Fiore, A., Torres-Lezama, A., Dourdain, A., Marimon, B., Marimon, B. H., Burban, B., van Ulft, B., Herault, B., Quesada,
2238   C., Mendoza, C., Stahl, C., Bonal, D., Galbraith, D., Neill, D., de Oliveira, E. A., Hase, E., Jimenez-Rojas, E., Vilanova,
2239   E., Arets, E., Berenguer, E., Alvarez-Davila, E., Honorio Coronado, E. N., Almeida, E., Coelho, F., Valverde, F. C., Elias,
2240   F., Brown, F., Bongers, F., Arevalo, F. R., Lopez-Gonzalez, G., van der Heijden, G., Aymard C., G. A., Llampazo, G. F.,
2241   Pardo, G., Ramírez-Angulo, H., do Amaral, I. L., Vieira, I. C. G., Huamantupa-Chuquimaco, I., Comiskey, J. A., Singh,
2242   J., Espejo, J. S., del Aguila-Pasquel, J., Zwerts, J. A., Talbot, J., Terborgh, J., Ferreira, J., Barroso, J. G., Barlow, J.,
2243   Camargo, J. L., Stropp, J., Peacock, J., Serrano, J., Melgaço, K., Ferreira, L. V., Blanc, L., Poorter, L., Gamarra, L. V.,
2244   Aragão, L., Arroyo, L., Silveira, M., Peñuela-Mora, M. C., Vargas, M. P. N., Toledo, M., Disney, M., Réjou-Méchain, M.,
2245   Baisie, M., Kalamandeen, M., Camacho, N. P., Cardozo, N. D., Silva, N., Pitman, N., Higuchi, N., Banki, O., Loayza, P.

2246   A., Graça, P. M. L. A., et al.: Water table depth modulates productivity and biomass across Amazonian forests, Global
2247   Ecology and Biogeography, 31, 1571–1588, https://doi.org/10.1111/geb.13531, 2022.

2248 Sperry, J. S., Hacke, U. G., Oren, R., and Comstock, J. P.: Water deficits and hydraulic limits to leaf water supply, Plant Cell
2249   Environ., 25, 251–263, 2002.

2250 Sperry, J. S., Venturas, M. D., Anderegg, W. R. L., Mencuccini, M., Mackay, D. S., Wang, Y., and Love, D. M.: Predicting
2251   stomatal responses to the environment from the optimization of photosynthetic gain and hydraulic cost, Plant, Cell &
2252   Environment, 40, 816–830, https://doi.org/10.1111/pce.12852, 2017.

2253 Stahl, C., Herault, B., Rossi, V., Burban, B., Brechet, C., and Bonal, D.: Depth of soil water uptake by tropical rainforest trees
2254   during dry periods: does tree dimension matter?, Oecologia, 173, 1191–1201, https://doi.org/10.1007/s00442-013-2724-6,
2255   2013a.

2256 Stahl, C., Burban, B., Wagner, F., Goret, J.-Y., Bompy, F., and Bonal, D.: Influence of seasonal variations in soil water
2257   availability on gas exchange of tropical canopy trees, Biotropica, 45, 155–164, https://doi.org/10.1111/j.1744-
2258   7429.2012.00902.x, 2013b.

2259 Stephenson, N. L., Das, A. J., Condit, R., Russo, S. E., Baker, P. J., Beckman, N. G., Coomes, D. A., Lines, E. R., Morris, W.
2260   K., Rüger, N., Álvarez, E., Blundo, C., Bunyavejchewin, S., Chuyong, G., Davies, S. J., Duque, Á., Ewango, C. N., Flores,
2261   O., Franklin, J. F., Grau, H. R., Hao, Z., Harmon, M. E., Hubbell, S. P., Kenfack, D., Lin, Y., Makana, J.-R., Malizia, A.,
2262   Malizia, L. R., Pabst, R. J., Pongpattananurak, N., Su, S.-H., Sun, I.-F., Tan, S., Thomas, D., van Mantgem, P. J., Wang,
2263   X., Wiser, S. K., and Zavala, M. A.: Rate of tree carbon accumulation increases continuously with tree size, Nature, 507,
2264   90–93, https://doi.org/10.1038/nature12914, 2014.

2265 Strigul, N., Pristinski, D., Purves, D., Dushoff, J., and Pacala, S.: Scaling from trees to forests: tractable macroscopic equations
2266   for forest dynamics, Ecological Monographs, 78, 523–545, https://doi.org/10.1890/08-0082.1, 2008.

2267 Sun, S., Jung, E.-Y., Gaviria, J., and Engelbrecht, B. M. J.: Drought survival is positively associated with high turgor loss
2268   points in temperate perennial grassland species, Functional Ecology, 34, 788–798, https://doi.org/10.1111/1365-
2269   2435.13522, 2020.

2270 Swaine, M. D. and Whitmore, T. C.: On the definition of ecological species groups in tropical rain forests, Vegetatio, 75, 81–
2271   86, https://doi.org/10.1007/BF00044629, 1988.

2272 Tamme, R., Götzenberger, L., Zobel, M., Bullock, J. M., Hooftman, D. A. P., Kaasik, A., and Pärtel, M.: Predicting species'
2273   maximum dispersal distances from simple plant traits, Ecology, 95, 505–513, https://doi.org/10.1890/13-1000.1, 2014.

2274 Thornley, J. H. M. and Cannell, M. G. R.: Modelling the components of plant respiration: representation and realism, Ann
2275   Bot, 85, 55–67, https://doi.org/10.1006/anbo.1999.0997, 2000.

2276 Thuiller, W., Albert, C., Araújo, M. B., Berry, P. M., Cabeza, M., Guisan, A., Hickler, T., Midgley, G. F., Paterson, J., Schurr,
2277   F. M., Sykes, M. T., and Zimmermann, N. E.: Predicting global change impacts on plant species' distributions: Future
2278   challenges, Perspectives in Plant Ecology, Evolution and Systematics, 9, 137–152,
2279   https://doi.org/10.1016/j.ppees.2007.09.004, 2008.

2280 Tomasella, J. and Hodnett, M. G.: Estimating soil water retention characteristics from limited data in Brazilian Amazonia.,
2281   Soil science, 163, 190–202, 1998.

2282 Trueba, S., Pan, R., Scoffoni, C., John, G. P., Davis, S. D., and Sack, L.: Thresholds for leaf damage due to dehydration:
2283   declines of hydraulic function, stomatal conductance and cellular integrity precede those for photochemistry, New
2284   Phytologist, 223, 134–149, https://doi.org/10.1111/nph.15779, 2019.

2285 Trugman, A. T., Medvigy, D., Mankin, J. S., and Anderegg, W. R. L.: Soil Moisture Stress as a Major Driver of Carbon Cycle
2286   Uncertainty, Geophysical Research Letters, 45, 6495–6503, https://doi.org/10.1029/2018GL078131, 2018.

2287 Turner, B. L., Brenes-Arguedas, T., and Condit, R.: Pervasive phosphorus limitation of tree species but not communities in
2288   tropical forests, Nature, 555, 367–370, https://doi.org/10.1038/nature25789, 2018.

2289 Tuzet, A., Perrier, A., and Leuning, R.: A coupled model of stomatal conductance, photosynthesis and transpiration, Plant,
2290   Cell & Environment, 26, 1097–1116, https://doi.org/10.1046/j.1365-3040.2003.01035.x, 2003.

2291 Tymen, B., Vincent, G., Courtois, E. A., Heurtebize, J., Dauzat, J., Marechaux, I., and Chave, J.: Quantifying micro-
2292   environmental variation in tropical rainforest understory at landscape scale by combining airborne LiDAR scanning and a
2293   sensor network, Annals of Forest Science, 74, 32, https://doi.org/10.1007/s13595-017-0628-z, 2017.

2294 Urbina, I., Grau, O., Sardans, J., Margalef, O., Peguero, G., Asensio, D., LLusià, J., Ogaya, R., Gargallo-Garriga, A., Van
2295   Langenhove, L., Verryckt, L. T., Courtois, E. A., Stahl, C., Soong, J. L., Chave, J., Hérault, B., Janssens, I. A., Sayer, E.,
2296   and Peñuelas, J.: High foliar K and P resorption efficiencies in old-growth tropical forests growing on nutrient-poor soils,
2297   Ecology and Evolution, 11, 8969–8982, https://doi.org/10.1002/ece3.7734, 2021.

2298 Vacchiano, G., Ascoli, D., Berzaghi, F., Lucas-Borja, M. E., Caignard, T., Collalti, A., Mairota, P., Palaghianu, C., Reyer, C.
2299   P. O., Sanders, T. G. M., Schermer, E., Wohlgemuth, T., and Hacket-Pain, A.: Reproducing reproduction: How to simulate
2300   mast seeding in forest models, Ecological Modelling, 376, 40–53, https://doi.org/10.1016/j.ecolmodel.2018.03.004, 2018.

2301 Van Bodegom, P. M., Douma, J. C., and Verheijen, L. M.: A fully traits-based approach to modeling global vegetation
2302   distribution, PNAS, 111, 13733–13738, https://doi.org/10.1073/pnas.1304551110, 2014.

2303 Van Nes, E. H. and Scheffer, M.: A strategy to improve the contribution of complex simulation models to ecological theory,
2304   Ecological Modelling, 185, 153–164, https://doi.org/10.1016/j.ecolmodel.2004.12.001, 2005.

2305 Vanclay, J. K.: Aggregating tree species to develop diameter increment equations for tropical rainforests, Forest Ecology and
2306   Management, 42, 143–168, https://doi.org/10.1016/0378-1127(91)90022-N, 1991.

2307 Vanclay, J. K.: Modelling forest growth and yield: applications to mixed tropical forests., CAB INternational, Wallingford,
2308   312 pp., 1994.

2309 Vargas Godoy, M. R., Markonis, Y., Hanel, M., Kyselý, J., and Papalexiou, S. M.: The Global Water Cycle Budget: A
2310   Chronological Review, Surv Geophys, 42, 1075–1107, https://doi.org/10.1007/s10712-021-09652-6, 2021

2311 Verbeeck, H., Peylin, P., Bacour, C., Bonal, D., Steppe, K., and Ciais, P.: Seasonal patterns of CO2 fluxes in Amazon forests:
2312   Fusion of eddy covariance data and the ORCHIDEE model, J. Geophys. Res.-Biogeosci., 116,
2313   https://doi.org/10.1029/2010JG001544, 2011.

2314 Verheijen, L. M., Aerts, R., Brovkin, V., Cavender-Bares, J., Cornelissen, J. H. C., Kattge, J., and van Bodegom, P. M.:
2315   Inclusion of ecologically based trait variation in plant functional types reduces the projected land carbon sink in an earth
2316   system model, Glob Change Biol, 21, 3074–3086, https://doi.org/10.1111/gcb.12871, 2015.

2317 Verhoef, A. and Egea, G.: Modeling plant transpiration under limited soil water: Comparison of different plant and soil
2318   hydraulic parameterizations and preliminary implications for their use in land surface models, Agricultural and Forest
2319   Meteorology, 191, 22–32, https://doi.org/10.1016/j.agrformet.2014.02.009, 2014.

2320 Vezy, R., Christina, M., Roupsard, O., Nouvellon, Y., Duursma, R., Medlyn, B., Soma, M., Charbonnier, F., Blitz-Frayret, C.,
2321   Stape, J.-L., Laclau, J.-P., de Melo Virginio Filho, E., Bonnefond, J.-M., Rapidel, B., Do, F. C., Rocheteau, A., Picart, D.,
2322   Borgonovo, C., Loustau, D., and le Maire, G.: Measuring and modelling energy partitioning in canopies of varying
2323   complexity using MAESPA model, Agricultural and Forest Meteorology, 253–254, 203–217,
2324   https://doi.org/10.1016/j.agrformet.2018.02.005, 2018.

2325 Villar, R., Held, A. A., and Merino, J.: Dark Leaf Respiration in Light and Darkness of an Evergreen and a Deciduous Plant
2326   Species, Plant Physiology, 107, 421–427, https://doi.org/10.1104/pp.107.2.421, 1995.

2327 Visser, M. D., Bruijning, M., Wright, S. J., Muller-Landau, H. C., Jongejans, E., Comita, L. S., and de Kroon, H.: Functional
2328   traits as predictors of vital rates across the life cycle of tropical trees, Funct Ecol, 30, 168–180,
2329   https://doi.org/10.1111/1365-2435.12621, 2016.

2330 Vleminckx, J., Fortunel, C., Valverde-Barrantes, O., Timothy Paine, C. E., Engel, J., Petronelli, P., Dourdain, A. K., Guevara,
2331   J., Béroujon, S., and Baraloto, C.: Resolving whole-plant economics from leaf, stem and root traits of 1467 Amazonian
2332   tree species, Oikos, 130, 1193–1208, https://doi.org/10.1111/oik.08284, 2021.

2333 Wagner, F. H., Anderson, L. O., Baker, T. R., Bowman, D. M., Cardoso, F. C., Chidumayo, E. N., Clark, D. A., Drew, D. M.,
2334   Griffiths, A. D., Maria, V. R., and others: Climate seasonality limits leaf carbon assimilation and wood productivity in
2335   tropical forests, Biogeosciences, 13, 2537, 2016.

2336 Walker, A. P., Beckerman, A. P., Gu, L., Kattge, J., Cernusak, L. A., Domingues, T. F., Scales, J. C., Wohlfahrt, G.,
2337   Wullschleger, S. D., and Woodward, F. I.: The relationship of leaf photosynthetic traits – Vcmax and Jmax – to leaf
2338   nitrogen, leaf phosphorus, and specific leaf area: a meta-analysis and modeling study, Ecol Evol, 4, 3218–3235,
2339   https://doi.org/10.1002/ece3.1173, 2014.

2340 Wang, Y. P. and Jarvis, P. G.: Description and validation of an array model — MAESTRO, Agricultural and Forest
2341   Meteorology, 51, 257–280, https://doi.org/10.1016/0168-1923(90)90112-J, 1990.

2342 Wang, Y.-P. and Leuning, R.: A two-leaf model for canopy conductance, photosynthesis and partitioning of available energy
2343   I:, Agricultural and Forest Meteorology, 91, 89–111, https://doi.org/10.1016/S0168-1923(98)00061-6, 1998.

2344 Warneke, C. R., Caughlin, T. T., Damschen, E. I., Haddad, N. M., Levey, D. J., and Brudvig, L. A.: Habitat fragmentation
2345   alters the distance of abiotic seed dispersal through edge effects and direction of dispersal, Ecology, 103, e03586,
2346   https://doi.org/10.1002/ecy.3586, 2022.

2347 Watt, A. S.: Pattern and Process in the Plant Community, Journal of Ecology, 35, 1–22, https://doi.org/10.2307/2256497, 1947.

2348 Weemstra, M., Mommer, L., Visser, E. J. W., van Ruijven, J., Kuyper, T. W., Mohren, G. M. J., and Sterck, F. J.: Towards a
2349   multidimensional root trait framework: a tree root review, New Phytol, 211, 1159–1169,
2350   https://doi.org/10.1111/nph.14003, 2016.

2351 Weerasinghe, L. K., Creek, D., Crous, K. Y., Xiang, S., Liddell, M. J., Turnbull, M. H., and Atkin, O. K.: Canopy position
2352   affects the relationships between leaf respiration and associated traits in a tropical rainforest in Far North Queensland, Tree
2353   Physiol, tpu016, https://doi.org/10.1093/treephys/tpu016, 2014.

2354 Williams, M., Rastetter, E. B., Fernandes, D. N., Goulden, M. L., Wofsy, S. C., Shaver, G. R., Melillo, J. M., Munger, J. W.,
2355   Fan, S.-M., and Nadelhoffer, K. J.: Modelling the soil-plant-atmosphere continuum in a Quercus–Acer stand at Harvard
2356   Forest: the regulation of stomatal conductance by light, nitrogen and soil/plant hydraulic properties, Plant, Cell &
2357   Environment, 19, 911–927, https://doi.org/10.1111/j.1365-3040.1996.tb00456.x, 1996.

2358 Williams, M., Law, B. E., Anthoni, P. M., and Unsworth, M. H.: Use of a simulation model and ecosystem flux data to examine
2359   carbon–water interactions in ponderosa pine, Tree Physiol, 21, 287–298, https://doi.org/10.1093/treephys/21.5.287, 2001.

2360 Wilson, J. B., Peet, R. K., Dengler, J., and Pärtel, M.: Plant species richness: the world records, Journal of Vegetation Science,
2361   23, 796–802, https://doi.org/10.1111/j.1654-1103.2012.01400.x, 2012.

2362 Wolf, A., Anderegg, W. R. L., and Pacala, S. W.: Optimal stomatal behavior with competition for water and risk of hydraulic
2363   impairment, PNAS, 113, E7222–E7230, https://doi.org/10.1073/pnas.1615144113, 2016.

2364 Wolz, K. J., Wertin, T. M., Abordo, M., Wang, D., and Leakey, A. D. B.: Diversity in stomatal function is integral to modelling
2365   plant carbon and water fluxes, Nat Ecol Evol, 1, 1292–1298, https://doi.org/10.1038/s41559-017-0238-z, 2017.

2366 Woodruff, D. R. and Meinzer, F. C.: Water stress, shoot growth and storage of non-structural carbohydrates along a tree height
2367   gradient in a tall conifer, Plant, Cell & Environment, 34, 1920–1930, https://doi.org/10.1111/j.1365-3040.2011.02388.x,
2368   2011.

2369 Wright, S. J., Kitajima, K., Kraft, N. J. B., Reich, P. B., Wright, I. J., Bunker, D. E., Condit, R., Dalling, J. W., Davies, S. J.,
2370   Díaz, S., Engelbrecht, B. M. J., Harms, K. E., Hubbell, S. P., Marks, C. O., Ruiz-Jaen, M. C., Salvador, C. M., and Zanne,
2371   A. E.: Functional traits and the growth–mortality trade-off in tropical trees, Ecology, 91, 3664–3674,
2372   https://doi.org/10.1890/09-2335.1, 2010.

2373 Wu, J., Albert, L. P., Lopes, A. P., Restrepo-Coupe, N., Hayek, M., Wiedemann, K. T., Guan, K., Stark, S. C., Christoffersen,
2374   B., Prohaska, N., Tavares, J. V., Marostica, S., Kobayashi, H., Ferreira, M. L., Campos, K. S., Silva, R. da, Brando, P. M.,
2375   Dye, D. G., Huxman, T. E., Huete, A. R., Nelson, B. W., and Saleska, S. R.: Leaf development and demography explain
2376   photosynthetic seasonality in Amazon evergreen forests, Science, 351, 972–976, https://doi.org/10.1126/science.aad5068,
2377   2016.

2378 Wu, J., Serbin, S. P., Xu, X., Albert, L. P., Chen, M., Meng, R., Saleska, S. R., and Rogers, A.: The phenology of leaf quality
2379   and its within-canopy variation is essential for accurate modeling of photosynthesis in tropical evergreen forests, Global
2380   Change Biology, 23, 4814–4827, https://doi.org/10.1111/gcb.13725, 2017.

2381 Wu, J., Serbin, S. P., Ely, K. S., Wolfe, B. T., Dickman, L. T., Grossiord, C., Michaletz, S. T., Collins, A. D., Detto, M.,
2382   McDowell, N. G., Wright, S. J., and Rogers, A.: The response of stomatal conductance to seasonal drought in tropical
2383   forests, Global Change Biology, 26, 823–839, https://doi.org/10.1111/gcb.14820, 2020.

2384 Xu, X., Medvigy, D., Powers, J. S., Becknell, J. M., and Guan, K.: Diversity in plant hydraulic traits explains seasonal and
2385   inter-annual variations of vegetation dynamics in seasonally dry tropical forests, New Phytol, 212, 80–95,
2386   https://doi.org/10.1111/nph.14009, 2016.

2387 Yang, X., Wu, J., Chen, X., Ciais, P., Maignan, F., Yuan, W., Piao, S., Yang, S., Gong, F., Su, Y., Dai, Y., Liu, L., Zhang, H.,
2388   Bonal, D., Liu, H., Chen, G., Lu, H., Wu, S., Fan, L., Gentine, P., and Wright, S. J.: A comprehensive framework for
2389   seasonal controls of leaf abscission and productivity in evergreen broadleaved tropical and subtropical forests, The
2390   Innovation, 2, 100154, https://doi.org/10.1016/j.xinn.2021.100154, 2021.

2391 Yao, Y., Joetzjer, E., Ciais, P., Viovy, N., Cresto Aleina, F., Chave, J., Sack, L., Bartlett, M., Meir, P., Fisher, R., and Luyssaert,
2392   S.: Forest fluxes and mortality response to drought: model description (ORCHIDEE-CAN-NHA r7236) and evaluation at
2393   the Caxiuanã drought experiment, Geoscientific Model Development, 15, 7809–7833, https://doi.org/10.5194/gmd-15-
2394   7809-2022, 2022.

2395 Yao, Y., Ciais, P., Viovy, N., Joetzjer, E., and Chave, J.: How drought events during the last century have impacted biomass
2396   carbon in Amazonian rainforests, Global Change Biology, 29, 747–762, https://doi.org/10.1111/gcb.16504, 2023.

2397 Yao, Y., Ciais, P., Joetzjer, E., Li, W., Zhu, L., Wang, Y., Frankenberg, C., and Viovy, N.: The impacts of elevated CO2 on
2398   forest growth, mortality and recovery in the Amazon rainforest, Earth System Dynamics Discussions, 1–23,
2399   https://doi.org/10.5194/esd-2024-5, 2024.

2400 Yoda, K., Shinozaki, K., Ogawa, H., Hozumi, K., and Kira, T.: Estimation of the total amount of respiration in woody organs
2401   of trees and forest communities., J. Biol. Osaka City Univ, 16, 15–26, 1965.

2402 Yu, W., Albert, G., Rosenbaum, B., Schnabel, F., Bruelheide, H., Connolly, J., Härdtle, W., von Oheimb, G., Trogisch, S.,
2403   Rüger, N., and Brose, U.: Systematic distributions of interaction strengths across tree interaction networks yield positive
2404   diversity–productivity relationships, Ecology Letters, 27, e14338, https://doi.org/10.1111/ele.14338, 2024.

2405 Zaehle, S., Sitch, S., Smith, B., and Hatterman, F.: Effects of parameter uncertainties on the modeling of terrestrial biosphere
2406   dynamics, Global Biogeochem. Cycles, 19, GB3020, https://doi.org/10.1029/2004GB002395, 2005.

2407 Zellweger, F., Frenne, P. D., Lenoir, J., Rocchini, D., and Coomes, D.: Advances in Microclimate Ecology Arising from
2408   Remote Sensing, Trends in Ecology & Evolution, 34, 327–341, https://doi.org/10.1016/j.tree.2018.12.012, 2019.

2409 Zhou, S., Duursma, R. A., Medlyn, B. E., Kelly, J. W. G., and Prentice, I. C.: How should we model plant responses to drought?
2410   An analysis of stomatal and non-stomatal responses to water stress, Agric. For. Meteorol., 182, 204–214,
2411   https://doi.org/10.1016/j.agrformet.2013.05.009, 2013.

2412 Zhou, S., Medlyn, B., Sabaté, S., Sperlich, D., Prentice, I. C., and others: Short-term water stress impacts on stomatal,
2413   mesophyll and biochemical limitations to photosynthesis differ consistently among tree species from contrasting climates,
2414   Tree Physiology, 34, 1035–46, 2014.

2415   Ziegler, C., Coste, S., Stahl, C., Delzon, S., Levionnois, S., Cazal, J., Cochard, H., Esquivel-Muelbert, A., Goret, J.-Y., Heuret,
2416   P., Jaouen, G., Santiago, L. S., and Bonal, D.: Large hydraulic safety margins protect Neotropical canopy rainforest tree
2417   species against hydraulic failure during drought, Annals of Forest Science, 76, 115, https://doi.org/10.1007/s13595-019-
2418   0905-0, 2019.

2419   **Appendix A**

2420   **Table A1. List of symbols and variables.**

Symbols	Definition	Units	Nature	Equations
Physical constants				
M_w	Molar mass of water vapor	kg mol^{-1}	Constant	12
R	ideal gas constant	J mol^{-1} K^{-1}	Constant	12-13, 28-31, 46-47
V_w	Partial molal volume of water	m^3 mol^{-1}	Constant	13
κ	von Karman constant	unitless	Constant	8, 15
g	Gravity constant	m s^{-2}	Constant	37
ρ	Density of water	kg m^{-3}	Constant	37
M_a	Molecular mass of air	kg mol^{-1}	Constant	41, 48
C_p	Heat capacity of air	J kg^{-1} K^{-1}	Constant	41, 48
γ	Psychrometric constant	Pa K^{-1}	Constant	41
D_H	Molecular diffusivity to heat	m^2 s^{-1}	Constant	46
σ	Stefan-Boltzmann constant	W m^{-2} K^{-4}	Constant	44, 48
Aboveground environment				
PPFD$_{top}$	Photosynthetic photon flux density at canopy top	μmol photons m^{-2} s^{-1}	Updated at half hourly step, given as input	1
T_{top}	Temperature at canopy top	°C	Updated at half hourly step, given as input	4, 6, 44
VPD_{top}	Vapour pressure deficit at canopy top	kPa	Updated at half hourly step, given as input	5, 7
u$_{top}$	Wind speed at a reference height above the canopy	m s^{-1}	Updated at half hourly step, given as input	Sections 2.1 and 2.2
T$_{night}$	Nighttime temperature	°C	Updated daily, given as input	Section 2.2
$PPFD$	Incident photosynthetic photon flux density	μmol photons m^{-2} s^{-1}	Computed every half hour	1, 25
T	Temperature	°C	Computed every half hour	4, 42, 46-48
VPD	Vapour pressure deficit	kPa	Computed every half hour	5
u	Wind speed	m s^{-1}	Computed every half hour	8, 9, 15, 47
c$_a$	CO$_2$ concentration	μmol mol^{-1} (ppm)	Constant	Section 2.5
P$_{ress}$	Atmospheric pressure	Pa	Constant	46-47
$PPFD_{abs}$	Absorbed photosynthetic photon flux density	μmol photons m^{-2} s^{-1}	Computed every half hour	2
T_{mean}	Temperature, averaged per crown layer	°C	Computed every half hour	6
VPD_{mean}	Vapour pressure deficit, averaged per crown layer	kPa	Computed every half hour	7
LAI	Cumulated leaf area per ground area	m^2 m^{-2}	Computed daily for each voxel	1-3, 11, 43
dens	Averaged leaf area density per unit ground area	m^2 m^{-2}	Computed daily, averaged per layer	3, 6-7

k	Effective light extinction coefficient	unitless	Fixed, computed from k_{geom} and absorptance$_{leaves}$	1
k_{geom}	Light extinction coefficient reflecting the geometric arrangement of leaves	unitless	Constant, given as input	1
absorptance$_{leaves}$	Fraction of absorbed light within a single leaf	unitless	Constant, given as input	1
LAI_{sat}	LAI threshold for computing microenvironemntal variation within the canopy	$m^2\ m^{-2}$	Constant	4-7
ΔT	Parameter of the within-canopy variation in temperature	°C	Constant	4, 6
C_{VPD0}	Parameter of the within-canopy variation in vapour pressure deficit	unitless	Constant	5, 7
u*	friction velocity	$m\ s^{-1}$	Constant	
d	zero-plane displacement height	m	Computed from the locally averaged canopy height (H)	8
z_0	aerodynamic roughness	m	Computed from the locally averaged canopy height (H)	8
H	Top canopy height	m	Computed daily	8-9
α	Parameter of wind speed decrease within the canopy	unitless	Constant	9
Water balance				
P	Precipitation	mm	Updated daily, given as input	10
I	Interception	mm	Computed daily	10, 11
Q	Run-off	m^3	Computed daily	10
E	Evaporation from the soil	$kg\ m^{-2}\ s^{-1}$	Computed daily	10, 12
T	Tree transpiration	m^3	Computed daily	10
L	Leakage	m^3	Computed daily	10
K	Parameter for rainfall interception	mm	Constant	11
T_s	Temperature at soil surface	K	Computed daily	12, 13
e_s	Vapor pressure of the soil surface	Pa	Computed daily	12
e_a	Vapor pressure of air above the soil surface	Pa	Computed daily	12
e_{sat}	saturated vapor pressure	Pa	Computed daily	13
r_{soil}	Soil surface resistance	$s\ m^{-1}$	Computed daily	12, 14
r_{aero}	Aerodynamic resistance to heat transfer	$s\ m^{-1}$	Computed daily	12, 15
Z	Reference height for r_{aero} computation	m	Constant	15
Z_m	Momentum soil roughness	m	Constant	15
ψ_l	Soil water potential of layer l	MPa	Computed daily	21
K_l	Soil hydraulic conductivity of layer l	$kg\ m^{-2}\ s^{-1}$	Computed daily	22

$\psi_{soil,top}$	Water potential of the top soil belowground voxel	MPa	Computed daily	13
θ_{top}	Water content of the top soil belowground voxel	m^3	Computed daily	14
$\theta_{fc,top}$	water content at field capacity of the top soil belowground voxel	m^3	Computed daily	14
Species and tree characteristics				
LMA	Leaf mass per area	$g\ m^{-2}$	Species-specific means: constant, provided as input; tree-specific values: randomly attributed at tree birth	26, 27, 32, 56
LA	Leaf area	cm^2	Species-specific means: constant, provided as input; tree-specific values: randomly attributed at tree birth	46-47
N	Leaf nitrogen content per dry mass	$mg\ g^{-1}$	Species-specific means: constant, provided as input; tree-specific values: randomly attributed at tree birth	26, 27, 32
P	Leaf phosphorous content per dry mass	$mg\ g^{-1}$	Species-specific means: constant, provided as input; tree-specific values: randomly attributed at tree birth	26, 27, 32
wsg	Wood specific gravity	$g\ cm^{-3}$	Species-specific means: constant, provided as input; tree-specific values: randomly attributed at tree birth	36, 55, 60-61, 66
π_{tlp}	Leaf water potential at turgor loss point	MPa	Species-specific means: constant, provided as input; tree-specific values: randomly attributed at tree birth	39-40, 58, 68, section 2.7.1
dbh$_{thres}$	Threshold diameter at breast height, beyond which growth senescence starts	m	Species-specific means: constant, provided as input; tree-specific values: randomly attributed at tree birth	62, 63

dbh_{max}	Maximal tree diameter at breast height	m	Computed once per tree	Section 2.6.4
h_{lim}	Asymptotic height (parameter of Michaelis-Menten function)	m	Species-specific means: constant, provided as input	16
h_{max}	Maximal tree height	m	Species-specific means: constant, provided as input	67
a_h	Parameter of Michaelis-Menten function	m	Species-specific means: constant, provided as input	16
$f_{reg,s}$	Relative abundance of species s in the external seed rain	unitless	Species-specific, provide as input	64
w_l	Leaf width	m	Computed for each tree	46-47
LL	Leaf lifespan	yr	Computed for each tree	57
$\varepsilon_{i,j}$	Individual effects for trait or variable i and tree j	See traits	Randomly attributed at tree birth	Sections 2.4.1 and 2.4.2
σ_i	standard deviation for intraspecific variability in trait or variable i	See traits	Constant, provided as input	Sections 2.4.1 and 2.4.2
dbh	Tree diameter at breast height	m	Tree variable, updated at each timestep	16, 17, 19, 60-62
h	Tree height	m	Tree variable, updated at each timestep	16, 37, 54-55, 58, 60
cr	Tree crown radius	m	Tree variable, updated at each timestep	17
cd	Tree crown depth	m	Tree variable, updated at each timestep	18, 54
a_{cr}	Coefficients of crown radius allometry	unitless	Species-independent constant, provided as input	17
b_{cr}	Coefficients of crown radius allometry	unitless	Species-independent constant, provided as input	17
a_{cd}	Coefficients of crown depth allometry	m	Species-independent constant, provided as input	18
b_{cd}	Coefficients of crown depth allometry	unitless	Species-independent constant, provided as input	18
$shape\_crown$	Ratio between the radius of the crown at the top of the tree to the radius at the bottom of the crown being a global parameter	unitless	Global parameter, provided as input	Section 2.4.2
f_{gap}	Fraction of gaps (openings) in tree crowns	unitless	Constant, provided as input	Section 2.4.2
RD	Tree root depth	m	Tree variable, updated at each timestep	19
RB_t	Total tree fine root biomass	g	Tree variable, updated at each timestep	20

RB_l	Tree fine root biomass in layer l	g	Tree variable, updated at each timestep	20
ψ_{root}	Soil water potential in the tree root zone	MPa	Tree variable, updated at each timestep	21, 37
$\psi_{R,min}$	Root water potential below which there is no soil water uptake	MPa	Constant	21
G_l	soil-to-root water conductance in layer l	mmol H_2O m^{-2} s^{-1} MPa^{-1}	Variable, computed for each tree and layer at each timestep	21, 22
$L_{a,l}$	Tree total root length per unit area in layer l	m m^{-2}	Variable, computed for each tree and layer at each timestep	22
$L_{v,l}$	Tree total root length per unit soil volume in layer l	m m^{-3}	Variable, computed for each tree and layer at each timestep	23
SRL	Specific root length	m g^{-1}	Constant	22
r_s	Mean fine root radius	m	Constant	22
r_s	half of the mean distance between roots	m	Variable, computed for each tree and layer at each timestep	22, 23
Leaf physiology				
T_l	Leaf temperature	°C	Computed half-hourly for each crown layer	24, 25, 28-31, 33, 46
VPD_s	Vapor pressure deficit at the leaf surface	kPa	Computed half-hourly for each crown layer	35
c_s	CO_2 concentration at the leaf surface	μmol mol^{-1} (ppm or μbar)	Computed half-hourly for each crown layer	34
c_i	CO_2 concentration at carboxylation sites	μmol mol^{-1} (ppm or μbar)	Computed half-hourly for each crown layer	24, 34
A_n	Leaf-level net carbon assimilation rate	μmol CO_2 m^{-2} s^{-1}	Computed half-hourly for each crown layer	24, 52
A_v	Leaf-level net carbon assimilation rate limited by Rubisco activity	μmol CO_2 m^{-2} s^{-1}	Computed half-hourly for each crown layer	24
A_j	Leaf-level net carbon assimilation rate limited by RuBP regeneration	μmol CO_2 m^{-2} s^{-1}	Computed half-hourly for each crown layer	24
R_p	Photorespiration rate	μmol C m^{-2} s^{-1}	Computed half-hourly for each crown layer	24
R_d	Leaf dark respiration rate	μmol C m^{-2} s^{-1}	Computed half-hourly for each crown layer	33
R_{d-M}	Leaf dark respiration rate on a leaf dry mass basis	nmol CO_2 g^{-1} s^{-1}	Computed half-hourly for each crown layer	32
V_{cmax}	Maximum rate of carboxylation	μmol CO_2 m^{-2} s^{-1}	Computed half-hourly for each crown layer	24, 26, 28
V_{cmax-M}	Maximum rate of carboxylation on a leaf dry mass basis	μmol CO_2 g^{-1} s^{-1}	Computed half-hourly for each crown layer	26
J	Electron transport rate	μmol e^- m^{-2} s^{-1}	Computed half-hourly for each crown layer	24, 25
J_{max}	maximal electron transport capacity	μmol e^- m^{-2} s^{-1}	Computed half-hourly for each crown layer	25, 29

J_{max-M}	maximal electron transport capacity on a leaf dry mass basis	µmol e^- g^{-1} s^{-1}	Computed half-hourly for each crown layer	27
Γ^*	CO$_2$ compensation point in the absence of dark respiration	μbar	Computed half-hourly for each crown layer	24, 30
K_m	Apparent kinetic constant of the Rubisco	μbar	Computed half-hourly for each crown layer	24, 31
θ	Curvature factor	unitless	Constant	25
α	Apparent quantum yield to electron transport	mol e^- mol $photons^{-1}$	Constant	25
LSQ	Effective spectral quality of light	unitless	Constant	25
g_s	stomatal conductance to CO$_2$	mol CO_2 m^{-2} s^{-1}	Computed half-hourly for each crown layer	34
g_{sw}	stomatal conductance to water vapor	mol H$_2$0 m^{-2} s^{-1}	Computed half-hourly for each crown layer	35
g_0	minimum leaf conductance for water vapor	mol H$_2$0 m^{-2} s^{-1}	Constant, provided by the user	35
g_1	Parameter of the stomatal conductance model	kPa$^{0.5}$	Computed daily for each tree	35, 36
ψ_{pd}	Leaf predawn water potential	MPa	Tree variable, computed daily	24, 25, 28, 29, 36-40
WSF_{ns}	Water stress factor for non-stomatal limitation	unitless	Tree variable, computed daily	28, 29, 40
WSF_s	Water stress factor for stomatal limitation	unitless	Tree variable, computed daily	36, 38-39
a	Parameter of WSF_{ns}	unitless	Constant	40
b	Parameter of WSF_s	unitless	Computed from tree-specific ψ_{tlp}	39, 39
E_l	Leaf-level transpiration rate	mol H$_2$0 m^{-2} s^{-1}	Computed half-hourly for each crown layer	41
λ	Latent heat of water vapor	J mol^{-1}	Computed half-hourly for each crown layer	41, 42
s	slope of the (locally linearized) relationship between saturated vapor pressure and temperature	Pa K^{-1}	Computed half-hourly for each crown layer	41
R_{ni}	isothermal net radiation	J m^{-2} s^{-1}	Computed half-hourly for each crown layer	41, 43
g_H	total leaf conductance to heat	mol m^{-2} s^{-1}	Computed half-hourly for each crown layer	41, 45
g_{bHf}	boundary layer conductance for free convection	mol m^{-2} s^{-1}	Computed half-hourly for each crown layer	45, 46, 50
g_{bHu}	boundary layer for forced convection	mol m^{-2} s^{-1}	Computed half-hourly for each crown layer	45, 47, 50
g_r	radiation conductance	mol m^{-2} s^{-1}	Computed half-hourly for each crown layer	45, 48
g_w	total leaf conductance to water vapor	mol H$_2$0 m^{-2} s^{-1}	Computed half-hourly for each crown layer	41, 49
g_{bw}	boundary layer conductance to water vapor	mol H$_2$0 m^{-2} s^{-1}	Computed half-hourly for each crown layer	49, 50
S_{abs}	Absorbed solar radiation (PAR and NIR)	J m^{-2} s^{-1}	Computed half-hourly for each crown layer	43

$B_{n,0}$	Net longwave radiation at the top of the canopy	J m⁻² s⁻¹	Computed every half hour	43, 44
k_d	Coefficient of extinction of longwave radiation	Unitless	Constant	43
ε_l	Emissivity of the canopy leaves	Unitless	Constant	44, 48
ε_a	Emissivity of the atmosphere	Unitless	Computed every half hour	44
Tree carbon allocation and demography				
GPP_{ind}	Tree-level gross primary productivity	gC	Computed daily	51
NPP_{ind}	Tree-level net primary productivity	gC	Computed daily	51
NPP_{leaves}	Tree-level net primary productivity allocated to leaf production	gC	Computed daily	56
NPP_{wood}	Tree-level net primary productivity allocated to woody growth	gC	Computed daily	61
AGB	Tree aboveground biomass	kg	Computed daily	59-60
$R_{maintenan}$	Tree-level maintenance respiration	gC	Computed daily	51
R_{stem}	Stem maintenance respiration	μmol C s⁻¹	Computed daily	54
R_{growth}	Tree-level growth respiration	gC	Computed daily	51
LA$_t$	Tree-level total leaf area	m²	Updated daily	55
LA$_{opt}$	Optimal tree leaf area	m²	Updated daily	Section 2.6.2
LA_l	Leaf area in tree crown layer l	m²	Updated daily	51, 52-53
LA$_{young}$	Tree-level young leaf area	m²	Updated daily	52-53, 56
LA$_{mature}$	Tree-level mature leaf area	m²	Updated daily	52-53, 56
LA$_{old}$	Tree-level old leaf area	m²	Updated daily	52-53, 56
ϱ	Ratio of young or old leaf assimilation rate over mature leaf assimilation rate	unitless	Constant	52
ϱ'	Ratio of young or old leaf respiration rate over mature leaf respiration rate	unitless	Constant	53
τ_{young}	Leaf residence time in the young age pool	yr	Computed for each tree	56
τ_{mature}	Leaf residence time in the young age pool	yr	Computed for each tree	56
τ_{old}	Leaf residence time in the young age pool	yr	Computed for each tree	56
SA	Tree sapwood area	m²	Updated daily	54, 55
λ_1	Parameter for sapwood area computation	m² cm⁻²	Constant	55
λ_2	Parameter for sapwood area computation	m cm⁻²	Constant	55
δ_1	Parameter for sapwood area computation	m² cm⁻²	Constant	55
δ_2	Parameter for sapwood area computation	cm³ g⁻¹	Constant	55

f_{canopy}	Fraction of NPP_{ind} allocated to tree canopy (including leaves, fruits and twigs)	unitless	Constant, given as input	Sections 2.6.1 and 2.6.2
f_{leaves}	Fraction of NPP_{ind} allocated to leaves	unitless	Constant	Section 2.6.2, 56
f_{fruit}	Fraction of NPP_{ind} allocated to fruits	unitless	Constant	Section 2.6.1
f_{twigs}	Fraction of NPP_{ind} allocated to twigs	unitless	Constant	Section 2.6.1
f_{wood}	Fraction of NPP_{ind} allocated to wood	unitless	Constant, given as input	Section 2.6.2
$\psi_{T,o}$	Water potential threshold for accelerating old leaf shedding	MPa	Computed daily for each tree	58
$a_{T,o}$	Parameter to compute $\psi_{T,o}$ (modulates old leaf drought tolerance)	unitless	Constant, given as input	58
$b_{T,o}$	Parameter to compute $\psi_{T,o}$ (modulates the height dependence of leaf susceptibility to drought)	MPa	Constant, given as input	58
f_o	Factor of the acceleration of old leaf shedding	unitless	Updated daily for each tree	Section 2.6.2
δ_o	Parameter controlling the pace of old leaf shedding acceleration (Δf_0)	unitless	Constant, given as input	
NSC_r	Maximal amount of stored non-structural carbohydrates	gC	Updated daily for each tree	59
ΔV	Increment of stem volume	m³	Computed daily for each tree	61
$Senesc$	Growth senescence factor	unitless	Computed daily for each tree	61-62
Δdbh	Trunk diameter growth	m	Computed daily for each tree	Section 2.6.4
dbh_{mature}	Diameter threshold beyond which the tree is fertile	m	Computed once for each tree	63
σ_{disp}	Scale parameter of the Rayleigh distribution for seed dispersal	m	Constant	Section 2.7.1
n_s	Number of reproduction opportunities per mature tree	number of seeds	Constant	Section 2.7.1
N_{tot}	Intensity of the external seed rain	number of seeds per hectare	Constant, given as input	64
$n_{ext,s}$	Species-specific number of dispersal events due to the external seed rain	number of seeds	Computed once for each species	64
n_{ha}	Area of the simulated plot	ha	Constant, computed from dimensions given as input	64
LAI_{max}	LAI threshold beyond which the seedling leaf carbon balance is negative	m² m⁻²	Computed once for each tree	Section 2.7.1

d	Tree death rate	events yr^{-1}	Updated daily at tree level	65-66
d_b	Background death rate	events yr^{-1}	Computed once per tree	65
m	reference background mortality rate	events yr^{-1}	Constant, provided as input	66
wsg_{lim}	Parameter of d_b	g cm^{-3}	Constant	66
d_{starv}	Death rate due to carbon starvation	events yr^{-1}	Updated daily at tree level	65
$d_{treefall}$	Death rate due to treefall	events yr^{-1}	Updated daily at tree level	65
Θ	Parameter of treefall probability	m	Computed once per tree	67
$d_{drought}$	Death rate due to drought	events yr^{-1}	Updated daily at tree level	65
v_T	Variance for treefall probability	unitless	Computed once per tree	67
hurt	Parameter of secondary treefall probability	m	Updated daily for each tree	Section 2.7.2
ψ_{lethal}	Water potential threshold for drought-induced mortality	MPa	Computed once per tree	68

2421

Appendix B

Table B1. Representation of stomatal conductance, water stress effect on leaf gas exchange and tree transpiration in several vegetation models. g_0, cuticular or minimal stomatal conductance, i.e. g_s when $A \rightarrow 0$; A, CO_2 assimilation rate; c_s, CO_2 concentration at the leaf surface; D_s, vapour pressure deficit at the leaf surface; h_s, fractional relative humidity at the leaf surface; Γ, CO_2 compensation point; V_{cmax} and J_{max} are the maximum carboxylation rate and electron transport rate. All 0 subscript denotes the values without water stress (except for g_0 by convention). Note stomatal conductance to H_2O is 1.6 times higher than stomatal conductance to CO_2, we here only represent stomatal conductance to H_2O.

| Vegetation model | | Stomatal conductance | | Water stress effect on leaf gas exchange | | Tree transpiration |
Name	Reference	Type	Model	Reference/type	Stomatal limitations	Non-stomatal limitations	
ED2	(Longo et al., 2018; Medvigy et al., 2009)	Cohort-based vegetation model	$g_s = g_0 + \dfrac{a_1 \times A}{(c_s - \Gamma)(1 + \frac{D_s}{D_0})}$	(Leuning, 1995)/ empirical model	The plant net CO_2 assimilation and evapotranspiration rates (x_{net}) are computed as a linear combination of their rates under open (x_o) and close (x_c) stomata: $x_{net} = f x_o + (1-f) x_c$ with $f = \dfrac{1}{1 + \frac{Demand}{Supply}} = \dfrac{1}{1 + \frac{E_0 \times LA}{K \times W_{avail,tot} \times B_{root}}}$ where E_0 is the evapotranspiration rate under conditions of open stomata times and LA the total plant leaf surface area, and $W_{avail,tot}$ is the amount of water accessible by the vegetation layer, B_{root} the plant root biomass, and K an optimized constant.		Computed with: $E_0 = \varphi_0 \times SLA \times B_{leaf}$ with B_{leaf} the tree leaf biomass and φ_0 its evapotranspiration rate, obtained by solving a set of 6 equations of 6 unknowns (after determining the leaf temperature using a surface energy balance submodel), among which: $\varphi_0 = g_{bw} \times (e_s - e_a)$ $\varphi_0 = g_s \times (e_l - e_s)$
ED2-hydro	(Powell et al., 2018; Xu et al., 2016)	ED2 with a new module of plant hydraulics	Solution of : $\dfrac{\partial}{\partial g_w}(A_{net} - \lambda g_w D_a) = 0$ with $g_w = \frac{g_s g_b}{g_s + g_b}$ and λ is the Lagrangian multiplier of the optimization problem, representing the marginal water use efficiency (marginal increase in A_{net} per unit change of water loss)	(Vico et al., 2013)/ optimization model, under CO_2 (Rubisco) and light (RuBP regeneration/electron transport) co-limitations	$\lambda = \lambda_0 \times \exp(\beta \times \psi_{pd})$ with λ_0 the value of λ when there is no water stress and β an empirical factor taken from Manzoni et al. (2011)	$V_{cmax} = V_{cmax,0} \times \left[1 + \left(\frac{\psi_{leaf}}{\pi_{ttp}}\right)^{\alpha}\right]^{-1}$ $J_{max} = J_{max,0} \times \left[1 + \left(\frac{\psi_{leaf}}{\pi_{ttp}}\right)^{\alpha}\right]^{-1}$ where $V_{cmax,0}$ and $J_{max,0}$ denotes the photosynthetic capacities without water stress, and α is a shape factor estimated from Brodribb et al. (2003).	Similarly to Medvigy et al. 2009, $E_0 = \dfrac{g_s g_b}{g_s + g_b} \times D_a \times LA$
TFS	(Fyllas et al., 2014)		$g_s = g_0 + 1.6 \times (1 + \frac{g_1}{\sqrt{D_s}}) \times \frac{A}{c_s}$ g_1 is an empirical coefficient*, associated to the water use efficiency (to the Lagrangian).	(Medlyn et al., 2011)/ optimization, for electron-transport limited photosynthesis (light limitation)	$g_s = g_{s,0} \times \dfrac{\theta_i - \theta_{wp}}{\theta_{fc} - \theta_{wp}}$ where θ_{wp}, θ_{fc}, θ_{wp} are the actual soil water available for tree i, and the soil water content at field capacity and wilting point respectively.	-	Following MAESTRA (Medlyn et al., 2007), an iterative procedure is used to solve the energy balance of the canopy of each tree, under which the Penman-Monteith equation is used to estimate canopy transpiration.

	CLM5	Multi-layer CLM4.5	TFS-Hydro
Reference	(Kennedy et al., 2019)	(Bonan et al., 2014)	(Christoffersen et al., 2016)
Type	Stand-based	DGVM	TFS with a new module of plant hydraulics
Stomatal conductance	$g_s = g_0 + 1.6 \times (1 + \dfrac{g_1}{\sqrt{D_s}}) \times \dfrac{A}{c_s}$ (Medlyn et al., 2011)/ optimization, under light	$g_s = g_0 + g_1 \times A \times \dfrac{h_s}{c_s}$ (Ball et al., 1987; Collatz et al., 1991)/ empirical	$g_s = g_{s,0} \times \left[1 + \left(\dfrac{\psi_{leaf}}{\psi_{g_s,50}} \right)^{a_{g_s}} \right]^{-1}$ where $\psi_{g_s,50}$ is the leaf water potential at 50% stomatal closure (assumed a 1:1 relationship between $\psi_{g_s,50}$ and the water potential at 20% loss of xylem hydraulic conductivity ($P_{20,x}$), following results from (Brodribb et al., 2003)), and a_{g_s} is the slope of the curve at $\psi_{leaf} = \psi_{g_s,50}$, computed from $\psi_{g_s,50}$ using the same relationship that relates a_x and $P_{50,x}$.
		g_s is iteratively computed such that (1) further opening does not yield a sufficient carbon gain per unit water loss (defined by a stomatal efficiency parameter) or (2) further opening causes leaf water potential to decrease below the minimum sustainable leaf water potential that prevents xylem cavitation Inspired from the SPA model (Williams et al., 1996)/ optimization within limitations imposed by water use efficiency, plant water storage, and soil-to-leaf water transport	—
	$V_{c,max} = V_{c,max,0} \times \sum_j r_j \dfrac{\psi_j - \psi_c}{\psi_o - \psi_c}$ CML4.5 default	$g_0 = g_{0,0} \times \sum_j r_j \dfrac{\psi_j - \psi_c}{\psi_o - \psi_c}$ where ψ_j is the soil water potential of soil layer j, and ψ_o and ψ_c are the leaf water potential at which the stomata are fully open and fully closed respectively, and r_j is the relative root fraction of soil layer j.	$V_{c,max} = V_{c,max,0} \times \sum_j r_j \dfrac{\psi_j - \psi_c}{\psi_o - \psi_c}$
		The optimization includes a dependence to ψ_{leaf}, where ψ_{leaf} is computed at each timestep (30-60 min) with Darcy's law (soil-to-leaf pathway, including capacitance).	—
	An iterative procedure is used to solve the energy balance (determine the leaf temperature and internal CO_2)	—	Iterative procedure

	ORCHIDEE EE	CABLE	MAESPA
Reference	(Krinner et al., 2005; Naudts et al., 2015)	(De Kauwe et al., 2015a, b)	(Duursma et al., 2012)
Structure	DGVM	DGVM (vegetation is represented using a single layer, two-leaf canopy model separated into sunlit and shaded leaves)	Individual- and stand-based model
g_s equation	$g_s = mA\dfrac{h_r}{c_a} + b$	$g_s = g_0 + 1.6 \times (1 + \dfrac{g_1}{\sqrt{D_s}}) \times \dfrac{A}{c_s}$	$g_s = g_0 + 1.6 \times \dfrac{A}{c_s} \times \dfrac{1 + e^{s_f\psi_f}}{1 + e^{s_f(\psi_f - \psi_{leaf})}}$ where ψ_{leaf} is computed at each time step using Darcy's law ($E_L = k_L \times (\psi_{soil} - \psi_{leaf})$)
Model / type	(Ball et al., 1987)	(Medlyn et al., 2011)/ optimization, under light limitation (RuBP regeneration) (was the model of (Leuning, 1995) in previous versions of CABLE (Wang et al., 2011))	(Tuzet et al., 2003)/ empirical
	-	Standard version of CABLE (De Kauwe et al., 2015a) : $g_1 = g_{1,0} \times \sum_i r_i \dfrac{\theta_i - \theta_{wp}}{\theta_{fc} - \theta_{wp}}$ with θ_i the volumetric soil water content and r_i the fraction of root mass in soil layer j, and θ_{wp} the soil wilting point and θ_{fc} its field capacity. New expression for drought sensitivity of gas exchange: $g_1 = g_{1,0} \times \exp(b \times \psi_{pd})$, where b is a fitted (species-specific) parameter representing the sensitivity of g_1 to leaf predawn water potential ψ_{pd} and taken from (Zhou et al., 2013, 2014), while $g_{1,0}$ values are drawn from (Lin et al., 2015).	Already implemented in g_s computation. g_1, is an empirical coefficient*, associated to the water use efficiency (to the Lagrangian).
$V_{c,max}$	In the version of (Krinner et al., 2005): The photosynthetic capacities, Vcmax and Jmax, are multiplied by a water stress factor that is:	$V_{c,max} = V_{c,max,0} \times \dfrac{1 + e^{s_f\psi_f}}{1 + e^{s_f(\psi_f - \psi_{pd})}}$ where s_f and ψ_f are fitted (species-specific) parameters drawn from (Zhou et al., 2013, 2014).	limitation (RuBP regeneration) $V_{c,max} = V_{c,max,0} \times 2^{-\left(\frac{\psi_{leaf}}{\psi_{g_s,50}}\right)^{a_{g_s}}}$ where $\psi_{g_s,50}$ is the leaf water potential at 50% loss of stomatal conductance and a_{g_s} is a shape-fitting parameter. The solution for vegetation water potential is the set of values that matches supply with demand, maintaining water balance across each of the vegetation water potential nodes ($\psi_{root}, \psi_{stem}, \psi_{sunlit-leaf}, \psi_{shade-leaf}$) based on Darcy's law (without capacitance).
Transpiration		Following MAESTRA (Medlyn et al., 2007), an iterative procedure is used to solve the energy balance of the canopy of each tree, under which the Penman-Monteith equation is used to estimate canopy transpiration. transpiration from the vegetation to the atmosphere is controlled by several resistances operating in series, both above (aerodynamic) and within the canopy (stomatal and leaf boundary layer), and a longwave radiative balance through radiative conductance on net available energy. These resistances in serial, result in a relatively weak coupling between the canopy surface and the atmosphere.	concentration), under which transpiration is computed as $E_0 = \dfrac{g_s g_b}{g_s + g_b} \times D_a \times LA$.

$$1 \ if \ f_w > f_o$$

$$1 - \frac{f_w - f_c}{f_o - f_c} \ if \ f_c < f_w < f_o$$

$$0 \ if \ f_w < f_c$$

with f_w the water fraction available for the plant in the root zone, and f_c and f_o the soil water fractions inducing, respectively, closure and maximum opening of stomata.

In the CAN version of (Naudts et al., 2015): The model calculates plant water supply according to the implementation of hydraulic architecture by (Hickler et al., 2006), i.e. using Darcy's law and accounting for the hydraulic resistances of fine roots, sapwood and leaves. If the transpiration calculated by the energy budget exceeds the amount of water a plant can transport from the soil to its stomata, transpiration is limited to the plant water supply, and stomatal conductance is then recalculated such that the transpiration equals the amount of water a plant can transport. The energy budget and photosynthesis are then recalculated. This may require up to 10 iterations to converge.

-

with m and b derived from laboratory measurements.

LPj	(Sitch et al., 2003)	DGVM		(Collatz et al., 1991)	
			The model uses the Farquhar model of photosynthesis as generalized for global modelling purposes by (Collatz et al., 1991). In absence of water stress, canopy conductance is derived from the daytime carbon assimilation rate: $$g_c = g_{min} + \frac{1.6\,A}{c_a(1-\lambda)}$$		Under water stress i.e. when min $[1; \frac{E_{supply}}{E_{dema,d}}] < 1$, The equations of evapotranspiration rate, assimilation rate and the one related assimilation rate and canopy conductance are solved simultaneously to yield values of canopy conductance consistent with the transpiration rate.	< 1 Daily evapotranspiration is calculated for each PFT as the minimum of a plant- and soil-limited supply function (E_{supply}) and the atmospheric demand (E_{demand}). E_{supply} is the product of a plant root-weighted soil moisture availability and a maximum transpiration rate; E_{demand} is calculated following Monteith's empirical relation between evaporation efficiency and surface conductance, that uses gpot, the nonwater-stressed potential canopy conductance calculated by the photosynthesis routine

*although fitted empirically to leaf exchange experimental data (Lin et al., 2015), attempts have been made to relate g1 to functional traits and/or

climatological variables (wood density, Lin *et al.*, 2015; leaf δ13C, Franks *et al.*, 2018), based on the premise that water use efficiency should be

associated to functional strategies. See also values reported in Domingues *et al.* (2014).

Table B2. Examples of observational or experimental studies that explored the relative roles of stomatal and non-stomatal limitations of photosynthesis under drought conditions.

Key message for vegetation models	Reference	Studied system	Main results
Stomatal-limitation only	Santos et al., 2018	57 canopy and understory trees within a central Amazonian forest	Photosynthesis decreased during the extreme dry season, and this was only related to stomatal closure (decline in stomatal conductance) and not to leaf biochemical changes (sustained chlorophyll concentration and fluoresecnce, and nutrient concentration).
	Rowland et al., 2015	Trees in the ThroughFall Exclusion and control plots in Caixuana, Amazonia.	No differences in V_{cmax} and J_{max} between the throughfall exclusion plot and the control plot.
	Trueba et al., 2019	Mature individuals of 10 angiosperms species located on the campus of UCLA and a park in LA	The stomatal and leaf hydraulic systems (50% lost of gs, K_{leaf}) show early functional declines before cell integrity is lost. Substantial damage to the photochemical apparatus (maximum quantum yield of the photosystem) occurs at extreme dehydration, after turgor loss and complete stomatal closure, and seems to be irreversible.
Both stomatal and non-stomatal limitations	Zhou et al., 2013	Meta-analysis of 22 experimental datasets where photosynthesis, stomatal conductance and predawn leaf water potential were measured at increasing water stress, spanning a range of plant functional types	Photosynthesis was found almost universally to decrease more than could be explained by the reduction in g_1 (parameter of the Medlyn model), implying a decline in apparent carboxylation capacity (V_{cmax}).
	Zhou et al., 2014	Two experiments, one in Australia on Eucalyptus, one in Spain on Quercus, on plants grown in glasshouses under control conditions. The non-stomatal response was partitioned into effects on mesophyll conductance (g_m), the maximum Rubisco activity (V_{cmax}) and the maximum electron transport rate (J_{max}).	They found consistency among the drought responses of g_1, g_m, V_{cmax} and J_{max}, suggesting that drought imposes limitations on Rubisco activity and RuBP regeneration capacity concurrently with declines in stomatal and mesophyll conductance. Within each experiment, the more xeric species showed relatively high g_1 under moist conditions, low drought sensitivity of g_1, g_m, V_{cmax} and J_{max}, and more negative values of the critical pre-dawn water potential at which V_{cmax} declines most steeply, compared with the more mesic species. Results showed that the decline in Vcmax is not explained just by the decline in gm, but by the decline in both gm and Vcmax.
	Egea et al., 2011	Outputs from a coupled A-gs model that uses a soil water content-dependent water stress factor were compared to leaf-level values obtained from the literature.	The sensitivity analyses emphasized the necessity to combine both stomatal and non-stomatal limitations of A in coupled A–gs models to accurately capture the observed functional relationships A vs. gs and A/gs vs. gs in response to drought. Accounting for water stress in coupled A–gs models by imposing either stomatal or biochemical limitations of A, as commonly practiced in most ecosystem models, failed to reproduce the observed functional relationship between key leaf gas exchange attributes.
	Drake et al., 2017	Plants in pots of four tree species originating from constrating	as soil water content (θ) was reduced under increasing drought, all species responded by reducing gs, resulting in reduced Ci and Asat. However, Asat was reduced to

		hydrological environment, placed in the field under rainout shelters. Comparison with coupled stomatal conductance-photosynthesis model.	a larger degree than would be predicted only by stomatal reduction of Ci, indicating a coincident reduction in photosynthetic capacity with declining θ. The best model include both stomatal and non-stomatal limitations.

References of Appendix B

Ball, J. T., Woodrow, I. E., and Berry, J. A.: A model predicting stomatal conductance and its contribution to the control of photosynthesis under different environmental conditions, in: Progress in photosynthesis research, edited by: Biggins, J., Springer Netherlands, 221–224, https://doi.org/10.1007/978-94-017-0519-6_48, 1987.

Bonan, G. B., Williams, M., Fisher, R. A., and Oleson, K. W.: Modeling stomatal conductance in the earth system: linking leaf water-use efficiency and water transport along the soil–plant–atmosphere continuum, Geosci. Model Dev., 7, 2193–2222, https://doi.org/10.5194/gmd-7-2193-2014, 2014.

Bondeau, A., Smith, P. C., Zaehle, S., Schaphoff, S., Lucht, W., Cramer, W., Gerten, D., Lotze-Campen, H., Müller, C., Reichstein, M., and Smith, B.: Modelling the role of agriculture for the 20th century global terrestrial carbon balance, Global Change Biology, 13, 679–706, https://doi.org/10.1111/j.1365-2486.2006.01305.x, 2007.

Brodribb, T. J., Holbrook, N. M., Edwards, E. J., and Gutiérrez, M. V.: Relations between stomatal closure, leaf turgor and xylem vulnerability in eight tropical dry forest trees, Plant, Cell & Environment, 26, 443–450, https://doi.org/10.1046/j.1365-3040.2003.00975.x, 2003.

Christoffersen, B. O., Gloor, M., Fauset, S., Fyllas, N. M., Galbraith, D. R., Baker, T. R., Kruijt, B., Rowland, L., Fisher, R. A., Binks, O. J., Sevanto, S., Xu, C., Jansen, S., Choat, B., Mencuccini, M., McDowell, N. G., and Meir, P.: Linking hydraulic traits to tropical forest function in a size-structured and trait-driven model (TFS v.1-Hydro), Geosci. Model Dev., 9, 4227–4255, https://doi.org/10.5194/gmd-9-4227-2016, 2016.

Collatz, G. J., Ball, J. T., Grivet, C., and Berry, J. A.: Physiological and environmental regulation of stomatal conductance, photosynthesis and transpiration: a model that includes a laminar boundary layer, Agricultural and Forest Meteorology, 54, 107–136, https://doi.org/10.1016/0168-1923(91)90002-8, 1991.

De Kauwe, M. G., Kala, J., Lin, Y.-S., Pitman, A. J., Medlyn, B. E., Duursma, R. A., Abramowitz, G., Wang, Y.-P., and Miralles, D. G.: A test of an optimal stomatal conductance scheme within the CABLE land surface model, Geoscientific Model Development, 8, 431–452, https://doi.org/10.5194/gmd-8-431-2015, 2015a.

De Kauwe, M. G., Zhou, S.-X., Medlyn, B. E., Pitman, A. J., Wang, Y.-P., Duursma, R. A., and Prentice, I. C.: Do land surface models need to include differential plant species responses to drought? Examining model predictions across a mesic-xeric gradient in Europe, Biogeosciences, 12, 7503–7518, https://doi.org/10.5194/bg-12-7503-2015, 2015b.

Domingues, T. F., Martinelli, L. A., and Ehleringer, J. R.: Seasonal patterns of leaf-level photosynthetic gas exchange in an eastern Amazonian rain forest, Plant Ecology & Diversity, 7, 189–203, https://doi.org/10.1080/17550874.2012.748849, 2014.

Drake, J. E., Power, S. A., Duursma, R. A., Medlyn, B. E., Aspinwall, M. J., Choat, B., Creek, D., Eamus, D., Maier, C., Pfautsch, S., Smith, R. A., Tjoelker, M. G., and Tissue, D. T.: Stomatal and non-stomatal limitations of photosynthesis for four tree species under drought: A comparison of model formulations, Agricultural and Forest Meteorology, 247, 454–466, https://doi.org/10.1016/j.agrformet.2017.08.026, 2017.

Duursma, R. A., Medlyn, B. E., and others: MAESPA: a model to study interactions between water limitation, environmental drivers and vegetation function at tree and stand levels, with an example application to [CO_2]$\times$ drought interactions, 2012.

Egea, G., Verhoef, A., and Vidale, P. L.: Towards an improved and more flexible representation of water stress in coupled photosynthesis–stomatal conductance models, Agricultural and Forest Meteorology, 151, 1370–1384, https://doi.org/10.1016/j.agrformet.2011.05.019, 2011.

Franks, P. J., Bonan, G. B., Berry, J. A., Lombardozzi, D. L., Holbrook, N. M., Herold, N., and Oleson, K. W.: Comparing optimal and empirical stomatal conductance models for application in Earth system models, Global Change Biology, 24, 5708–5723, https://doi.org/10.1111/gcb.14445, 2018.

Fyllas, N. M., Gloor, E., Mercado, L. M., Sitch, S., Quesada, C. A., Domingues, T. F., Galbraith, D. R., Torre-Lezama, A., Vilanova, E., Ramírez-Angulo, H., Higuchi, N., Neill, D. A., Silveira, M., Ferreira, L., Aymard C., G. A., Malhi, Y., Phillips, O. L., and Lloyd, J.: Analysing Amazonian forest productivity using a new individual and trait-based model (TFS v.1), Geosci. Model Dev., 7, 1251–1269, https://doi.org/10.5194/gmd-7-1251-2014, 2014.

Hickler, T., Prentice, I. C., Smith, B., Sykes, M. T., and Zaehle, S.: Implementing plant hydraulic architecture within the LPJ Dynamic Global Vegetation Model, Global Ecology and Biogeography, 15, 567–577, https://doi.org/10.1111/j.1466-8238.2006.00254.x, 2006.

Kennedy, D., Swenson, S., Oleson, K. W., Lawrence, D. M., Fisher, R., Costa, A. C. L. da, and Gentine, P.: Implementing Plant Hydraulics in the Community Land Model, Version 5, Journal of Advances in Modeling Earth Systems, 11, 485–513, https://doi.org/10.1029/2018MS001500, 2019.

Krinner, G., Viovy, N., de Noblet-Ducoudré, N., Ogée, J., Polcher, J., Friedlingstein, P., Ciais, P., Sitch, S., and Prentice, I. C.: A dynamic global vegetation model for studies of the coupled atmosphere-biosphere system, Global Biogeochem. Cycles, 19, GB1015, https://doi.org/10.1029/2003GB002199, 2005.

Leuning, R.: A critical appraisal of a combined stomatal-photosynthesis model for C3 plants, Plant, Cell & Environment, 18, 339–355, https://doi.org/10.1111/j.1365-3040.1995.tb00370.x, 1995.

Lin, Y.-S., Medlyn, B. E., Duursma, R. A., Prentice, I. C., Wang, H., Baig, S., Eamus, D., de Dios, V. R., Mitchell, P., Ellsworth, D. S., de Beeck, M. O., Wallin, G., Uddling, J., Tarvainen, L., Linderson, M.-L., Cernusak, L. A., Nippert, J. B., Ocheltree, T. W., Tissue, D. T., Martin-StPaul, N. K., Rogers, A., Warren, J. M., De Angelis, P., Hikosaka, K., Han,

2500   Q., Onoda, Y., Gimeno, T. E., Barton, C. V. M., Bennie, J., Bonal, D., Bosc, A., Löw, M., Macinins-Ng, C., Rey, A.,
2501   Rowland, L., Setterfield, S. A., Tausz-Posch, S., Zaragoza-Castells, J., Broadmeadow, M. S. J., Drake, J. E., Freeman, M.,
2502   Ghannoum, O., Hutley, L. B., Kelly, J. W., Kikuzawa, K., Kolari, P., Koyama, K., Limousin, J.-M., Meir, P., Lola da
2503   Costa, A. C., Mikkelsen, T. N., Salinas, N., Sun, W., and Wingate, L.: Optimal stomatal behaviour around the world, Nature
2504   Clim. Change, 5, 459–464, https://doi.org/10.1038/nclimate2550, 2015.

2505   Longo, M., Knox, R. G., Levine, N. M., Alves, L. F., Bonal, D., Camargo, P. B., Fitzjarrald, D. R., Hayek, M. N., Restrepo-
2506   Coupe, N., Saleska, S. R., Silva, R. da, Stark, S. C., Tapajós, R. P., Wiedemann, K. T., Zhang, K., Wofsy, S. C., and
2507   Moorcroft, P. R.: Ecosystem heterogeneity and diversity mitigate Amazon forest resilience to frequent extreme droughts,
2508   New   Phytologist,   914–931,   https://doi.org/10.1111/nph.15185@10.1111/(ISSN)1469-
2509   8137.DroughtImpactsonTropicalForests, 2018.

2510   Manzoni, S., Vico, G., Katul, G., Fay, P. A., Polley, W., Palmroth, S., and Porporato, A.: Optimizing stomatal conductance
2511   for maximum carbon gain under water stress: a meta-analysis across plant functional types and climates, Functional
2512   Ecology, 25, 456–467, https://doi.org/10.1111/j.1365-2435.2010.01822.x, 2011.

2513   Medlyn, B. E., Pepper, D. A., O'Grady, A. P., and Keith, H.: Linking leaf and tree water use with an individual-tree model,
2514   Tree Physiol, 27, 1687–1699, https://doi.org/10.1093/treephys/27.12.1687, 2007.

2515   Medlyn, B. E., Duursma, R. A., Eamus, D., Ellsworth, D. S., Prentice, I. C., Barton, C. V. M., Crous, K. Y., De Angelis, P.,
2516   Freeman, M., and Wingate, L.: Reconciling the optimal and empirical approaches to modelling stomatal conductance,
2517   Global Change Biology, 17, 2134–2144, https://doi.org/10.1111/j.1365-2486.2010.02375.x, 2011.

2518   Medvigy, D., Wofsy, S. C., Munger, J. W., Hollinger, D. Y., and Moorcroft, P. R.: Mechanistic scaling of ecosystem function
2519   and dynamics in space and time: Ecosystem Demography model version 2, J. Geophys. Res., 114, G01002,
2520   https://doi.org/10.1029/2008JG000812, 2009.

2521   Naudts, K., Ryder, J., McGrath, M. J., Otto, J., Chen, Y., Valade, A., Bellasen, V., Berhongaray, G., Bönisch, G., Campioli,
2522   M., Ghattas, J., De Groote, T., Haverd, V., Kattge, J., MacBean, N., Maignan, F., Merilä, P., Penuelas, J., Peylin, P., Pinty,
2523   B., Pretzsch, H., Schulze, E. D., Solyga, D., Vuichard, N., Yan, Y., and Luyssaert, S.: A vertically discretised canopy
2524   description for ORCHIDEE (SVN r2290) and the modifications to the energy, water and carbon fluxes, Geosci. Model
2525   Dev., 8, 2035–2065, https://doi.org/10.5194/gmd-8-2035-2015, 2015.

2526   Powell, T. L., Koven, C. D., Johnson, D. J., Faybishenko, B., Fisher, R. A., Knox, R. G., McDowell, N. G., Condit, R., Hubbell,
2527   S. P., Wright, S. J., Chambers, J. Q., and Kueppers, L. M.: Variation in hydroclimate sustains tropical forest biomass and
2528   promotes functional diversity, New Phytologist, 219, 932–946, https://doi.org/10.1111/nph.15271, 2018.

2529   Rowland, L., Lobo-do-Vale, R. L., Christoffersen, B. O., Melém, E. A., Kruijt, B., Vasconcelos, S. S., Domingues, T., Binks,
2530   O. J., Oliveira, A. A. R., Metcalfe, D., da Costa, A. C. L., Mencuccini, M., and Meir, P.: After more than a decade of soil
2531   moisture deficit, tropical rainforest trees maintain photosynthetic capacity, despite increased leaf respiration, Glob Change
2532   Biol, 21, 4662–4672, https://doi.org/10.1111/gcb.13035, 2015.

2533 Sakschewski, B., von Bloh, W., Boit, A., Rammig, A., Kattge, J., Poorter, L., Peñuelas, J., and Thonicke, K.: Leaf and stem
2534   economics spectra drive diversity of functional plant traits in a dynamic global vegetation model, Glob Change Biol, n/a-
2535   n/a, https://doi.org/10.1111/gcb.12870, 2015.

2536 Sakschewski, B., von Bloh, W., Boit, A., Poorter, L., Peña-Claros, M., Heinke, J., Joshi, J., and Thonicke, K.: Resilience of
2537   Amazon forests emerges from plant trait diversity, Nature Climate Change, 6, 1032–1036,
2538   https://doi.org/10.1038/nclimate3109, 2016.

2539 Santos, V. A. H. F. dos, Ferreira, M. J., Rodrigues, J. V. F. C., Garcia, M. N., Ceron, J. V. B., Nelson, B. W., and Saleska, S.
2540   R.: Causes of reduced leaf-level photosynthesis during strong El Niño drought in a Central Amazon forest, Global Change
2541   Biology, 24, 4266–4279, https://doi.org/10.1111/gcb.14293, 2018.

2542 Sitch, S., Smith, B., Prentice, I. C., Arneth, A., Bondeau, A., Cramer, W., Kaplan, J. O., Levis, S., Lucht, W., Sykes, M. T.,
2543   Thonicke, K., and Venevsky, S.: Evaluation of ecosystem dynamics, plant geography and terrestrial carbon cycling in the
2544   LPJ dynamic global vegetation model, Glob. Change Biol., 9, 161–185, https://doi.org/10.1046/j.1365-2486.2003.00569.x,
2545   2003.

2546 Smith, B., Prentice, I. C., and Sykes, M. T.: Representation of vegetation dynamics in the modelling of terrestrial ecosystems:
2547   comparing two contrasting approaches within European climate space, Global Ecology and Biogeography, 10, 621–637,
2548   https://doi.org/10.1046/j.1466-822X.2001.t01-1-00256.x, 2001.

2549 Trueba, S., Pan, R., Scoffoni, C., John, G. P., Davis, S. D., and Sack, L.: Thresholds for leaf damage due to dehydration:
2550   declines of hydraulic function, stomatal conductance and cellular integrity precede those for photochemistry, New
2551   Phytologist, 223, 134–149, https://doi.org/10.1111/nph.15779, 2019.

2552 Tuzet, A., Perrier, A., and Leuning, R.: A coupled model of stomatal conductance, photosynthesis and transpiration, Plant,
2553   Cell & Environment, 26, 1097–1116, https://doi.org/10.1046/j.1365-3040.2003.01035.x, 2003.

2554 Vico, G., Manzoni, S., Palmroth, S., Weih, M., and Katul, G.: A perspective on optimal leaf stomatal conductance under CO2
2555   and light co-limitations, Agricultural and Forest Meteorology, 182–183, 191–199,
2556   https://doi.org/10.1016/j.agrformet.2013.07.005, 2013.

2557 Wang, Y. P., Kowalczyk, E., Leuning, R., Abramowitz, G., Raupach, M. R., Pak, B., Gorsel, E. van, and Luhar, A.: Diagnosing
2558   errors in a land surface model (CABLE) in the time and frequency domains, Journal of Geophysical Research:
2559   Biogeosciences, 116, https://doi.org/10.1029/2010JG001385, 2011.

2560 Williams, M., Rastetter, E. B., Fernandes, D. N., Goulden, M. L., Wofsy, S. C., Shaver, G. R., Melillo, J. M., Munger, J. W.,
2561   Fan, S.-M., and Nadelhoffer, K. J.: Modelling the soil-plant-atmosphere continuum in a Quercus–Acer stand at Harvard
2562   Forest: the regulation of stomatal conductance by light, nitrogen and soil/plant hydraulic properties, Plant, Cell &
2563   Environment, 19, 911–927, https://doi.org/10.1111/j.1365-3040.1996.tb00456.x, 1996.

2564 Xu, X., Medvigy, D., Powers, J. S., Becknell, J. M., and Guan, K.: Diversity in plant hydraulic traits explains seasonal and
2565   inter-annual variations of vegetation dynamics in seasonally dry tropical forests, New Phytol, 212, 80–95,
2566   https://doi.org/10.1111/nph.14009, 2016.

2567 Zhou, S., Duursma, R. A., Medlyn, B. E., Kelly, J. W. G., and Prentice, I. C.: How should we model plant responses to drought?
2568 An analysis of stomatal and non-stomatal responses to water stress, Agric. For. Meteorol., 182, 204–214,
2569 https://doi.org/10.1016/j.agrformet.2013.05.009, 2013.
2570 Zhou, S., Medlyn, B., Sabaté, S., Sperlich, D., Prentice, I. C., and others: Short-term water stress impacts on stomatal,
2571 mesophyll and biochemical limitations to photosynthesis differ consistently among tree species from contrasting climates,
2572 Tree Physiology, 34, 1035–46, 2014.
2573